Aus dem

Max-Planck-Institut für Herz- und Lungenforschung, Bad Nauheim

Am Fachbereich Biologie und Chemie

der Justus-Liebig Universität Gießen

The bidirectional crosstalk between macrophages and cancer cells via CX3CR1- and CCR2-signaling: fundamental for lung cancer growth and metastasis

Inauguraldissertation
zur Erlangung des Doktorgrades
der Naturwissenschaften
(Dr. rer. nat.)
Fachbereich Biologie und Chemie
der Justus-Liebig-Universität Gießen

vorgelegt von
Anja Mareike Emily Schmall
aus Köln
Gießen 2014

Gutachter: Prof. Dr. rer. nat. Michael Martin

Gutachter: Prof. Dr. rer. nat. Ralph Theo Schermuly

Tag der Disputation: 23-05-2014

Table of Contents

1 Introduction

1.1 General introduction

1.1.1 Epidemiology and risk factors

Lung cancer is characterized by the unlimited growth of cells of epithelial background in the lung and manifests with shortness of breath, hoarseness, cough and blood in sputum. Lung cancer is currently the leading cause of cancer deaths worldwide in both, men and women, and it accounts for over 30% of all deaths in both genders. Lung cancer is much more frequent than both prostate and breast cancer (*Figure 1*) and is among the 10 most common cancers. This is remarkable, since the number of estimated new cases for prostate and breast cancer together (470,930 new cases) is more than double the number of new lung cancer cases (228,190 cases, both genders combined). The incidence of lung cancer is especially elevated in North America, Europe and China. Overall, there is an aggregated (e.g. also non-smoker's) probability of 7.77% for men and 6.35% for women of developing lung cancer in their lifetimes.

The prognosis for lung cancer is poor, with an overall five-year survival rate of 15% at diagnosis (all stages combined). The survival rates according to the different lung cancer stages are summarized in *Table 1*.

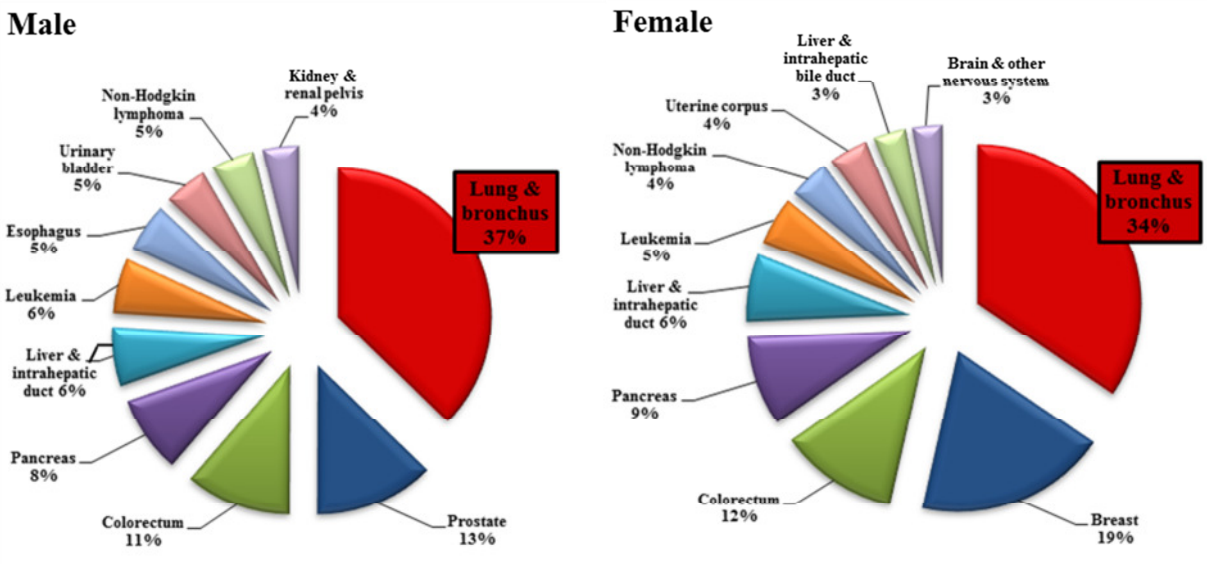

Figure 1 **Estimated deaths of the 10 leading cancer types in 2013 (Siegel et al., 2013).**

Notably, the five-year survival rate dramatically decreases to less than 5% as soon as invasive or metastatic processes are involved (from stage IIIB).

Up from stage IIIB, the one-year survival rate is just 10%. When it is taken into account, that 56% of all lung cancers are already stage III or more at the point of diagnosis, the highest fatality of lung cancer within all cancer diseases can be explained. Furthermore, 65-80% of patients present with already unresectable disease due to the advanced stage (Ferlay et al., 2010; Malvezzi et al., 2012; Siegel et al., 2013; Siegel et al., 2011).

Stage	5-year-survival rate
I	**60-80%**
II	**25-50%**
IIIA	**10-30%**
IIIB	**< 5%**
IV	**< 5%**

Table 1 **Overall 5-year-survival in relation to the stage**

By far, the greatest risk factor for lung cancer is tobacco use. Between 80% and 90% of all lung cancers worldwide are attributable to smoking, with a 20-fold increased risk of lung cancer in smokers compared to non-smokers. Interestingly, the increased risk of developing lung cancer is more dependent on the length of smoking history compared to smoking a greater amount of cigarettes. Moreover, these trends closely follow the rates of tobacco use of men and women over the years, and recent data show that the rates of lung cancer incidence are finally expected to decrease for both men and women as smoking demographics have changed.

Nevertheless, this leaves a large number of lung cancer victims who have never smoked, and lung cancer deaths are the seventh leading cause of cancer mortality among individuals who have never smoked.

A second risk factor is second-hand smoke, often referred to as environmental tobacco smoke (ETS), which is estimated to cause approximately 3,000 cases of lung cancer deaths each year. Studies reveal that spousal smoking increases the lung cancer risk of the non-smoking spouse by 30% and is dependent on duration and level of exposure. Similar increased risks are found in non-smokers exposed to ETS at work.

In addition to smoking, there are several occupational exposure hazards that have been identified as risk factors for lung cancer, including chronic exposure to cooking fumes, ionizing radiation generated during CT scans, radon gas and asbestos, with heavy exposure to asbestos doubling the risk (Alberg and Samet, 2003; Sun et al., 2007; Taylor et al., 2007; Thun et al., 2008; Truong et al., 2010; Veglia et al., 2007).

A more considerable contributor to lung cancer risk is pre-existing lung diseases, such as chronic obstructive pulmonary disease (COPD), asthma, pneumonia and tuberculosis. The most likely explanation for the increased lung cancer risk is the underlying inflammatory effect from these diseases, including the recruitment and activation of inflammatory cells that are accompanied by the expression of pro-inflammatory cytokines and chemokines, as well as the establishment of chemotactic gradients. Moreover, inflammation further initiates and promotes processes such as anti-apoptotic signaling, increased angiogenesis and increased generation of genetic mutations (Fitzpatrick, 2001; Kundu and Surh, 2008; McCarthy et al., 2012; Zhang et al., 2000).

Finally, genome-wide association studies have also identified several chromosome regions that suggest an inherited genetic susceptibility to lung cancer. The 5p15.33 locus, as well as the telomerase gene TERT (telomerase reverse transcriptase), was confirmed as being significantly correlated with lung cancer risk. TERT is critical for telomere replication and stabilization by controlling telomere length. Two additional loci, 6p21 and 6q23-25, could be related to increased lung cancer risk, although the direct involvement remains unclear (Gao et al., 2009; Schwartz and Ruckdeschel, 2006; Wang et al., 2009).

1.1.2 Pathogenesis

Lung carcinogenesis is influenced by a variety of environmental factors such as tobacco smoke, radiation and pre-existing inflammation that interact and may work synergistically with non-environmental factors, including genetic susceptibility, genetically determined variation in carcinogen metabolism and/or variability in DNA repair capacity (Caporaso et al., 1991; Wei and Spitz, 1997). The initial step of carcinogenesis in lung cancer is DNA-damage in the epithelial layers of the bronchi, bronchioli and alveoli, most likely induced by carcinogens such as benzo[a]pyrene, a classic DNA damaging carcinogen abundantly found in tobacco smoke and the environment as a result of fuel combustion (Phillips, 1983). The metabolic processes in the human body itself generate highly toxic, electrophilic and free

radical reactive intermediates that form DNA adducts through covalent binding or oxidation (Gelboin, 1980; MacLeod and Tang, 1985). In tobacco smoke alone, over 55 pro-carcinogens and ultimate carcinogens can be found. The human organism is capable of repairing damaged DNA through various pathways, such as the nucleotide excision repair pathway (Sancar, 1995). When the homeostasis of DNA damage and DNA repair becomes unstable and the level of DNA damage exceeds repair capabilities, genetic and epigenetic changes of the DNA remain permanent via mutations, loss of heterozygosity or promoter methylation (Wei et al., 2000).

Chronic changes on the DNA level can result in global transcriptome changes with deregulated pathways involved in proliferation and apoptosis. Epithelial cells can gain unlimited proliferative capacities and resistance to apoptosis and anoikis. These changes can persist over the long term and eventually lead to premalignant changes, including dysplasia and clonal patches (Mao et al., 1997; Spira et al., 2004). Premalignant patches contain clones and subclones (socalled insets), that can carry different mutations. Additionally, DNA damage or involvement of the tumor microenvironment can result in *in situ* cancer and further invasion to an advanced cancer with distant metastasis. Many molecular changes in the earliest stage of cancer also occur in advanced disease (Bianchi et al., 2004; Sato et al., 2007; Zudaire et al., 2008).

Lung cancers differ in their localization within the lung, depending on the association with smoking: primary cancers related to smoking most often develop in the central airway (squamous cell carcinoma and small-cell lung cancer; see classification in 1.1.3), while cancers unrelated to smoking develop in the peripheral airways (adenocarcinoma) (Mao et al., 1997; Wistuba et al., 2000). Moreover, lung cancers have strikingly different molecular profiles in smoking patients versus patients without a smoking history.

***Table* 2** summarizes the most common DNA changes detected in lung cancer tissue from patients with different lung cancer subtypes. Genetic changes can be divided into two subtypes: either a mutation or amplification leads to higher activity of an oncogene, e.g. KRas or EGFR (epithelial growth factor receptor), or a tumor suppressor gene is suppressed or its tumor protecting function abolished, e.g. p53 (tumor protein 53).

The most common mutation (accounting for approximately 70%), in SCLC (small-cell lung cancer) and NSCLC (non-small cell lung cancer) is the mutation of the tumor suppressor gene p53. The second-most abundant mutation (90%) in adenocarcinomas of the lung is the

activating G→T transversion affecting exon12 in p53. KRas-mutations in adenocarcinomas are smoking-related and they generally mark a poor prognosis (Riely et al., 2008; Sun et al., 2007; Westra, 2000).

Abnormality	Non-Small-Cell Lung Cancer (NSCLC)		Small-Cell Lung Cancer (SCLC)
	Squamous-Cell Carcinoma	Adenocarcinoma	
KRAS mutation	Very rare	10-30%	Very rare
BRAF mutation	3%	2%	Very rare
EGFR			
Kinase Domain mutation	Very rare	10-40%	Very rare
Amplification	30%	15%	Very rare
Variant III mutation	5%	Very rare	Very rare
HER2			
Kinase Domain mutation	Very rare	4%	Very rare
Amplification	2%	6%	Not known
ALK fusion	Very rare	7%	Not known
MET			
Mutation	12%	14%	13%
Amplification	21%	20%	Not known
TITF-1 amplification	15%	15%	Very rare
p53 mutation	60 to 70%	50 to 70%	75%
LKB1 mutation	19%	34%	Very rare
PIK3CA			
Mutation	2%	2%	Very rare
Amplification	33%	6%	4%

***Table* 2 Summary of genetic abnormalities specific in lung cancer, adapted from (Herbst et al., 2008).** **ALK**, anaplastic lymphoma kinase; **EGFR**, epidermal growth factor receptor; **HER**, human epidermal growth factor receptor 2; **LKB1**, liver kinase B1; **MET**, hepatocyte growth factor receptor; **PIK3**, Phosphatidylinositide 3-kinases; **TTF**, thyroid transcription factor.

Also notable is the kinase domain mutation of the EGFR, which is detected in 10%–40% of all adenocarcinomas. EGFR regulates important tumorigenic processes, including proliferation, apoptosis, angiogenesis, and invasion. Among the mutations of the kinase domain, over 80% are involved in frame deletions in exon19. In contrast to the Kras mutations, EGFR mutations in adenocarcinomas have been identified in non-smokers and are associated with an improved prognosis (Lynch et al., 2004; Paez et al., 2004; Pao et al., 2004).

Amplification (increased gene copy numbers or polysomy) of EGFR is the second-most frequent abnormality in squamous cell carcinoma (30%), and in this NSCLC subtype, it is related to smoking and associated with a poor prognosis (Hirsch et al., 2008; Tsao et al., 2005).

Further progression of lung tumors is still partially dependent on these initially occurring mutations, although the tumor microenvironment with non-neoplastic stromal cells might play a more important role in advanced stages of lung cancer and the metastatic spread of the primary tumor. In particular, the molecular mechanisms that initiate intravasation of tumor cells, circulation and the sub sequent extravasation at distant sites are incompletely understood and require further investigation.

1.1.3 Classification

Lung cancer is divided into two main groups based on histological features: small-cell lung cancer (SCLC) and non-small-cell lung cancer (NSCLC). NSCLC is further divided into squamous cell carcinoma, adenocarcinoma and large-cell carcinoma. *Table 3* provides an overview and direct comparison of different lung cancer subtypes.

Notably, adenocarcinoma is represented by distinct histological subtypes, which show significant differences in prognosis and treatment options, although most lung adenocarcinomas exhibit combinations of morphologic patterns. Further classification is based on invasiveness and ability to secrete mucins and include bronchoalveolar carcinoma (BAC; carcinoma *in situ*), minimally invasive adenocarcinoma (MIA) and invasive adenocarcinoma (IA) with lepidic, acinary, pappillary, micropappillary or solid growth (Finberg et al., 2007; Motoi et al., 2008; Travis et al., 2011). The applied therapy is selected based on the correct differential diagnosis of the lung cancer subtype and is therefore crucial for the patient's prognosis.

	Small cell lung cancer (SCLC)	Non-small cell lung cancer (NSCLC)		
		Adenocarcinoma	Squamous cell carcinoma	Large cell carcinoma
Histology	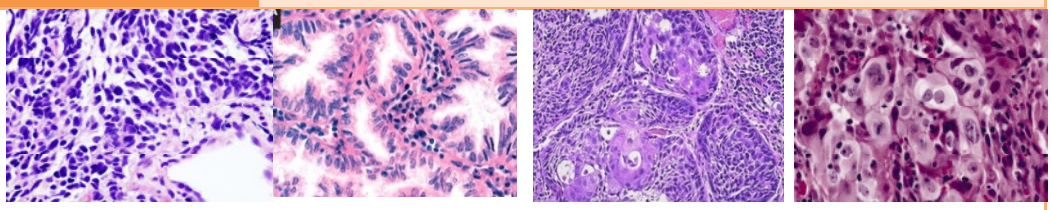			
Incidence [%]	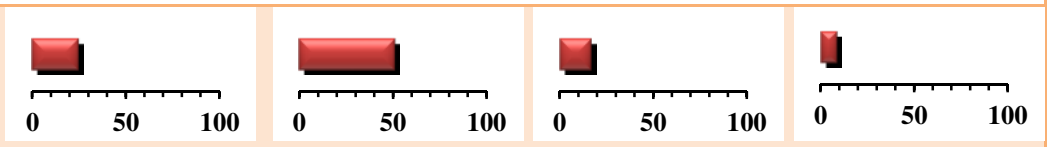			
Male vs. female	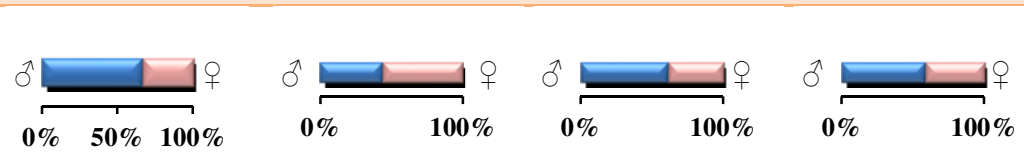			
Location	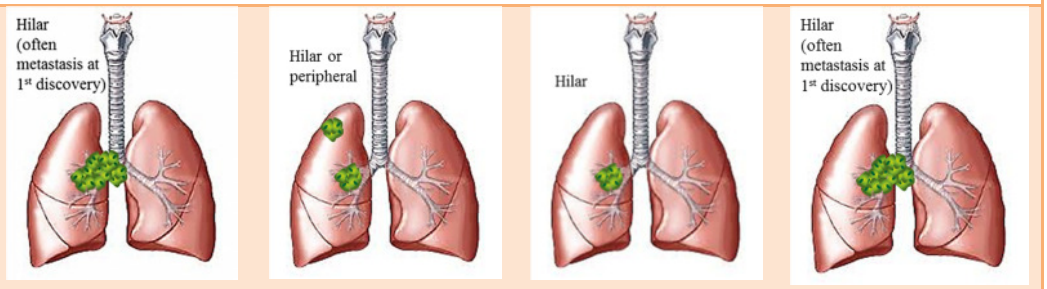			
Marker	NSE, proGRP	TTF-1, Napsin A, CK7, CEA	P63, CK5/6, Sox2. CYFRA 21-1	CEA
Smoking relation	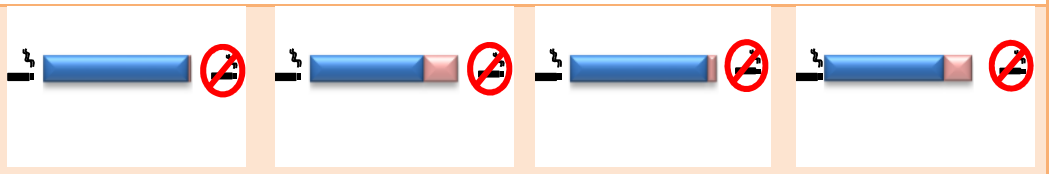			
Growth	Very rapid	Intermediate	Relatively slow	Rapid
Metastatic tendency	Very early; to mediastinum or distaly	Intermediate	Later, then primarly to hilar nodes	Early
Resectability	almost none	poor	fair	poor

Table 3 **Characteristics of histological lung cancer subtypes. NSE, neuron specific enolase; TTF-1, thyreoid transcription factor 1; CK, cytokeratin; CEA, Carcinoembryonic antigen; CYFRA 21-1 cytokeratin 19 fragment.**

The summary provided in *Table 3* is based on multiple recent studies (Barletta et al., 2009; Chen et al., 2009; Devesa et al., 2005; Janssen-Heijnen and Coebergh, 2001; Kenfield et al., 2008; Molina et al., 2003; Noh and Shim, 2012; Russell et al., 2011; Sarrafzadegan et al., 2007; Shibayama et al., 2001; Tacha et al., 2012).

1.2 Therapeutical options with special regards to the tumor stroma

The major challenge in lung cancer therapy arises from the fact that the majority of patients present with either locally advanced disease (stage III) or metastatic disease (stage IV). The first-choice approach is curative surgical resection. Importantly, patient survival ranges between 50% and 80% after surgery, implying that a significant number of patients require systematic treatment. Furthermore, occult and therefore untreated micrometastatic disease at the time of resection leads to relapse. Patients presenting with advanced disease, tumor relapse after surgery or metastatic spread are dependent on alternative therapeutic approaches.

1.2.1 Radiation therapy

Patients who are poor candidates for surgery because of their age, condition or advanced disease receive radiation treatment. Radiation is also used prior to surgery to shrink the tumor or maintain cells in a state of higher sensitivity to chemotherapeutic agents and therefore might be combined with chemotherapy.

Moreover, radiation combined with chemotherapy is the treatment for SCLC, since this highly aggressive tumor tends to spread very quickly and eludes surgical treatment options (Stupp et al., 2004).

1.2.2 Chemotherapy

Chemotherapy (in combination with radiation) is the method of choice for advanced NSCLC, although chemotherapy regimens show only a modest improvement in survival and no regimen has been completely effective. Postoperative adjuvant chemotherapy has been shown to improve survival for patients with stage II disease and may also have a role in the treatment of stage IB NSCLC.

Combination regimens, including platinum-based chemotherapy with either cisplatin or carboplatin, have become the standard of care for treating NSCLC, and these drugs modestly

improve survival (Arriagada et al., 2004). Various clinical trials failed to show an advantage of using more than two drugs in a chemotherapy regimen. First-line chemotherapeutic agents used in combination with cisplatin or carboplatin include taxanes (paclitaxel and docetaxel), gemcitabine (a deoxycytidine analogue), vinorelbine, and irinotecan or topotecan (topoisomerase I inhibitors).

Therapy with chemotherapeutic agents is associated with severe side effects and significantly impairs the quality of the patient's life. Even cisplatin and carboplatin, the mainstay of lung cancer chemotherapy, only increase the one-year survival to 30%, which appears relatively minimal if compared to the impact on the patient's life. Overall, no chemotherapeutic agent or combination regimes showed a better one-year survival than the 40.3% reported with cisplatin together with paclitaxel (Bonomi et al., 2000; Crino et al., 1999; Haura, 2001; Le Chevalier et al., 1994; Sandler et al., 2000). This lack of success underlines the mandatory research to find alternatives to chemotherapy.

1.2.3 Targeted therapy

The most advanced approach of lung cancer therapy is targeted therapy. Thus far, only three pharmaceuticals have been approved for treatment of lung cancer in the past 10 years: gefitinib, erlotinib and crizotinib.

As described above, NSCLCs exhibit genetic changes such as KRas mutations and EGFR-abnormalities. Such genetic alterations can be detected in patients' biopsies and provide a basis for a patient-optimized, targeted therapy. The first targeting agent to be approved for lung cancer treatment was gefitinib in 2002, and shortly after erlotinib in 2003. Both agents are tyrosine kinase inhibitors (TKIs) and designed to target EGFR mutations. An EGFR mutation is a valid biomarker of treatment response, and prospective clinical trials demonstrated a progression-free survival benefit of TKI as first-line therapy in EGFR mutant patients (Mok et al., 2009; Sharma et al., 2007). The EGFR mutation status can be determined by gene sequencing, *in situ* hybridization or immunohistochemistry with mutation-specific antibodies (Cagle and Chirieac, 2012).

A second success for the approach of targeted therapies is crizotinib, which was approved in 2011 and which was designed to target advanced or metastatic NSCLC that is positive for anaplastic lymphoma kinase (ALK). This tyrosine kinase receptor is usually expressed only in neuronal cell types. In NSCLC, ALK is rearranged to a protein with constitutive kinase

activity. Interestingly, none of the adenocarcinomas with rearranged ALK showed coexisting mutations of EGFR. A recently published clinical trial showed that lung cancers expressing ALK are sensitive to inhibitors of ALK kinase activity. Although only 7% of adenocarcinomas and nearly none of the squamous cell carcinomas show ALK mutations, crizotinib serves as an example for a successful targeted therapy (Koivunen et al., 2008; Kwak et al., 2010; Soda et al., 2007).

More inhibitors for various genetic alterations are currently in clinical trials, such as trastuzumab, a chimerized monoclonal antibody against HER2/neu, a member of the human epidermal growth factor receptor family (Azzoli et al., 2002).

Overall targeted therapy is a very promising approach, and in the future patients diagnosed for lung cancer will most likely be tested for a panel of oncogenes/mutations to optimize the therapy. Although the benefits of individualized therapy are obvious, one should consider both economic aspects and potential ethical questions. For example, what might be the consequence of a positive screen for lung cancer common mutations on the insurance status in countries without compulsory health insurance?

1.2.4 Targeting the tumor microenvironment

The tumor microenvironment surrounds the virtual tumor and consists of accumulated non-neoplastic host cells, such as tumor-associated macrophages (TAM), cancer-associated fibroblasts (CAF), leucocyte subsets and non-cellular alterations including angiogenesis, abundant production of extracellular matrix (ECM) and secretion of cytokines and growth factors. Below is more detailed information regarding the tumor microenvironment (*Figure 2*).

Thus far, the only clinically approved therapeutic approach directed against the tumor microenvironment is bevacizumab (Avastin, Roche), a monoclonal antibody against VEGF. Overall, the survival benefits of antiangiogenetic drugs have been rather modest (Sounni and Noel, 2013). Moreover, therapy with bevacizumab requires an accurate diagnosis of the NSCLC subtype and is currently contraindicated in patients with lung squamous cell carcinoma, due to severe adverse side effects (bleeding complications) (Johnson et al., 2004). The only patient groups that benefit from bevacizumab treatment (and only in combination with chemotherapy) are those with non-squamous NSCLC. Furthermore, bevacizumab is not curative and treatment withdrawal leads to tumor regrowth (Sandler et al., 2006).

Since it is well-established that chronic inflammation contributes to cancer development, several studies have attempted to inhibit the inflammatory processes. A key pathway in inflammation is the activation of NF-κB, which leads to secretion of inflammatory cytokines. Chronic activation of NF-κB enhances resistance to chemotherapy and radiotherapy, and several NF-κB inhibitors have been reported to improve the effect of chemotherapeutic agents against lung cancer and induce tumor regression and prolonged survival in mice. However, sustained NF-kB inhibition results in neutrophilia, enhanced acute inflammation and liver damage (Greten et al., 2007; Izzo et al., 2006; Xue et al., 2011).

An approach to directly target stromal cells was developed with sibrotuzumab, a humanized monoclonal antibody against FAP (fibroblast activation protein α), a membrane-bound serine protease expressed by CAFs. Immunohistochemical studies revealed that FAP is mainly localized in the stroma of tumor cells, but not in the stroma of healthy tissue, thus providing a potential cancer-specific target. However, phase I and II studies targeting FAP failed to show clinical benefits (Xing et al., 2010).

Several researchers employed a completely different strategy, whereby instead of targeting specific stromal cells, the immune system was manipulated with the aim of overcoming tumor -mediated immune suppression. Tumor cells are known to thrive in an immunosuppressed environment. In normal cells, antigen-presenting cells (APCs) phagocytes tumor cell fragments and display the antigens on their surface to naïve T-lymphocytes in adjacent lymph nodes, which in turn are activated to tumor-specific $CD4^+$ T-helper and $CD8^+$ cytotoxic T-cells. This process is abrogated in lung cancer development (Gridelli et al., 2009; Kelly et al., 2010). Several groups attempted to restore this co-stimulatory pathway with approaches such as vaccine therapy or antigen-independent immunotherapy. The most successful tumor-antigen based vaccine was L-BLP25 against MUC-1 (mucin-1), which is overexpressed in various cancers. However, it eventually failed in clinical phase II studies (Butts et al., 2005; Sangha and Butts, 2007). Dendritic cells (DCs) vaccines are based on DCs cultured with necrotic tumor cells or electroporated tumor lysates and injected either intradermally or into the patient's lymph nodes. These vaccines seem to be tolerated in patients with NSCLC and are currently in phase I studies. This therapy approach is individualized for patients and accordingly economically difficult to accomplish (Chang et al., 2005; Um et al., 2010).
Antigen-independent therapy appears to be a more feasible option, and two approaches are currently in advanced clinical trials. The first involves ipilimumab, a humanized IgG1 anti-CTLA-4 antibody (cytotoxic T-lymphocyte antigen 4, CD152), which binds a receptor that

induces downregulation of the immune system upon stimulation. Ipilimumab blocks this inhibitory signal and thus enhances and prolongs the activation and proliferation of tumor-specific T-cells (Fong and Small, 2008; Tarhini and Iqbal, 2010) Ipilimumab was found to improve the survival in metastatic melanoma patients in a phase III clinical study (Hodi et al., 2010).

A similar approach for improving the immune reaction again tumor cells is provided with talactoferrin alfa, a recombinant human lactoferrin that enhances the movement of immune cells to lymphoid tissue, where it stimulates their maturation. This leads to increased levels of DCs bearing tumor antigens, as well as secretion of cytokines that promote maturation and proliferation of antitumor $CD8^+$ T-cells. Talactoferrin alfa demonstrated a significantly improved median overall survival in a phase II trial with NSCLC patients (Digumarti et al., 2011; Parikh et al., 2011).

1.3 The tumor microenvironment

1.3.1 Characterization of the tumor microenvironment

Over recent decades, the conventional view of tumorigenesis as a cell-autonomous process based solely on genetic mutations has shifted, as experimental evidence has revealed that the presence of mutations alone is not sufficient for primary tumor growth and metastasis. Moreover, it has become increasingly apparent that non-neoplastic host cells present in solid tumors play a key role in achieving and promoting an oncogenic microenvironment with dynamic and sustained signaling cascades. The most important microenvironmental alterations include the accumulation of TAMs, CAFs and various leucocyte subsets, as well as non-cellular alterations such as neoangiogenesis, abundant production of ECM, and secretion of cytokines and growth factors (Cavallo et al., 2011; Coussens and Werb, 2002; Hanahan and Weinberg, 2000).

While the co-dependent relationship that exists between tumor and stromal cells is well-documented, the regulatory pathways that underlie these interactions are not well understood. A better understanding of the crosstalk between cancer cells and their tumor stroma will likely provide new therapeutic targets. This knowledge is invaluable, since the currently available chemotherapeutic agents are not efficacious, particularly in the case of lung cancer.

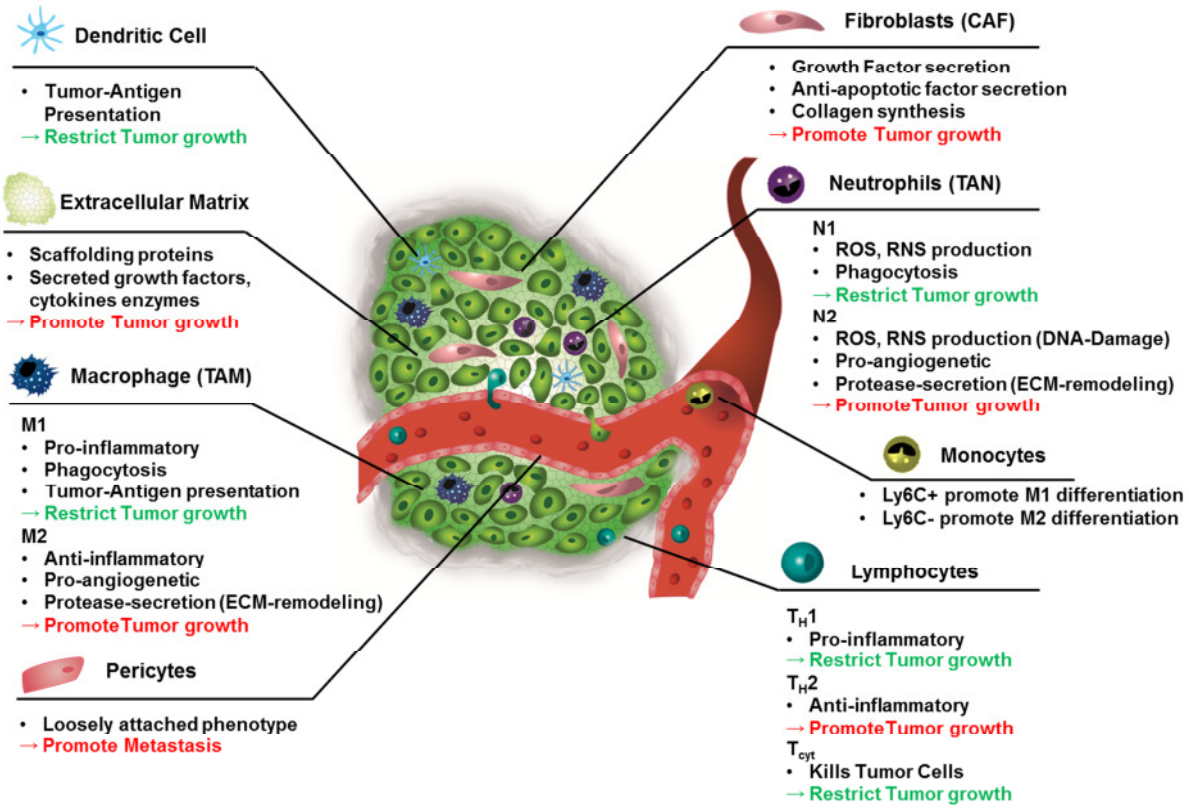

Figure 2 **The tumor microenvironment. CAF,** Cancer associated fibroblast; **ECM**, Extracellular Matrix; **N1/N2,** Neutrophil-polarization; **M1/M2,** Macrophage-polarization; **RNS,** reactive nitrogen species; **ROS,** reactive oxygen species; **TAN,** Tumor associated Neutrophil; **TAM,** Tumor associated Macrophage; **T_H1/T_H2,** T-Lymphocyte-polarization; **T_{cyt},** cytotoxic T-Lymphocyte.

Cancer-associated fibroblasts (CAF)

CAF are the most prominent cell type within the tumor stroma and are divided into several subpopulations based on their derivation and marker expression. CAF can derive from resident local interstitial fibroblasts, bone marrow-derived progenitor cells or trans-differentiating epithelial cells (Anderberg and Pietras, 2009). Most overlapping markers for CAF are α-smooth muscle actin (SMA), platelet-derived growth factor receptors (PDGFR) and fibroblast specific protein-1 (FSP-1) (Sugimoto et al., 2006). CAF promote tumor cell proliferation via secretion of hepatocyte growth factor (HGF), fibroblast growth factors (FGF), Wnt-family members and CXCL12 and further convey cancer cells by producing anti-apoptotic stimuli such as insulin-like growth factor-1 and -2 (Bhowmick et al., 2004; Strnad et al., 2010). Moreover, they abundantly supply the ECM with different collagens and their

tumor-promoting capacities were demonstrated in several *in vivo* studies (Anderberg et al., 2009; Karnoub et al., 2007). Interestingly, CAF display a different phenotype compared to normal fibroblasts (Chaudhri et al., 2013).

Pericytes

Pericytes are crucial for maturation and stabilization of vessels. However, pericytes localized in the tumor microenvironment appear to have a more loosely attached phenotype and fail to interact properly with endothelial cells, resulting in leaky and disorganized vessels, which might promote metastatic spread (Morikawa et al., 2002; Xian et al., 2006).

Myeloid leukocytes

Cells of myeloid origin such as mast cells, granulocytes (neutrophils, basophils and eosinophils), DCs, macrophages (MΦ) and monocytes (MC) are abundantly accumulated in pre-malignant and malignant tissues. They orchestrate a myriad of signaling cascades by releasing cytokines, chemokines, matrix metalloproteinases, serine proteases, reactive oxygen species (DNA damage!), histamine and other bioactive mediators, which influence tissue remodeling and angiogenesis and as a consequence tumor cell migration and metastasis (Coukos et al., 2005; Coussens et al., 1999; De Palma and Naldini, 2006). Whereas the contributions of basophils and eosinophils to lung cancer development are less intensively studied, recent data suggest that tumor associated neutrophil (TAN) subpopulations show a Janus face similar to different polarized MΦ, i.e. they can be divided into a N1-tumor limiting and a N2-tumor promoting fraction. Key cytokines in TAN polarization include TGFβ (promoting N2) and IFNβ (promoting N1). Typical characteristics of N1 are a hyper-segmented nucleus and restriction of angiogenesis. The N1 subpopulation is highly cytotoxic due to secretion of proteases, ROS and RNS (reactive oxygen species and reactive nitrogen species). The N2 subpopulation is identified by circular nuclei. Similar to MΦ sub-populations, they promote angiogenesis, invasiveness and metastasis of lung cancer cells (DeNardo et al., 2010; Piccard et al., 2012).

The involvement of mast cells in tumor progression and rejection remains overall controversial. Immature mast cell progenitors are released from the bone marrow and remain circulating. They mature as they migrate into tissue, with adapting tissue specific

characteristics that guide a division of mast cells into two general subtypes: connective tissue mast cells with chymase expression and mucosal mast cells with tryptase expression, such as abundantly found in the mucosa of the lungs (Irani et al., 1986). In NSLC, mast cells and mast cell-derived histamine were shown to increase proliferation and tumor growth in a histamine receptor dependent pathway (Stoyanov et al., 2012). Controversially, studies with non-small cell lung cancer patients demonstrated a correlation of low microenvironmental infiltration of mast cells with a worse prognosis (Carlini et al., 2010) and abundant accumulation of mast cells in tumor islets with an improved prognosis (Welsh et al., 2005)

Lymphoid leukocytes

Accumulation of the lymphocyte subpopulation described thus far can be observed in the tumor microenvironment. There are two distinct subpopulations: the $CD8^+$ cytotoxic T-lymphocyte and NK (natural killer) cells, with a more clarified role in lung cancer development. Both cell populations play a critical role in restraining tumor progression (Dunn et al., 2004). This tumor-restraining effect might be masked by other lymphocyte populations, as in the entire tumor stroma the balance between both forces is critical and the dominating effect dictates tumor-progression or -regression (Balkwill et al., 2005; de Visser et al., 2006; Karin et al., 2006).

The contribution of $CD4^+$ T-cells, the most prominent T-cell subset, is quite controversial. Infiltration of $CD4^+$ cells in human lung cancer tissue correlates with a positive outcome, whereas in other cancer types, $CD4^+$ accumulation is associated with a decreased survival rate (Siddiqui et al., 2007; Wakabayashi et al., 2003). The two subpopulations of $CD4^+$ cells, T_{H1} and T_{H2} cells, might explain these controversial effects. Polarization towards T_{H1} or T_{H2} is determined by different cytokines. In general, T_{H1} cells maintain tumor restrictive processes, such as enhancing APCs and prolonging the response of $CD8^+$ cytotoxic cells (Romagnani et al., 1997). They are further able to kill tumor cells directly by secreting IFNγ, TNFα and cytolytic granules (Munk and Emoto, 1995). T_{H2} cells release abundant amounts of IL-4, IL-10 and IL-13, which promote tumor growth indirectly by favoring MΦ-polarization towards an M2-phenotype, inhibiting apoptosis and inducing proliferation.

In conclusion, it is the ratio of T_{H2} to T_{H1}-cells that correlates more consistently with parameters of clinical disease progression and thus is more important than an overall determination of infiltrating $CD4^+$ lymphocytes in cancer tissue (Chin et al., 1992).

Another subpopulation thought to play a role in regulating tumor progression is the $CD4^+FoxP3^+$ T regulatory (T_{REG}) cell population. T_{REG}-infiltrations in NSCLC correlate with a poor prognosis (Petersen et al., 2006), and these cells seem to influence tumor development via suppression of the anti-tumor activities of $CD8^+$ cytotoxic lymphocytes, NK-cells and DC (Fehervari and Sakaguchi, 2004; Trzonkowski et al., 2004). Obviously, T_{REG} cells shift the cytokine secretion pattern towards immunosuppressive-acting cytokines such as TGFβ, IL-35 and IL-10, and further interfere with the metabolic activity of cyclic adenosine monophosphate (cAMP) transfer, as well as inhibiting APC function by inducing binding of cytotoxic T-lymphocytes to CD80/86, which is necessary for T-cell activation and survival (Strauss et al., 2007; Tang and Bluestone, 2008).

A more recently discovered T-cell subset is the T_{H17}-cell group that differentiates upon stimulation of IL-6 and TGFß and mediates their effect through secretion of IL-17, IL-21 and IL-22 (Dong, 2008; Weaver et al., 2006). Secretion of IL-17 promotes the growth of NSCLC in a mouse model by enhancing neoangiogenesis (Numasaki et al., 2003; Numasaki et al., 2005).

Extra-cellular Matrix (ECM)

Although not an active cellular component of the tumor stroma, the ECM plays a crucial role in tumor progression and migration. Collagen is the most abundantly expressed protein in the ECM, and its crosslinking results in ECM stiffening, thus facilitating tumor growth, invasion and metastatic spread (Levental et al., 2009; Lo et al., 2000).

1.3.2 Macrophages (MΦ) in the tumor microenvironment

MΦ represent a key component of the innate immune system, with effector functions that are far beyond their classical functions as phagocytic and antigen-presenting immune cells. With their plasticity and ability to secret a wide variety of cytokines, chemokines, growth factors and enzymes, they are major players in regulating tissue homeostasis both in normal physiological and pathophysiological conditions (Mosser and Edwards, 2008; Murray and Wynn, 2011). Accumulated MΦ in tissue can have different origins: (1) they derive from proliferation of local tissue MΦ, (2) they differentiate from myeloid progenitors from the bone marrow over a monocyte state to MΦ or (3) they differentiate from splenic monocytes.

Several tissues have more than one resident MΦ population, mostly with different functions. In the lung, for example, alveolar MΦ reside on alveolar septae in the alveolar space, and alveolar interstitial MΦ reside in the interstitium of the lung (Cortez-Retamozo et al., 2012; Galli et al., 2011; Kugathasan et al., 2008; Laskin et al., 2001). MΦ have been shown to enhance tumor growth in a variety of cancers, including breast, prostate, colorectal and hepatocellular carcinomas (Cortez-Retamozo et al., 2012; Mroczko et al., 2007; Qian and Pollard, 2010; Zhu et al., 2008). In addition, enhanced infiltration of MΦ within tumors is associated with a poor outcome and shorter survival times. In contrast, it is well-documented that directed activation of immune cells leads to cancer regression (Aarntzen et al., 2012; Freire and Osinaga, 2012; Nars and Kaneno, 2012; Savai et al., 2007). Hence, an ambiguity remains regarding the role of MΦ in cancer initiation and progression. Part of this ambiguity may be explained by the fact that MΦ can polarize into either pro-inflammatory (M1) or "alternatively activated" anti-inflammatory (M2) cells (*Figure 3*). The M1-phenotype develops upon contact with LPS or bacteria, IFNγ or activation of Toll-like receptors (TLR). In response, iNOS expression and activity is upregulated to produce reactive oxygen or nitrogen species, histamine and proteolytic enzymes to kill microorganisms. Furthermore, classical pro-inflammatory cytokines are upregulated, such as IL-1β, IL-12, IL-6 and an overall inflammatory reaction, including activation of NK-cells and T_{H1} response is induced. In the context of cancer development, M1 cells were considered the "good guys" with tumor-restrictive properties that are mainly based on tumor antigen presentation and phagocytosis of malignant cells. M2-polarization was recently divided into more subtypes, such as M2a, M2b and M2c, based on cytokine secretion patterns. However, all M2-subtypes have tumor supporting features in common, so MΦ will be considered to divide only into M1 and M2. MΦ polarize into M2 upon stimulation with cytokines known of a T_{H2}-immune response, such as IL-4, IL-13, IL-33 and IL-10. Furthermore, MΦ can adapt an M2-phenotype upon interaction with B-cells, which secrete immune complexes in combination with IL-1β and IL-10. With polarization to an M2-phenotype, the ability of tumor restriction is lost and M2-MΦ work as anti-inflammatory agents and strongly promote angiogenesis and tissue remodeling. M2-MΦ express arginase1 and CD206, and secrete high levels of IL-10 and IL-RA. MΦ-polarization can be retraced to their progenitor monocytes and is even reflected in certain signal transduction patterns with distinct kinases and transcription factors as summarized in *Figure 3* (Biswas and Mantovani, 2010; Lawrence and Natoli, 2011; Sica et al., 2008).

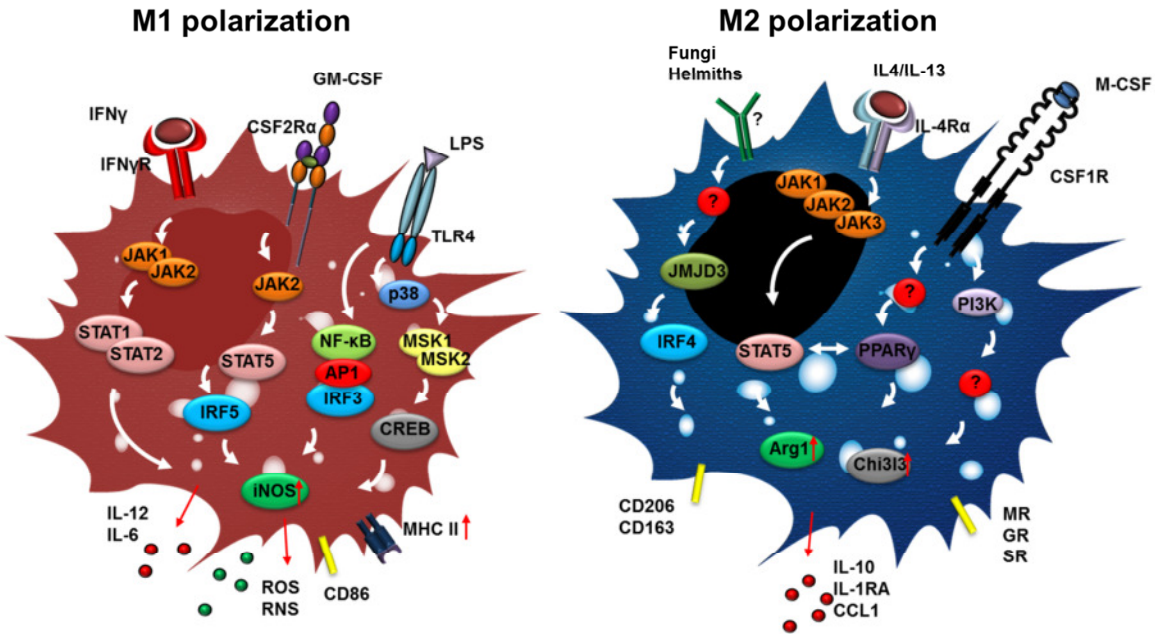

***Figure 3* Summary of MΦ-*polarization (above* MΦ*:* stimuli, intracellular: signal transduction pathways; under MΦ: target genes). Arg1**, arginase 1; **Chi3l3**, chitinase 3-like 3; **CREB**, cAMP-responsive element-binding protein; **GM-CSF**, granulocyte-macrophage colony stimulating factor; **GR**, galactose receptor; **IFNγ**, interferonγ; **iNOS**, inducible NO-synthase; **IL**, interleukin; **IRF**, Interferon-regularoty factor; **JAK**, Janus kinase; **LPS**, lipopolysaccharide; **M-CSF**, macrophage colony stimulating factor; **MSK**, mitogen- and stress-activated kinase; **MR**, mannose receptor; **NF-κB**, nuclear factor-κB; **PI3K**, phosphoinositied 3-kinase; **PPARγ**, peroxisome proliferator-activated receptor γ; **RNS**, reactive nitrogen species; **ROS**, reactive oxygen species; **STAT**, signal transducer and activator of transcription; **SR**, scavenging receptor; **TLR**4, toll-like receptor 4 [adapted from (Biswas and Mantovani, 2010; Lawrence and Natoli, 2011)

Although some research was done in the field of MΦ-polarization, there is still no validated marker specific for M2-MΦ, and overall marker expression often displays heterogeneity between M1 and M2-markers (Gordon and Martinez, 2010; Mantovani et al., 2002). These observations suggest that MΦ-polarization is dynamic and the effector functions of discrete MΦ populations are incompletely understood. Due to the heterogeneity of MΦ subpopulations (especially *in vivo*) and their pleiotropic effects, research with MΦ has proven challenging, especially in a setting such as lung cancer where long-term studies are required.

1.4 Chemokine receptors CCR2 and CX3CR1

MΦ direct distinct cytokine- and chemokine -networks in various, mainly inflammatory diseases. Two important chemokine receptors within these networks are CCR2, the receptor for CCL2 (MCP-1, *monocyte chemoattractant protein 1)* and CX3CR1, the receptor for CX3CL1 (*Fractalkine, Neurotactin*). The chemokine receptor nomenclature reflects their

binding ligands, which are named based on the number and location of the cysteine residues at the N-terminus of the molecule. (*Figure 4*).

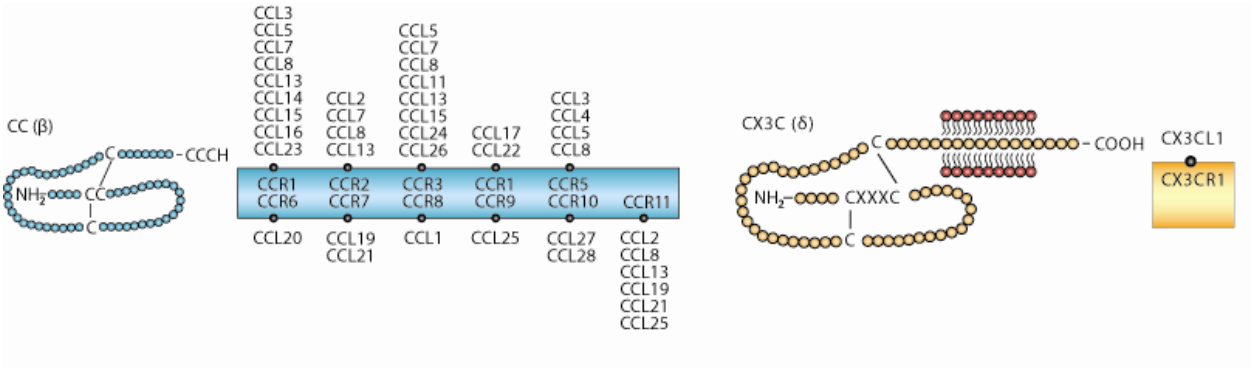

***Figure 4* Structure and ligands of CCR2 and CX3CR1 [modified after (Burke-Gaffney et al., 2002)].**

CCR2 exists in two isoforms, CCR2A and CCR2B, and both are encoded by a single CCR2 gene. The isoforms are derived by alternative splicing and gene-sequencing uncovered, that the 47-amino acid carboxyl tail of CCR2B was located together with the seven transmembrane domains in the same exon, and the 61-amino acid tail of CCR2A was in a downstream exon. Accordingly, the splicing variants differ only in their terminal carboxyl tail. Both isoforms are G-protein-coupled receptors and bind CCL2 with high affinity. The differences in the terminal carboxyl tail result in a different signal transduction and localization of the receptor. Binding of the agonist CCL2 results in a rapid Ca^{2+} (*Calcium*) influx after activation of CCR2B, but not CCR2A. Moreover, the trafficking to the membrane of CCR2A is impaired, implying that the amino acid sequence responsible for the receptor localization is within the terminal carboxyl tail. Finally, CCR2B is the more abundantly expressed receptor overall and the low expression of CCR2A makes studies challenging, so that the exact functions of this splicing variant remain unclear. (Sanders et al., 2000; Wong et al., 1997) In the following explanations CCR2 refers to the isoform CCR2B. Additionally to CCL2, studies revealed CCL7 (MCP-3, monocyte chemoattractant protein 3), CCL8 (MCP-2, monocyte chemoattractant protein 2) and CCL13 (MCP-4, monocyte chemoattractant protein 4) as agonists of CCR2 (*Figure 4*). However, CCL2 is the ligand with the highest affinity and potency, as measured as Ca^{2+} flux. Moreover, CCL2 amplifies its own receptor binding affinity via CCR2 binding (Kito et al., 2001; Moore et al., 1997; Uguccioni et al., 1995).

Although three isoforms are reported for CX3CR1 – the “standard” and two prolonged amino acid sequences - , the functional differences are poorly investigated. However, the extended

isoforms display an increased sensitivity upon CX3CL1 binding with increased Ca^{2+} mobilization (Garin et al., 2003). The only CX3-chemokine, CX3CL1 binds exclusively to CX3CR1, thus implying a tighter regulation of CX3CR1-CX3CL1 signaling as compared to CCR2-CCL2 signaling (Deshmane et al., 2009; Rodriguez-Frade et al., 1999).

Both, CCR2 and CX3CR1 are transmembrane G-protein coupled receptors, which activate multiple signaling pathways including JAK-STAT, MAPK and PI-3K pathways, upon dimerization (Mellado et al., 1998; Wolf et al., 2012). Agonist-mediated activation leads to chemotaxis of CCR2-expressing cells towards the CCL2 concentration gradient. In contrast, CX3CR1-CX3CL1 binding leads not only to chemotaxis but also to integrin independent adhesion of the CX3CR1-expressing cell, since CX3CL1 can be expressed as a membrane-bound protein as well as a cleaved and then chemotactic peptide. This dual function is unique in the group of chemokines (Kim et al., 2011). CX3CR1-CX3CL1 signaling is further important for angiogenesis and proliferation (Imai et al., 1997; Lee et al., 2006). Both receptors are expressed abundantly by MΦ and monocytes as well as other leucocytes.

CCL2-CCR2 and CX3CL1-CX3CR1 signaling plays a crucial role in many inflammatory diseases where chemotactic attraction of immune cells to the site of inflammation is crucial and a lack of CCR2/CX3CR1 results in decreased MC/MΦ-accumulation. CCR2-mediated emigration of MC from the bone marrow to the blood stream and following trafficking to the foci of infection is important for clearance of several bacteria, viruses, fungi and protozoa. However, persistent accumulation of CX3CL1/CCL2-attracted inflammatory cells results in chronic inflammation, severe tissue destruction and remodeling. For example, high CX3CL1-levels are associated with COPD, pulmonary hypertension and pulmonary fibrosis in a negative sense (Shi and Pamer, 2011; Zhang and Patel, 2010).

The importance of CCL2 in tumor growth and metastasis was demonstrated in several types of cancers, with the focus on CCL2-secreting cancer cells. The main discovery in most of the studies was that CCL2 attracts monocytes to establish a tumor microenvironment (Bailey et al., 2007; Erreni et al., 2010; Qian et al., 2011; Tanaka et al., 2009).

Overall, the role of CX3CL1 in cancer progression is more contrary. CX3CL1 and CX3CR1 were found to be expressed and functional on glioma cells but inhibited invasiveness of cancer cells. In contrast, another study could correlate high CX3CL1-expression with a later stage and worse survival in oligodendrogliomas, anaplastic astrocytomas and glioblastomas. Furthermore, CX3CL1 expression in breast cancer tissue correlates with a poor outcome.

Additionally, CX3CL1 was able to promote cancer development in a spontaneous model of breast cancer by activating EGF signaling. (Erreni et al., 2010; Sciume et al., 2010; Tardaguila et al., 2013; Tsang et al., 2013)

However, the role of chemokine receptors, CCR2 and CX3CR1, as well on MΦ or cancer cells during cancer progression and metastasis, is poorly understood.

2 Aims of the Study

Lung cancer is the leading cause of cancer death worldwide. This high death rate in relation to newly diagnosed lung cancer cases is due to (1) advanced stage of the disease at the time of diagnosis without possibility of resection, (2) failure of existing chemotherapeutic acting agents especially in late stage and metastatic lung cancer and (3) the lack of reliable preventive screenings. One of the important reasons for these dilemmas is the lack of knowledge of the underlying mechanisms of lung cancer development and progression besides the triggering mutations of oncogenes. In particular, the involvement of the tumor microenvironment with innumerable interacting cell types and signaling cascades remains unclear.

The present study was performed to contribute to elucidate dysregulated key pathways in the tumor microenvironment with particular attention to MΦ-tumor cell interactions. This study was conducted to

(1) Determine the magnitude of contribution of different MΦ-populations to tumor growth and metastasis.

(2) Determine fundamental mechanisms of MΦ-contribution to the tumor microenvironment.

(3) Identify aberrant signaling pathways in MΦ and cancer cells provoked by their interactions.

(4) Identify new targets for anti-cancer drugs apart from chemotherapeutic agents to treat lung cancer.

These aims were accomplished using long-term MΦ-depleted animal models, pathway-specific knockout animals and *in vitro* co-cultures of MΦ and cancer cells.

3 Materials and Experimental Procedures

3.1 Experimental procedures – *in vitro*

3.1.1 Cell culture

Murine lung cancer cell line

Experimental analyses were performed using the LLC1 (Lewis lung carcinoma 1) cell line, which was originally established from a Lewis lung carcinoma bearing C57/Bl6 mouse. Although this cell line originated from a distinct epithelial background, some epithelial characteristics were lost due to its malignant transformation. This results in a mixed morphology, with a more elongated and attached as well as rounded cell population that grows in suspension.

The LLC1 cell line is an ideal tool for investigating the development of lung cancer *in vitro* and *in vivo* since it is syngeneic with the C57/Bl6 mouse, which is the basis for genetically modified animals such as Knock out and transgenic mice. LLC1 cells are highly tumorigenic in mice with a well reproducible tumor growth curve and the ability to form metastasis. (Bertram and Janik, 1980). LLC1 cells were obtained from the American type culture collection (ATCC; CRL-1642™) and were cultured in tissue culture flasks in RPMI 1640 supplemented with 1% glutamine, 10% fetal calf serum (FCS) and penicillin (100U/ml) /streptomycin (0.1 mg/ml). Subcultures were prepared by aspirating the media, washing the cells once with 1× phosphate buffered saline (PBS) and incubating cells at 37°C with 1× Trypsine. After cell detachment FCS was added to stop the reaction and the cell suspension was centrifuged for 8 min at 1600 rpm. After subsequent resuspension in fresh media, the cells were plated again at a ratio of 1:6. Excessive cells were frozen as stock in liquid nitrogen for later use: one million LLC1 cells were resuspended in 1 ml of the culture media supplemented with 5% DMSO and stored in screw cap cryotubes overnight in an isopropanol filled freezing box at -80°C. The next day all cryotubes were moved to the liquid nitrogen storage tank.

Human lung cancer cell lines

Every human lung cancer cell line was cultured, subcultured and frozen analogue to the LLC1. A summary of media, histological subtype and ATCC-Nr is provided in

Table 4.

Cell Line	ATCC-No.	Media	Histological subtype
A549	(ATCC® CRL-5800™)	DMEM/F12	Adenocarcinoma
H23	(ATCC® CRL-5800™)	DMEM/F12	Adenocarcinoma
H226	ATCC® CRL-5826™)	DMEM/F12	Squamous cell carcinoma
H460	(ATCC® HTB-177™)	RPMI 1640	Large cell lung cancer
H520	(ATCC® HTB-182™)	RPMI 1640	Squamous cell carcinoma
H661	(ATCC® HTB-183™)	RPMI 1640	Large cell lung cancer
H1299	(ATCC® CRL-5803™)	DMEM/F12	Adenocarcinoma
H1437	(ATCC® CRL-5872™)	RPMI 1640	Adenocarcinoma
H1650	ATCC® CRL-5883™)	RPMI 1640	Adenocarcinoma
H1975	(ATCC® CRL-5908™)	RPMI 1640	Adenocarcinoma

***Table 4* Human lung cancer cell lines**

DMEM/F12 media was supplemented for all cell lines with 10% FCS, 1% penicillin (100U/ml) /streptomycin (0.1 mg/ml), 1% vitamins, 1% Glutamine and 1% non-essential amino acids. RPMI 1640 was supplemented for all cell lines with 10% FCS, 1% penicillin (100U/ml) /streptomycin (0.1 mg/ml), 0.11 g/l NatriumPyruvat and 2.383 g/l HEPES ((4-(2-hydroxyethyl)-1-piperazineethanesulfonic acid).

For cell culture experiments or injections, a single cell suspension was prepared by trypsinizing cultured cells as above and resuspending them in fresh media. Cells were counted with a Neubauer counting chamber and viable cells were distinguished with trypan blue staining. The cell concentration was adjusted for the according experiment by dilution with the necessary amount of fresh media. DMEM/F12, RPMI1640, L-glutamine, vitamins, non-essential amino acids, HEPES, NatriumPyruvat, trypsin 10×, FCS, penicillin (100U/ml) /streptomycin (0.1 mg/ml), trypan blue stain, PBS 1×, all cell culture materials (e.g. cell culture flasks) were purchased from Gibco® life technologies, Grand Island, USA. DMSO was purchased from Sigma-Aldrich, St. Louis, USA.

3.1.2 Lentiviral transduction of LLC1

Lentiviral vectors (pLKO.1-puro) containing short hairpin RNAi against mouse CCR2 and CX3CR1 were obtained from Mission shRNA®, Sigma-Aldrich. Scramble shRNA and empty vector pLKO.1-puro vector (Addgene plasmid 8453) were used as a negative control. Lentivirus particles were produced by co-transfection of HEK293T cells (obtained from ATCC) with lentiviral plasmid and packing plasmid (psPAX2 and pMD2.G) using TurboFect transfection reagent (Fermentas). Supernatants were collected 72h after transfection (Stewart et al., 2003). Lentivirus titers were determined with the QuickTiters lentivirus titer kit, an HIV p24-based ELISA (Cell Biolabs), according to the supplier's procedure. LLC1 cells were cultured in 75 cm^2 flasks and transduced with lentivirus (multiplicity of infection (MOI) = 50) in the presence of 7 µg/ml polybrene (Sigma-Aldrich). Twenty-four hours after infection, medium was replaced with fresh medium for 48h and experiments were performed.

3.1.3 Generation of bone marrow derived MΦ

Bone marrow from the femur and tibia of 5- to 7-week old wild type (WT), $CCR2^{-/-}$ or $CX3CR1^{-/-}$ mice were isolated, erythrocyte-depleted and cultured for 10 days in RPMI 1640 (20% FCS, 1% penicillin/streptomycin) in the presence of 50 ng/ml recombinant murine macrophage stimulating factor (rmM-CSF, R&D Systems, Minnesota, USA) (*Figure 5*). After 10 days, cells were harvested and used for co-culture experiments described above. Purity and correct differentiation were screened by Flow cytometry (FACS) and immunocytochemistry.

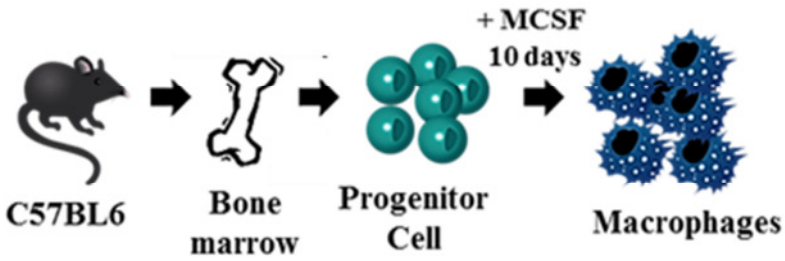

***Figure 5* Generation of bone-marrow derived macrophages**

3.1.4 Polarization of bone-marrow derived MΦ

To generate M1- or M2 polarized MΦ as a positive control for polarization studies or *in vivo* injection in mice, bone marrow generated MΦ were polarized *in vitro*. Two well established methods to generate MΦ are *in vitro* generation with either M-CSF (macrophage-colony stimulating factor) or GM-CSF (granulocyte/macrophage colony stimulating factor). Recent

data show that growth factors determine polarization of MΦ towards M1 (GM-CSF) or M2 (M-CSF), (Fleetwood et al., 2009). MΦ were generated with 20ng/ml rmGM-CSF (R&D Systems) and additionally treated with 100 ng lipopolysaccharide (LPS) from *E.coli* (Sigma-Aldrich) to obtain an M1-phenotype. To polarize the MΦ towards an M2-phenotype, MΦ were generated with 50 ng/ml rmM-CSF as described and stimulated with a combination of 10 ng/ml IL-4 and 10 ng/ml IL-13 (R&D Systems). Polarized MΦ were harvested and prepared for RNA-isolation or *in vivo* injection.

3.1.5 Generation of human monocyte derived MΦ

Buffy coats for isolation of peripheral blood mononuclear were obtained from the blood bank of the university hospital Gießen. The peripheral blood was mixed with culture media (DMEM/F12) in a 1:2 ratio. The mixed blood was carefully overlayed on Ficoll (BIOCOLL, Biochrom AG, Berlin, Germany). After a centrifugation without breaking for 20 min, the interphase of white blood cells was transferred in a new falcon with 5 ml media. After additional centrifugation (with breaks), cells were counted and prepared for antibody-mediated depletion of B-cells and T-cells.

Magenetic beads (Dynabeads®, life technologies) were washed three times with o.1% BSA in PBS. First, a CD2-antibody was added to deplete T-Cells. After incubation, cells were washed and Dynabeads were added. After an incubation of 30-45 min, the tube was placed in a magnet holder for 1 min and unbound cells were removed. In a second depletion step, CD19-antibody was added to remove B-Cells. After incubation, washing and addition of Dynabeads, the tube was placed in a magnet holder for 1 min and unbound cells were removed, washed and counted. Finally, cells were cultured in flasks in RMPI 1640, supplemented with 20% FCS and 20 ng/ml recombinant human M-CSF for 8-10 days (rhM-CSF, R&D Systems). For experimental use, MΦ were gently harvested with a rubber cell scraper (Sarstedt, Inc.; Newton, USA), washed and seeded for the according experiment.

3.1.6 Co-culture

Co-culture of LLC1 and MΦ from either WT, $CCR2^{-/-}$ or $CX3CR1^{-/-}$ mice was performed using a transwell system with a 6-well layout. First, LLC1 cells were seeded on inverted transwells (pore size 8 µm, BD BioSciences, Franklin Lakes, USA), left two hours to attach

and placed in companion plates (BD Biosciences). After 24 h MΦ were seeded in new companion plates and combined with the LLC1-populated transwells (*Figure 6*).

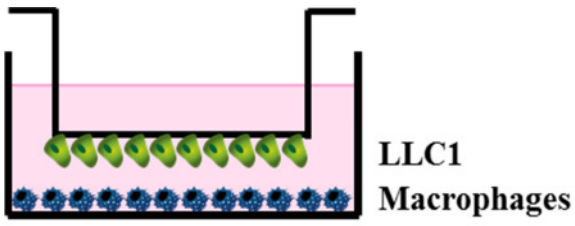

***Figure 6* Co-culture of LLC1 with macrophages**

LLC1 and MΦ were seeded separately as controls. All cells were cultured in RPMI-1640 supplemented with 1% FCS and penicillin (100U/ml) /streptomycin (0.1 mg/ml). After 12 h and 24 h, the supernatant (conditioned media; CM) was harvested, centrifuged, filtered and stored at –80°C for further experiments. Additionally, each cell type was harvested separately from the transwell filters (LLC1) or the companion plate (MΦ) and prepared for RNA-isolation. This resulted in following samples:

A. **conditioned media (CM)**: MΦ alone, LLC1 alone, co-culture of LLC1 and MΦ.

B. **mRNA**: MΦ alone, LLC1 alone, co-cultured LLC1 and co-cultured MΦ.

Each sample set was replicated at 3-5 times from co-cultures with MΦ from WT, $CCR2^{-/-}$ and $CX3CR1^{-/-}$ mice.

Human cancer cells were co-cultured analogue to LLC1 with human MC-derived MΦ for 24 h. All human cancer cells and MΦ were cultured in DMEM/F12 supplemented with 1% FCS and penicillin (100U/ml) / streptomycin (0.1 mg/ml). After co-culture, CM and each cell type were collected as described for LLC1/ MΦ co-cultures for further analysis.

3.1.7 Flow cytometry

Multiparameter flow cytometer analysis of MΦ was performed using a FACSCanto flow cytometer equipped with DIVA software (BD Biosciences). Cells ($5x10^{5)}$ were fixed for 15 minutes in cold 1% paraformaldehyde and incubated with fluorochrome labeled antibodies (CD45-APC-Cy7, GR-1-PE-Cy7, CD11b-PE, CD11c-PerCP-Cy5.5, F4/80-APC, MHC II-FITC, all BD Biosciences) for 20 min at 4°C. After two washes in FACS buffer ($PBS^{-/-}$

supplemented with 7.4 % EDTA and 0,5 % FCS) the cells were subjected to flow cytometric quantification of MΦ(CD45$^+$ GR$^{1low/neg}$ CD11b$^+$ CD11c$^+$ F4/80$^+$ MHC II^{low}).

3.1.8 RNA isolation, DNaseI treatment, cDNA-synthesis, real time RT-PCR

RNA was isolated using Trizol® Reagent (Invitrogen, Carlbad, CA, USA) according to manufacturer`s instructions. Trizol® is based on the method of Chomczynski and Sacchi and contains guanidiniumthiocyanate for cell lysis and inactivation of RNAses and phenol to dissolve DNA and protein. After phaseseparation by addition of chloroform and centrifugation, total RNA was precipitated with isopropanol from the resulting aqueous phase. Concentration and purity of the RNA was measured with NanoDrop (Peqlab Biotechnologie GmbH, Erlangen, Germany) and integrity of RNA was monitored with 1% agarose gels.

To avoid any DNA contamination in the real time RT-PCR reactions, all RNA-samples were treated with DNaseI under following conditions:

RNA [0.1 µg/µl]	**µl**
DEPC-H_20	30 µl – X
MasterMix	1
Buffer	4
RNAse Inhibitor	1
DNAseI	4

Table 5 **DNAseI treatment**

All samples were incubated at 37°C for 30 min. In the last step, 4 µl EDTA (25 mM) were added and each tube was incubated for 10 min at 65°C to inactivate DNAseI. All reagents were purchased from Fermentas (Waltham, USA). A total of 800 ng of total RNA was reverse transcribed using the ImPromII-Kit (Promega, Madison, USA) according to supplier's instructions.

Real time RT-PCR was performed with the Platinum®SYBR®Green qPCR SuperMix-UDG (Invitrogen, *Life Technologies*, Grand Island, USA) and the following conditions:

Master Mix	Volume	Final concentration
Platinum®SYBR®Green qPCR SuperMix-UDG	12.5 µl	1x
$MgCl_2$ [50mM]	1 µl	5 mM
Forward primer [10µM]	0.5 µl	0.1 µM
Reverse primer [10µM]	0.5 µl	0.1 µM
ROX reference dye [25µM]	0.1 µl	0.1 µM
cDNA [0.25µg/µl]	2 µl	0.5 µg
DEPC-H_2O	8.4 µl	
Gesamt	25 µl	

Table 6 **real-time RT-PCR master mix.**

Time [min]	Temperature [°C]	Cycles
10:00	95	1
0:30	95	40
1:00	58-60	
0:30	72	
10:00	95	1
0:30	55	
0:30	95	

Table 7 **Real-time RT-PCR conditions**

All real time RT-PCR reactions were performed on the Stratagene Mx3005P with the MxPro software and the program "SYBR Green with Dissociation curve" to confirm the specificity of each primer. PCR products were seperated on a 3% agarose gel, to confirm that every primer yielded one specific product. All primer pairs were blasted with the NCBI primer blast tool (http://www.ncbi.nlm.nih.gov/tools/primer-blast/) and purchased from Metabion (Metabion GmbH, Martinsried, Germany). Tables 8 and 9 provide all primer sequences, annealing temperatures and product sizes.

Gen Bank Accession	Name	Forward Primer 5'→3' Reverse Primer 5'→3'	product size	annealing temp.[°C]
NM_007482.3	Arginase	GGTTCTGGGAGGCCTATCTT CACCTCCTCTGCTGTCTTCC	127	58
NM_011333.3	CCL2	TTAAAAACCTGGATCGGAACCAA GCATTAGCTTCAGATTTACGGGT	121	60
NM_009915.2	CCR2	TCCTTGGGAATGAGTAACTGTGT TGGAGAGATACCTTCGGAACTT	142	60
NM_009914.4	CCR3	CAGATACCTGGCTATCGTCCA GGCTCGAAGGGCAAACACA	43	60
NM_009892.2	Chitinase	CCCTGGGTCTCGAGGAAGCCC GCAGCCTTGGAATGTCTTTCTCCAC	113	58
NM_011045	CX3CL1	CCAGAGCTGGCAATAACCTA GGCATACAGGGTACGATCTG	193	58
NM_009987	CX3CR1	GTGACATGAAGAGGGACCTG CCCTCGCTTGTGTAGTGAGT	247	58
NM_013556.2	HPRT	GCTGACCTGCTGGATTACAT TTGGGGCTGTACTGCTTAAC	242	58
NM_010548.2	IL-10	CAGAGAAGCATGGCCCAGA TGCTCCACTGCCTTGCTCTTA	130	58
NM_031167.5	IL-1RA	TCCTGTTTAGCTCACCCATGG CCAGCAATGAGCTGGTTGTTT	136	58
NM_008361.3	IL-1β	ACCCCAAAAGATGAAGGGCTG TACTGCCTGCCTGAAGCTCT	112	58
NM_031168.1	IL-6	TCTCTGCAAGAGACTTCC AGTAGGGAAGGCCGTGGTTGT	90	58
NM_008611.4	MMP 8	GGCCCTTCCTACCCAACGGT AGAGCCCAGTACTGTCTGCCTTT	91	58
NM_013599.2	MMP 9	ACGGGTATCCCTTCGACGGC AGTGGGGATCACGACGCCTTT	131	58
NM_011045	PCNA	GGGTTGGTAGTTGTCGCTGT TCCAGCACCTTCTTCAGGAT	172	58
NM_013693.2	TNFα	CATCTTCTCAAAATTCGAGTGACAA TGGGAGTAGACAAGGTACAACCC	175	58
NM_001025257.4	VEGFa	GGCCTCCGAAACCATGAACTT TGGGACCACTTGGCATGGT	87	58
NM_001185164.1	VEGFb	AGCCAGACAGCCCCAGGAT AGCAGCTTGTCACTTTCGCG	176	58
NM_009506.2	VEGFc	ACCTCCATGTGTGTCCGTCT TTCAAACAACGTCTTGCTGAGG	103	58
NM_010810.4	MMP 7	AGCTTCCCCTTTGATGGGCCA GGAAGTTCACTCCTGCGTCCT	130	58
NM_001081117	Ki67	CTCCACGAACCTCAAAGAGA TGTGGATTCCTTCACACCTT	164	58
NM_019471.2	MMP 10	TGAGAAATGGACACTTGCACCCTC ACCGGCTCCATACAGGGATTGAAT	199	58
NM_008606.2	MMP 11	CTTCGCCAGGTACTGGCATGGTG TGGCCAAATTCATGAGCCGCC	183	58
NM_008607.2	MMP 13	AGCAGTTCCAAAGGCTACAACTTGT GGGTTGGGTCTTCATCGCCT	199	58
NM_008610.2	MMP 2	GTCCCGAGACCGCTATGTCCA ACACCTTGCCATCGTTGCGG	126	58
NM_010809.1	MMP 3	TCCCTCTATGGAACTCCCACAGCA GGAGTCCTGAGAGATTTGCGCCA	185	58
NM_010927.3	iNOS	CACCAAGCTGAACTTGAGCG CCATAGGAAAAGACTGCACCG	105	58

Table 8 **Murine real-time RT-PCR primers.**

Gen Bank Accession	Name	Forward Primer 5'→3' Reverse Primer 5'→3'	product size	annealing temp.[°C]
NM_002982.3	CCL2	CAGCCAGATGCAATCAATGCC TGGAATCCTGAACCCACTTCT	190	58
NM_001123396	CCR2	TGTCCACATCTCGTTCTCGGT CCGCTCTCGTTGGTATTTCTGA	46	58
NM_002996.3	CX3CL1	CAAACGCGCAATCATCTTGG ATTTCGAGTTAGGGCAGCAG	121	58
NM_001171174.1	CX3CR1	ATATTGGGGACATCGTGGTCT TGGCAAAGATGACGGAGTAGA	66	58
NM_000194.2	HPRT	TGACACTGGCAAAACAATGCA GGTCCTTTTCACCAGCAAGCT	94	58

Table 9 **Human real-time RT-PCR primers**

3.1.9 Immunocytochemistry (ICC)

LLC1 (20.000) or MΦ (50.000) cells were seeded on 8-well glass chamber slides (BD Biosciences) and cultured for 24 h. LLC1 cells were stimulated with either control or co-culture CM and incubated for another 24 h. MΦ were directly subjected to ICC. Cells were fixed in ice cold methanol/acetone (1:1) (Roth, Karlsruhe, Germany), washed and blocked with blocking buffer (5% BSA, 0.5 % serum, according to secondary antibody (AB), 0.2% Triton-X in PBS), and incubated over night with the primary AB. After washing and incubation with the secondary AB, the slides were incubated with DAPI (Dako, Glostrup, Denmark) for nuclear counterstaining and mounted with fluorescence mounting media (Dako). Pictures were taken with the same gain and exposure time dependent on the primary AB. Fluorescence pictures were taken with the Leica DM6000B equipped with the Image Analysis & Processing Software for Quantitative Microscopy Leica QWin (Leica Microsystems GmbH, Wetzlar, Germany).

Antibody	Species/reactivity	Company, Catalogue-No.	Antigen-retrieval	Dilution
Alexa488® (2°)	Goat anti-rat and Goat anti-rabbit	Invitrogen A-11034; A-11006	-	1:1000
Alexa594® (2°)	Goat anti-rat and goat anti-rabbit	Invitrogen A-11012; A-11007	-	1:900
CCR2	Rabbit anti-mouse	Abcam; ab32144	Citrate ProteinaseK	1:100

Antibody	Species/reactivity	Company, Catalogue-No.	Antigen-retrieval	Dilution
CD11b	Rat anti-mouse	Millipore; MAB1387Z	Trypsin	1:200
CD68	Rat anti-mouse	AbD Serotec; MCA1957	Citrate	1:200
CX3CR1	Rabbit anti-mouse	NOVUS; NBP1-76949	Citrate	1:100
F4/80	Rat anti-mouse	Abcam; ab6640	Trypsin ProteinaseK	1:100
MoMa2	Rat anti-mouse	AbD Serotec; MCA519G	just ICC	1:200
PCNA	Rabbit anti mouse	Santa Cruz Biotechnology; Sc7907	Citrate	1:150

Table 10 **Antibodies**

3.1.10 Migration assay

Chemotactic migration was quantified using a Boyden chamber transwell assay (8µm pore size; uncoated filters; BD Biosciences). Either control (MΦ or LLC1 alone) or co-culture-CM (from 12 h and 24 h co-culture) was provided in the lower part of the chamber, LLC1 cells (4×10^4) were introduced into the upper chamber and left to migrate for 8 h. Additional controls were performed with media containing 0%, 1% or 20% FCS. The cells were fixed with methanol (Roth, Germany) and stained with crystal violet (Sigma-Aldrich, USA) and migrated cells in fifteen randomly chosen fields per filter were counted. Images were taken with the Leica Dm6000B using 20× magnification. The migration assay was repeated with 3-5 different co-cultures per MΦ genotype (WT, $CCR2^{-/-}$, $CX3CR1^{-/-}$), and each experiment was performed in triplicate.

3.1.11 Proliferation assay

Proliferation assays were performed with serum starved LLC1 cells exposed for 24 h to either control or co-culture-CM (12 h, 24 h). After incubation for 20 h, BrdU (bromdesoxyuridin) was added and its incorporation was detected using an HRP-coupled antibody by measuring the absorption of the HRP-substrate at 370 nm, according to the manufacturer's instructions

(Cell Proliferation ELISA, BrdU colorimetric, Roche,). Detection was performed with the Tecan infinite M200 Pro.

3.1.12 ELISA (enzyme-linked immunosorbent assay)

Mouse CCL2 and CX3CL1 levels were quantified in either control or co-culture-CM (12 h and 24 h) as well as in plasma levels of tumor-bearing WT, $CCR2^{-/-}$ and $CX3CR1^{-/-}$ mice with the Mouse CCL2/JE/MCP-1 Quantikine ELISA Kit and the Mouse CX3CL1/Fractalkine Quantikine ELISA Kit, respectively, according to the manufacturer's instructions. Human CCL2 in control or co-culture CM (24 h) was measured with the Human CCL2/MCP-1 Quantikine ELISA Kit (all R&D Systems).

The final colorimetric reaction was detected at 450 nm using the Tecan infinite M200 Pro and quantified using the Magellan V7.0 software (Tecan Group Ltd, Männedorf, Switzerland).

3.1.13 Cytokine arrays

Cytokine arrays (mouse cytokine antibody array, panel A, R&D Systems, Minnesota, USA) were performed to detect secreted mediators in either co-culture or control medium or plasma of tumor bearing mice. Samples of CM of LLC1, MΦ and co-culture or plasma of WT, $CCR2^{-/-}$ and $CX3CR1^{-/-}$ mice were incubated with the *Panel A Detection Antibody Cocktail* (Biotin-labeled). Nitrocellulose membranes spotted with capture antibodies against 40 different cytokines, as well as positive and negative controls, were first blocked and subsequently incubated with the prepared samples. The AB-Cytokine-AB-coupling reaction was detected by adding a streptavidin-HRP solution followed by incubation with *Chemi Reagent Mix.*. The reactions were visualized with Amersham Hyperfilm ECL films (GE Healthcare Europe GmbH, Freiburg, Germany). Analysis and quantification was performed with the BioDoc Analyze Software from Biometra.

3.2 Experimental procedures – *in vivo*

3.2.1 Mouse lines

Wildtype (WT) C57/Bl6 mice were obtained from Charles River GmbH, Sulzfeld, Germany. All knock out lines were obtained from The Jackson Laboratories, Maine, USA, and

maintained under pathogen-free conditions according to the European Communities recommendations for experimentation after approval by local authorities (animal proposal no. V54-19c20/15-B2/288).
Additionally, the following gene-manipulated mice were used for experimental analysis:

B6.129S4-Ccr2^{tm1Ifc}

The generation and characterization of this mouse line was previously described (Boring et al., 1997). Mice homozygous for the CCR2-deletion, show an abnormal leukocyte trafficking, especially impaired migration of myeloid-derived cells, e.g. MΦ. These mice also show a decreased acute inflammatory reaction with decreased MΦ infiltration.

B6.129P-Cx3cr1^{tm1Litt}

These mice were created with an enhanced GFP-expressing target vector that disrupted exon 2 of the coding region of the CX3CR1 gene. As a consequence, all CX3CR1-expressing cells exhibit green fluorescence. The mice display abnormal leukocyte-chemotaxis, in particular, the migration of monocytes and NK-cells is impaired. A more detailed description of the generation of this mouse strain was previously described (Jung et al., 2000).

C57BL/6-Tg(Csf1r-EGFP-NGFR/FKBP1A/TNFRSF6)2Bck/J

These transgenic mice carry an inducible Fas suicide/apoptotic gene driven by the mouse *Csfr* (macrophage colony stimulating factor receptor 1) promoter. The gene construct (containing an IRES sequence, human low affinity nerve growth factor receptor [ΔLNGFR], two copies of the 12kDa human FK506 binding protein 1A [FKBP12], and the intracellular domain region of the *Fas* gene) was inserted immediately downstream of the enhanced Green Fluorescent Protein (EGFP) gene (*Figure 7*). The resulting transmembrane protein binds the dimerization drug AP20187 (ClonTech, Takara holdings Inc., Kyoto, Japan) and induces apoptosis in MΦ and MΦ-derived DCs, resulting in an MΦ-depleted mouse. Seven days after cessation of treatment, the MΦ and MΦ-derived Dc populations undergo regrowth. The generation and characterization of this mouse strain was previously described (Burnett et al., 2004). These mice are referred to as MaFIA-(**Ma**crophage **F**as **I**nduced **A**poptosis)-mice.

Figure 7 **MaFIA Transgene**

3.2.2 Genotyping

B6.129S4-Ccr2^{tm1Ifc}

Following primer pairs detected CCR2-deletion:

Primer	Forward Primer 5'→3' Reverse Primer 5'→3'	Band size
Wildtype	CCACAGAATCAAAGGAAATGG CCAATGTGATAGAGCCCTGTG	424 bp
Mutant	CTTGGGTGGAGAGGCTATTC AGGTGAGATGACAGGAGATC	280 bp

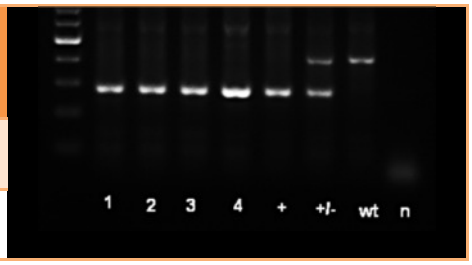

***Table 11* CCR2 Genotyping primer and band sizes**; (1-4) homozygous CCR2$^{-/-}$ mice, (+) positive control , (+/-) heterozygous mouse, (wt) wildtype, (n) negative control.

Sample preparation		
Reaction Component	**Volume [µl]**	**Final Concentration**
ddH2O	4.75	-
Buffer	12.5	1.00 X
25 mM MgCl2	0.5	2.00 mM
DMSO	1.25	0.20 mM
each Primer	1.25	1.00 uM
DNA	1.00	-

PCR		
Temp [°C]	**Time [sec]**	**Cycles**
95	120	1
95	15	
59	15	35
72	60	
72	120	1
4	∞	1

***Table 12* CCR2 Genotyping RT-PCR conditions**

PCR for genotyping was carried out with the reagents (KAPA Genotyping HOT Start Kit, peqlab Biotechnologie GmbH, Erlangen, Germany) and conditions listed in table 11 and 12.

B6.129P-Cx3cr1^{tm1Litt}

Following primer pairs detected CX3CR1-deletion:

Primer	Forward Primer 5'→3' Reverse Primer 5'→3'	Band size
Wildtype	GTCTTCACGTTCGGTCTGGT CCCAGACACTCGTTGTCCTT	410 bp
Mtant	CTCCCCCTGAACCTGAAAC CCCAGACACTCGTTGTCCTT	500 bp

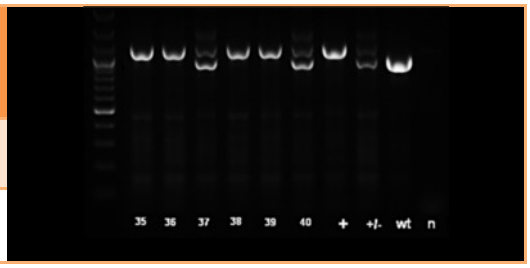

Table 13 **CX3CR1 Genotyping primer and band sizes; (35, 36,38,39) homozygous CX3CR1$^{-/-}$ mice, (37,40) heterozygous mice, (+) positive control, (+/-) heterozygous control, (wt) wildtype, (n) negative control.**

PCR for genotyping was carried out with following reagents (KAPA Genotyping HOT start Kit, peqlab Biotechnologie GmbH, Erlangen, Germany) and conditions:

Sample preparation		
Reaction Component	**Volume [µl]**	**Final Concentration**
ddH2O	6	-
Buffer	12.5	1.00 X
25 mM MgCl2	0.5	2.00 mM
DMSO	1.25	0.20 mM
each Primer	1.25	1.00 uM
DNA	1.00	-

PCR		
Temp [°C]	**Time [sec]**	**Cycles**
94	180	1
94	30	
65	30	35
72	60	
72	120	1
4	∞	1

Table 14 **CX3CR1 Genotpying RT-PCR conditions.**

C57BL/6-Tg(Csf1r-EGFP-NGFR/FKBP1A/TNFRSF6)2Bck/J

Following primer pairs detected MaFIA-transgene insertion:

Primer Type	Forward Primer 5'→3' Reverse Primer 5'→3'	Band size
Internal control	CTAGGCCACAGAATTGAAAGATCT GTAGGTGGAAATTCTAGCATCATCC	324 bp
Mutant	AAGTTCATCTGCACCACCG TCCTTGAAGAAGATGGTGCG	173 bp

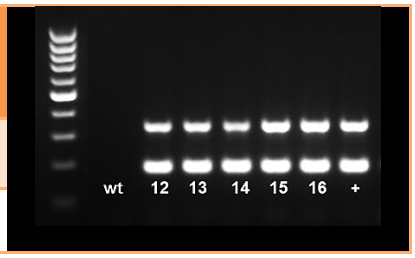

Table 15 **MaFIA Genotyping primer and band sizes,** (wt) wildtype, (12-16) mice positive for MaFIA-transgene, (+) positive control.

PCR for genotyping was carried out with following reagents (RED Taq Ready Mix. Sigma Aldrich, St. Louis, USA) and conditions:

Sample preparation		
Reaction Component	**Volume [µl]**	**Final Concentration**
ddH2O	7.8	-
Buffer	10	1.00 X
each Primer	0.3	1.00 uM
DNA	1.00	-

RT-PCR		
Temp [°C]	**Time [sec]**	**Cycles**
95	**180**	**1**
95	**30**	
60	**30**	**35**
72	**60**	
72	**120**	**1**
4	∞	**1**

Table 16 **MaFIA Genotyping RT-PCR conditions.**

3.2.3 MΦ -depletion with clodronate-liposomes or AP20187

MΦ were depleted in vivo with either clodronate liposomes (CLs) or AP20187 in MaFIA-mice. CLs (obtained from www.clodronateliposomes.org) are ingested by MΦ via endocytosis and after fusion with lysosomes in the cytoplasm of MΦ, clodronate is released and induces apoptosis via inhibition of the mitochondrial ADP/ATP translocase. CLs are unable to pass vascular barriers, e.g. after orotracheal aspiration, alveolar MΦ are depleted in the lung but not alveolar interstitial MΦ. The preparation and detailed analysis of tissue distribution has been previously described (van Rooijen and van Kesteren-Hendrikx, 2002). Control mice were treated with PBS Liposomes.

AP20187 was dissolved in 100% ethanol in a concentration of 62.5 µg/µl as a stock solution. 30 min prior to injection, the stock solution was diluted to 2.5 µg/µl with dilution buffer (1.7% Tween-20, 1% PEG-400 and 0.9% NaCl). Mice were balanced and injected at a dose of 10 mg/kg bodyweight, and the final injection volume was adjusted to 100 µl using a dilution buffer. Control mice were peritoneally injected with 100 µl dissolvent without AP20187.

For analysis of tumor growth in CL MΦ depleted- or in MaFIA mice, daily intraperitoneal pretreatment with either CL in WT-mice or AP20187 (ClonTech), respectively, was started 4 days prior to LLC1 injection, followed by continuous intraperitoneal and intratumoral injections every 4th day. Experimental schemes are provided in the according results section.

3.2.4 Syngeneic subcutaneous model of lung cancer

Primary tumor growth from LLC1 was monitored as described in (Savai et al., 2007). Briefly, 1×10^6 LLC1 cells were subcutaneously injected (24g needle, 0.55 × 25 mm, Neolus, Terumo Europe, Leuven, Belgium) subcutaneously into C57BL/6 WT, or MΦ-depleted mice (CL or MaFIA). Tumor growth was measured every 4 days with digital calipers. At day 21 mice were sacrificed and tumor, lung, liver and spleen were balanced and analyzed for FACS, immunohistochemistry or molecular biology techniques.

3.2.5 Syngeneic metastatic model of lung cancer (tumor relapse model)

Primary tumor growth was initiated as described above in WT, $CCR2^{-/-}$, $CX3CR1^{-/-}$ and CL treated mice. After 10 days, mice were intubated and anaesthetized using isoflurane anesthesia (Forane, Baxter, Deerfield, USA) with 4-5% to initiate and 2-3% to obtain anesthesia. Skin covering the subcutaneous (s.c) tumor was shaved and disinfected with 70% ethanol, Metamizol (200 mg/kg bodyweight) was subcutaneously injected for preoperative analgesia. The s.c. tumor was extracted and the wound sewed (Vicryl*Plus Absorbable, RB-1 plus, 17mm ½ c, Johnson&Johnson Intl., St-Stevens-Woluwe, Belgium). Postoperative analgesia was obtained using Metamizol (200 mg/kg bodyweight) in drinking water. All mice were intensively observed over a following period of 20-40 days. Tumor metastasis in the lung was evaluated by MRI (magnetic resonance imaging) on days 20 and 30. After the mice were sacrificed, according to humane endpoints (scoring sheet), the lungs (after perfusion), liver and spleen were extracted and photographed. All macroscopic nodules (≥ 1 mm) were counted and measured with digital calipers. All organs were fixed in 4% PFA for immunohistochemistry.

3.2.6 Tumor digestion for FACS analysis

To prepare subcutaneous tumors for flow cytometric analysis of infiltrating MΦ, extracted tumors were placed in 35 × 10 mm petri dishes (Greiner Bio-one, Frickenhausen, Germany) and cut in small cubes (< 1 mm^3) with a scalpel. Two ml of a digestion solution of 0.2 mg/ml collagenase-D (Roche Diagnostics, Mannheim, Germany), 1 mg/ml pronase (Roche Diagnostics, Mannheim, Germany) and 2 µl DNAseI (400 U/ml, Promega, Madison, USA) were added, and samples were incubated for 40 min at 37°C on a shaker. The digested tissue was resuspended in 10 ml PBS with 10% FCS to stop the digestion reaction and centrifuged

for 5 min with 1600 rpm. The pellet was washed with PBS and passed through a 40 µm cell strainer (BD Biosciences) and cells were counted. The cell suspension was then centrifuged, resupended in 1 ml ice-cold 1% PFA per 10^6 cells, and fixed for 15 min on ice. After centrifugation, cells were prepared in FACS buffer ($PBS^{-/-}$, 0.15% EDTA, 10% FCS, pH 7.2) for staining and flow cytometry (see point *3.1.7*). EDTA solution was purchased from Biochrom AG, Berlin, Germany.

3.2.7 Histology

3.2.7.1 Hematoxylin and eosin staining

Sections (3 µm) from paraffin embedded tissues were first rehydrated with a continuous xylol-ethanol 99%- ethanol 90%- ethanol 70% row. After washing in distilled H_2O, slides were incubated in fresh hematoxylin (Merck, Darmstadt, Germany) for 15 min and washed in distilled H_2O until was removed from the tissue. Next, the slides were incubated with freshly prepared eosin (Merck, Darmstadt, Germany) for 1 min. The slides were washed in ddH_2O again, dehydrated with ascending ethanol concentrations (70%, 90%, 99%) and finally mounted with Pertex Mounting Media (Leica Biosystems, Wetzlar, Germany. Pictures of whole H&E stained sections were acquired with the microscope SteREO Discovery. V8 microscope, equipped with the software AxioVision4.7.1 software. (Carl Zeiss AG, Oberkochen, Germany)

3.2.7.2 Immunohistochemistry (IHC)

For IHC staining, 3 µm sections were rehydrated and antigen retrieval was achieved with citrate buffer/heat, trypsin- or proteinase-K treatement as indicated in

Table 10. After blocking (5% BSA, 0.2% Triton-X, 0.5 % serum according to secondary AB), sections were incubated with the following primary antibodies: F4/80, CD11b or PCNA. Indirect immunofluorescence was conducted by incubation with Alexa488- or Alexa594-conjugated secondary antibodies (Invitrogen). Nuclei were counterstained with DAPI, and sections were mounted with fluorescent mounting media (Dako). All fluorescence images were acquired with the same exposure time in 40× and 20× magnification with a Leica DM6000B microscope equipped with the Image Analysis & Processing Software for Quantitative Microscopy Leica QWin (Leica Microsystems GmbH, Wetzlar, Germany). Positive cells were quantified from 15 randomly taken pictures per slide and calculation of the positive/total cell ratio.

3.2.8 µ-computed tomography (µCT)

3.2.8.1 Animal preparation

Animals were euthanized with a fatal dose of inhaled isoflurane and fixed in supine position. After thoracotomy, the left ventricle was cannulated with a 24 G needle and the right atrium was incised. 10 ml of heparinized saline were injected until the effluent from the right ventricle was free from blood. The injection rate was 0.3 ml/s, mimicking a physiological minute volume of 18 ml. Next, 10 ml of Microfil (Microfil® MV-122; Flow Tech, Carver, MA, USA), a plumbiferous intravasal polymerizing contrast agent, was injected at the same injection rate. Tumors were excised 45 min after injection with a sufficient intravasal hardening of the contrast agent and fixed in neutral buffered formaline.

3.2.8.2 µ-CT imaging

Tumors were wrapped in parafilm to prevent dehydration and scanned in a micro-computed tomograph (micro-CT; SkyScan (SkyScan1072_80 kV, Kontich, Belgium). The system is equipped with a microfocus tube (20-80 kV, 0-100 µA) reaching a minimum spot size of 8 µm at 8 W generating X-rays in cone-beam geometry and was described in detail (Langheinrich et al., 2004). The detector consists of a 1024 × 1024 pixel matrix with a 12 bit digital CCD high-resolution camera and digital frame-grabber. For this study, tube voltage was chosen at 75 kV with a beam hardening filter of 0.5 mm aluminium. To obtain an optimal resolution, geometric magnification, i.e. spatial resolution, was chosen individually depending on the tumor size. Side length of the resulting isotropic pixels was between 14 and 18 µm. Cross sectional images were reconstructed using a modified Feldkamp cone-beam reconstruction algorithm with a grey scale resolution of 8 bit (0-255).

3.2.8.3 nano-CT imaging

Cubic specimens of 5 mm side length were excised from well-perfused tumor areas as predetermined from the previous acquired micro-CT data sets. Specimens were stored in parafilm and scanned using nano-computed tomography (SkyScan 2011, Kontich, Belgium). The system is equipped with an open pumped type X-ray source, a LaB6 cathode, and a transmission anode consisting of a tungsten coated beryllium window. Superior edge sharpness is reached by a high focussed X-ray spot of 300 nm side length. Tube voltage was 70 kVp. The system was previously described in detail (Langheinrich et al., 2010). Cross sectional images were reconstructed with a modified Feldkamp cone-beam reconstruction

algorithm. Image resolution of the cross sectional images was 6 µm isotropic voxel side length with the same grey scale resolution of 8 bit.

3.2.8.4 Quantification

1) Micro-CT data sets

Measurements of tumor size and whole tumor vascularization were performed using the Analyze 10.0 software package (Biomedical Imaging Resource, Mayo Clinic, Rochester, MN, USA). Thresholding for object identification (air + wax vs. tumor tissue vs. vascularization) was adapted to the grey level of the compartments and carried out semi-automated. Tumor volume and vascular volume were determined. Vascular volume fraction (VVF) was measured according to the following:

VVF (%) = 3D CAV/ 3D TV × 100 %;

with 3D_CAV (total contrast agent volume) representing the sum of all voxels tagged as contrast agent and 3D_TV (tumour volume) representing the volume of the entire specimen.

2) Nano-CT data sets:

Vascular morphometry was evaluated using the CTAn-Software package (SkyScan, Kontich, Belgium). Morphometric parameters were determined after binarization using an adaptive method for a more precise segmentation of vessels with suppression of typical nano-CT artifacts. The following parameters were determined for binarized 3D data sets: Vascular volume fraction (VVF), mean vascular thickness (ST.Th), mean vascular separation (Sr.Sp) and structure linear density (Sr.Li.Dn). Mean vascular thickness and mean vascular separation are image editing algorithms which identify the centreline of a vessel or the intervascular space (tissue) and measure the radius of the described structure by placing virtual spheres along the centreline which fit into the depicted structure. Structure linaer density describes the number of traversals of vascular structures along any linear distance in the volume by measuring the inverse of the mean centre line distances.

3.2.9 Magnetic resonance imaging (MRI)

MRI measurements were performed on a 7.0 T Bruker Pharmascan equipped with a 300mT/m gradient system and using a custom-built circularly polarized birdcage resonator. The frequency for the ^{1}H isotope is 300.33 MHz. Localizer images were acquired by spin echo sequence (repetition time, TR = 205 ms; echo time, TE = 10 ms; slice thickness = 5 mm) with

three orthogonal slices (axial, coronal and sagittal) for rough positioning. RARE-(Rapid Acquisition with Relaxation Enhancement) sequences in axial, coronal and sagitall orientation (TR = 2500 ms, TE = 36.7 ms and slice thickness = 1 mm) were used to verify a strictly symmetric positioning of the mouse. For reducing inhomogeneity in the region of the lung a correction of the shim on the basis of a B_o field map was executed. For lung imaging we employed the respiratory gated UTE 3D- (Ultra-Short-Echo Time) sequence (TE = 20 µs; TR = 8.0 ms; FOV = 2.5 × 2.7 ×5.0 cm^3; matrix = 128×128×128; slice thickness = 0.39 mm) for WT, PBS-treated and $CCR2^{-/-}$ mice or the respiratory gated ZTE- (Zero Echo Time) sequence (TE = 0 µs; TR = 4,0 ms; FOV = 3,0x3,0x4,0 cm^2; matrix = 256x256; slice thickness = 0,16 mm) for CL-depleted and $CX3CR1^{-/-}$ mice. Mice were measured under volatile isoflurane (1.5 – 2.0 % in oxygen and air with a flow rate of 1.0 L/min) anesthesia; the body temperature was maintained at 37°C by a thermostatically regulated water flow system during the entire imaging protocol.

3.3 Data analysis

Statistical analyses were performed with the GraphPad Prism 5 Software following the guidelines found in GraphPad Prism. One-way ANOVA followed by Tukey's posttest was used to compare the means of more than two independent groups; two independent groups were compared with the Student's t test. All sample sizes were tested for Gaussian distribution and subjected to Grubbs' outlier test. Data are expressed mean ± SEM; statistical significance was set at $p \leq 0.05$. Significance level is noted as follows: * $p \leq 0.05$, ** $p \leq 0.01$, ***$p \leq 0.001$.

4 Results

4.1 Systemic depletion of MΦ in mice

4.1.1 CL mediated depletion of MΦ in primary tumor growth

MΦ are involved in various processes in tumor progression and metastasis (Pollard, 2004). However, long-term studies with a systemic depletion of MΦ are lacking. We depleted MΦ in C57/Bl6 mice bearing s.c. LLC1 tumors with CL, which specifically kill phagocytosing MΦ after engulfment of liposomes and accumulation of clodronate in their cytoplasm (Van Rooijen and Sanders, 1994). To ensure a complete MΦ depletion during tumor initiation and formation, we started MΦ depletion 4 successive days prior to LLC1 injection. Since the MΦ population starts to regenerate within seven days, we injected clodronate or PBS liposomes i.p., respectively, every 4^{th} day to maintain the systemic depletion (*Figure 8A*). To specifically target the TAM, we additionally injected CL directly in the tumor.

The chronic systemic MΦ depletion resulted in the expected significantly inhibited primary tumor growth from day 16 (1158.86 ± 143.13 mm^3 in the control group vs. 551.00 ± 94.784 mm^3 in CL-treated group) and was finally reduced about 56% from a volume of 3284.447 ± 176.48 mm^3 to 1452.55 ± 168.767 mm^3 compared to control (PBS-Liposomes). The weight of extracted tumors (day 21) was significantly decreased from 4.00 ± 0.4359 g to 1.667 ± 0.2140 g in the CL-treated group. Since the measurement with digital calipers also measures additionally skin and hair of the mice, we confirmed the significant difference in the tumor volume between the groups with a more exact µCT measurement of the extracted tumors, although the occurring error with digital calipers can be assumed to be a systemic error (*Figure 8B-E).*

Surprisingly, both groups showed no difference in gain of body weight. Whereas the control group still gained 4.23 ± 0.189 g in average, the CL-treated mice gain just 1.87 ± 0.491 g. Since the gain of weight includes also the weight of the growing tumor, these values don't represent a normal gain of weight due to growth. This might be a hint, that an unspecific targeting of the entire MΦ-population can decrease the primary tumor growth, but is eventually not beneficial for the mice (*Figure 8*F).

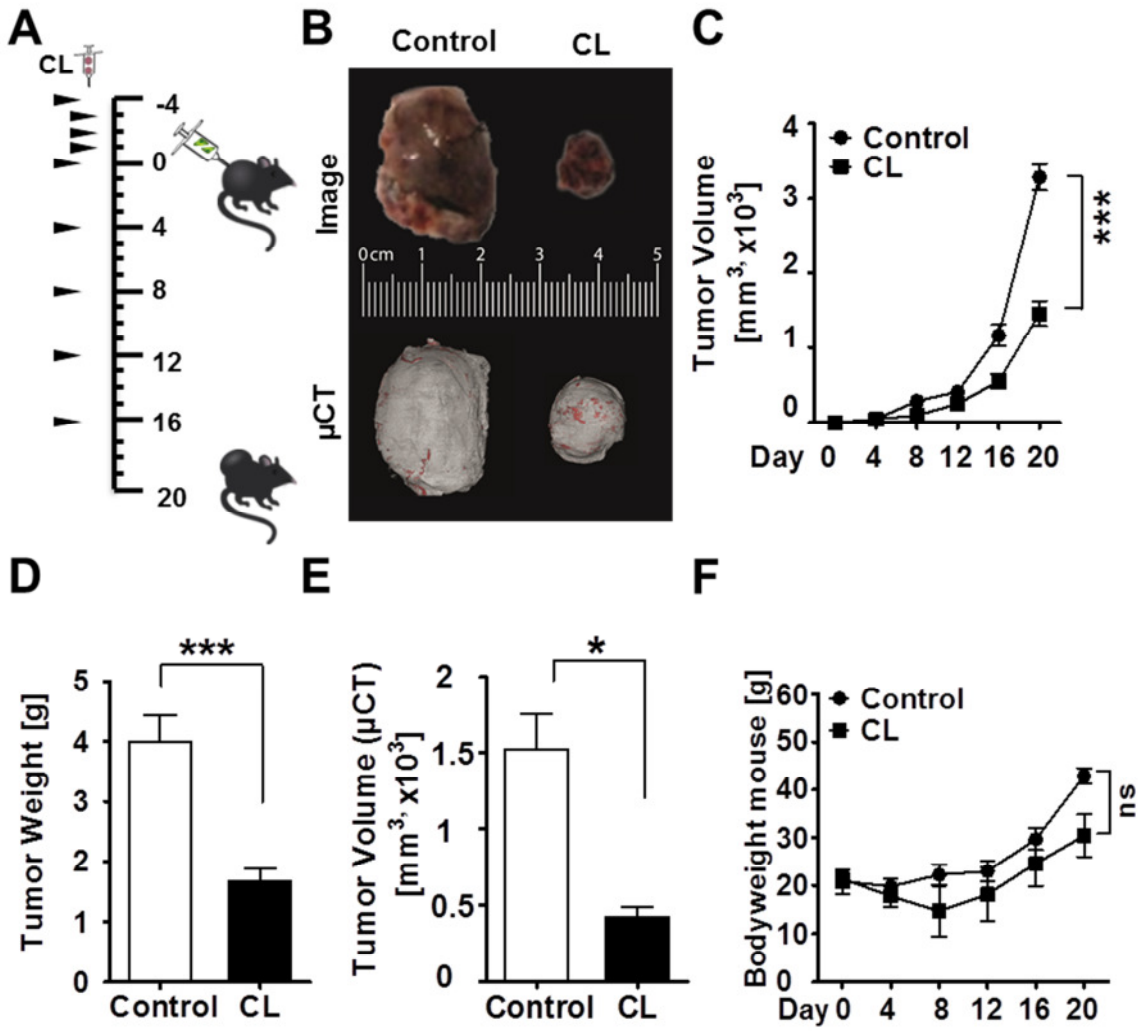

Figure 8 **CL-mediated MΦ depletion inhibits primary tumor growth.** (A) Schematic of the experimental procedure (▶, injections) (B) Representative pictures of extracted tumors (C) Volume (measured with digital calipers at the indicated time points) and (D) Weight of tumors from CL-treated or control mice (E) Tumor volume as assessed with µCT (F) Mice bodyweight. All data represents mean ± SEM, n = 10, * $p \leq 0.05$, ** $p \leq 0.01$, *** $p \leq 0.001$.

The number of $PCNA^+$ cells (positively stained cells per total cells) in tumor tissue was decreased from 82.57 ± 4.705 in the control group to 18.54 ± 12.03 in CL-treated mice, supporting the finding of decreased tumor growth in CL- treated mice (*Figure 9A-B).* Staining for $F4/80^+$ positive cells revealed a decrease of MΦ within the tumor microenvironment, which was confirmed and quantified with flow cytometric analysis. Interestingly, the flow cytometry results showed an approximate 56% reduction of MΦ accumulation, similar to the changes in primary tumor volume, indicating the direct involvement of MΦ in primary tumor growth (*Figure 9C-D).*

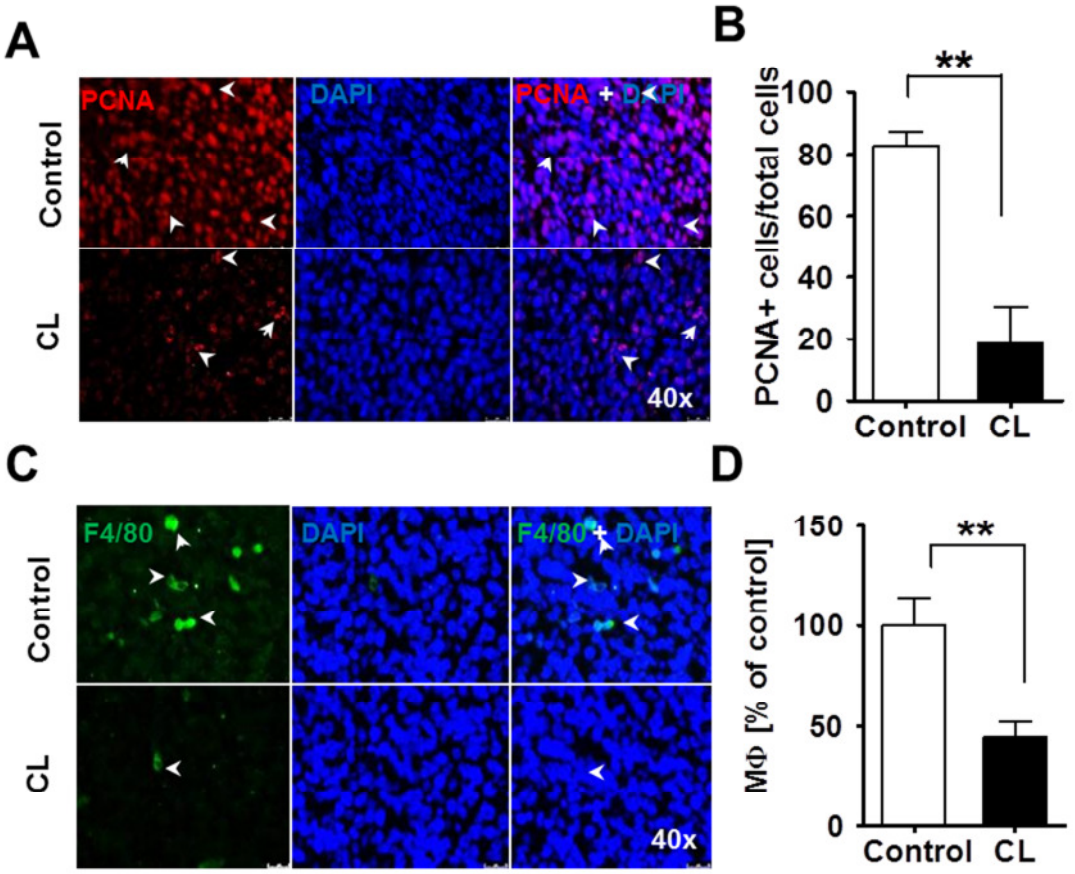

Figure 9 **CL-treatment decreases PCNA$^+$ cells and macrophages in the tumor microenvironment.** (A) Immunohistochemistry for and (B) Quantification of PCNA$^+$ in s.c. tumor tissue from CL-treated mice and controls (C) Immunohistochemistry for F4/80$^+$ cells (D) Flow cytometric analysis of Macrophage-accumulation in s.c. tumor tissue. White arrow indicates positive cells. All data represent mean ± SEM, n = 6-10, **p≤0.01.

To further examine the consequences of MΦ depletion on the tumor stroma, tumor tissue lysate was screened for different MΦ polarization markers and the expression of chemokine receptors. Levels of the M1-phenotype marker iNOS was increased in the tumor tissue, whereas the M2-marker arginase levels were decreased. The M2-marker chitinase showed no significant change (*Figure 10A*). Moreover, the mRNA levels of the chemokine receptors CCR2 and CX3CR1 were significantly decreased in the CL-treated group: CCR2 was decreased by 2.071±0.4836 ΔCt and CX3CR1 by 1.869±0.2360 ΔCt in tumor tissue of the CLgroup, revealing an involvement of a CCR2$^+$ cell population in tumor progression. Since CCR2 is typically expressed on monocytes and MΦ and the CX3CR1 is expressed on all leukocytes and due to this also on MΦ, this important CCR2$^+$CX3CR1$^+$ cell population can be, but not necessarily have to be MΦ. Additionally the chemokine receptor CCR3, mainly responsible for eosinophil granulocyte chemotaxis (Kampen et al., 2000) was not changed (*Figure 10B*).

To examine further consequences on the entire tumor microenvironment after MΦ depletion tumor tissue lysates were screened for mRNA expression of secreted MMPs and VEGFs, since these two groups can represent tissue remodeling and induced angiogenesis and MΦ are a concise source for these enzymes and growth factors (Goetzl et al., 1996; Lin and Pollard, 2004). Two members of VEGF group were decreased, with only VEGFc showing a significant decrease and VEGFb showing a trend towards decrease (*Figure 10C*). VEGFc is important for lymph angiogenesis and importantly, like VEGFa binds to VEGFR-2 (Flk1), which is the main receptor responsible for VEGF-mediated actions such as endothelial cell migration and angiogenesis. Furthermore, VEGFc was recently described to be the main angiogenetic factor in cancer (Carroll et al., 2013; Terme et al., 2013).

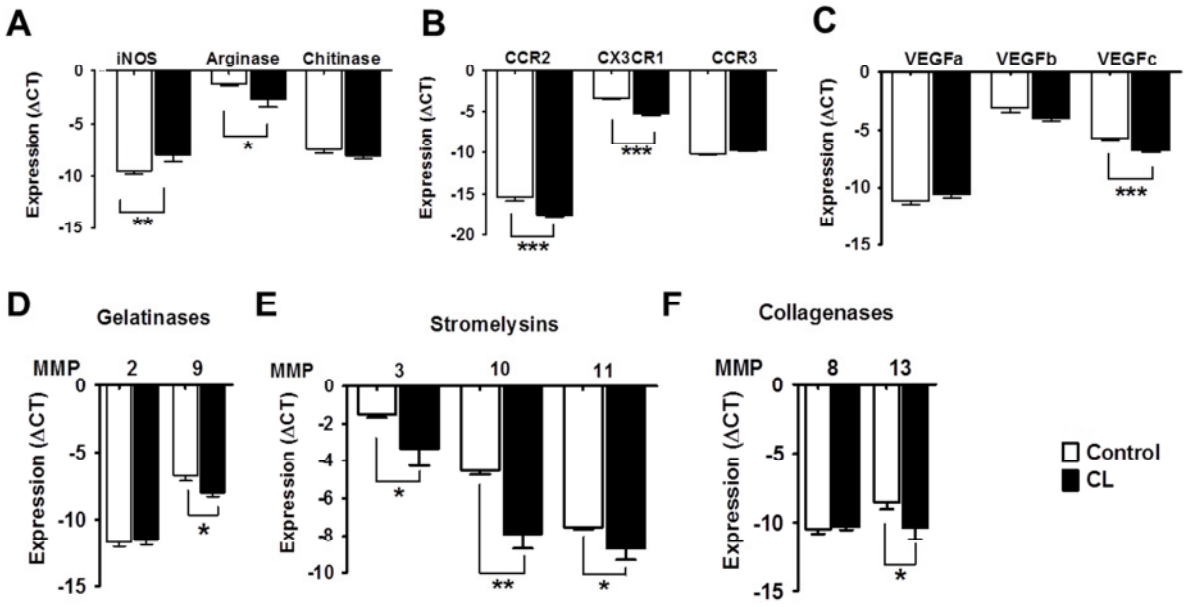

***Figure 10* Changed mRNA expression within a MΦ-depleted tumor microenvironment.** (A) Relative mRNA-expression levels of MΦ-polarization marker (B) Chemokine-receptors (C) VEGFs (D) Gelatinases (E) Stromelysins and (F) Collagenases. All data represent mean ± SEM, n = 6, *p≤0.05, **p≤0.01, *** p≤0.001.

We focused on the secreted isoforms of MMPs, as their involvement is already well described in tumor progression and found several MMPs were decreased in the CL-treated tumor tissues. In particular, level of the subgroup of stromelysins (MMP-3, -10 and -11) were entirely, significantly less expressed. Further less expressed are the gelatinase MMP-9, with type IV collagen as main substrate and the collagenase MMP-13, which can degrade triple-helical collagen as well (*Figure 10D-F*).

Considering these marked changes in tumor growth and the microenvironmental composition including MΦ accumulation, MMP, VEGF and chemokine-receptor expression one possible

underlying mechanism of MΦ contribution to cancer growth could be alterations of the vasculature. The total vessel supply of s.c. tumors was quantified and visualized with a µCT and nanoCT. While there was no significant change but a clear difference by trend in the total volume of the macro-vasculature between the groups as assessed with the µCT, there were highly irregular, leaky vessels in the CL-group that are inefficient to provide the tumor with nutrition (*Figure 11A-B*). Importantly, there is a significant decrease in the important nurturing microvasculature as revealed with the nanoCT. Moreover, the structure linear density, a value representing the vessel number on a virtual 1 cm line, is also significantly decreased in the CL-treated group (*Figure 11C*).

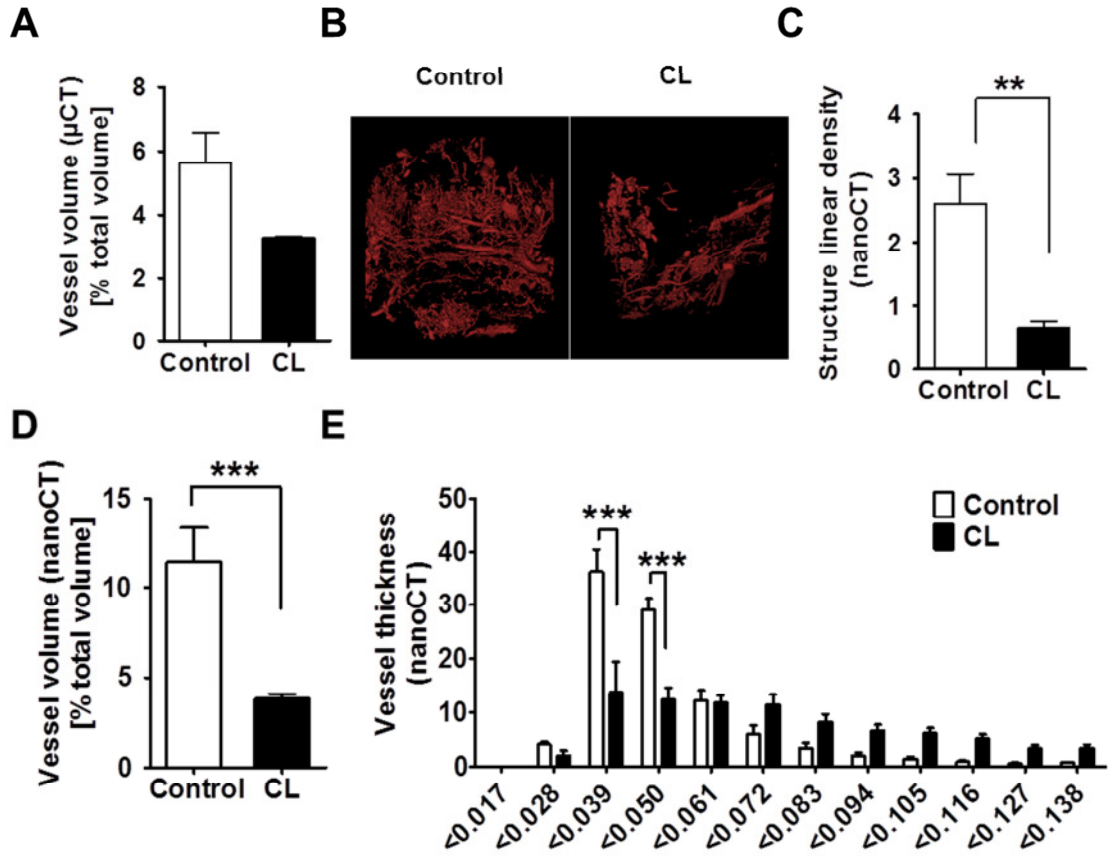

***Figure 11* CL-mediated macrophage depletion results in alterations of macro- and microvasculature.** (A) Vessel volume as assessed with µCT (B) Representative 3D-pictures of the microvasculatures evaluated with nano-CT (C) Vessel density and (D) Volume quantified with nanoCT (E) Vessel fractions according to theis diameter. All data represents mean ± SEM, n = 6, * p≤0.05, ** p≤0.01, * p≤0.001.

Analysis of the different vessel fractions according to their vessel diameter, revealed a major difference in vessels of 0.028 - 0.050 µm size (*Figure 11E*). These crucial findings highlight the nano-CT as a highly accurate and more powerful tool than µCT, especially for analysis of neoangiogenesis in solid tumors. Taken together, these findings underline the generation of a

malnourished tumor-environment that lost its full capacity to grow due to MΦ-depletion and subsequent tumor microenvironmental changes.

4.1.2 CL mediated depletion of MΦ in metastasis formation

Since MΦ-depletion is affects the entire tumor microenvironment and especially ECM remodeling enzymes and vascularization, a significant impact of MΦ on metastasis formation was expected. MΦ involvement in lung metastasis formation was examined using a new model, where the s.c. tumor was removed after ten days, which provokes metastasis, in the case of LLC1 primary to the lung. During the progression of the metastatic process, all animals were screened twice with an MRI (*Figure 12A*). The endpoint was defined according to the humane endpoint guidelines, which suggests the scarification of an animal that fails to pass a score sheet with defined point regarding outlook and behavior.

The number of metastatic nodules in the lung of CL-treated mice was markedly decreased. Overall, the number of macroscopic metastases, detectable with the naked eye on the surface of the extracted lung, was approximately seven fold higher in the control group. These results were confirmed in H&E stained sections, where the number of detected nodules decreased from 10.25 ± 2.658 in the control group to 2.571 ± 0.8411 in the CL-treated group. Additionally, the MRI evaluation of metastatic tumor formation in the lung confirms these findings (*Figure 12B-D).* Furthermore, additional liver-metastases were observed in several control-animals but never in CL-treated animals. Due to the reduced lung metastasis, survival of mice in the CL-group was slightly, but significantly longer *(Figure12E*). This result confirms the observation in primary tumor growth (4.1.1), that a general systemic MΦ depletion influences tumor growth and metastasis, but may not be beneficial for the mice. In line with that, MΦ accumulated less in the metastatic tumor microenvironment (*Figure 12F-G*).

Due to the less vascularized primary tumors and lower availability of basement membrane and ECM down breaking enzymes like MMPs and VEGFs, the extravasation of tumor cells might be impaired and this results in a strongly impaired formation of metastatic nodules. Additionally, the MΦ in the metastatic nodule are less as well, so the same effect as in the primary tumor microenvironment can be assumed: a reduced vascularization and with this a malnutrition of the tumor nodules and impaired growth.

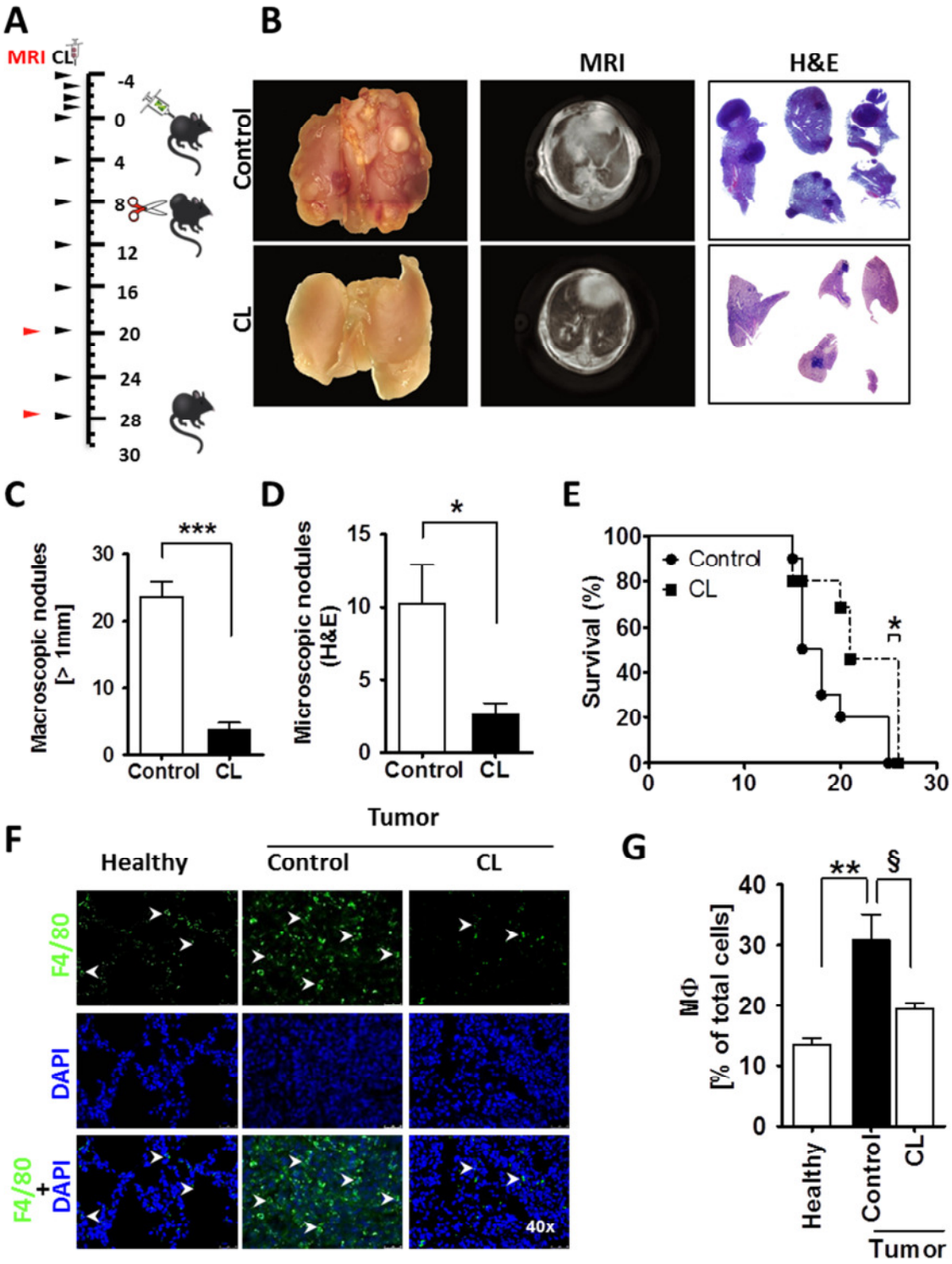

***Figure 12* CL-mediated MΦ depletion attenuates lung metastasis *in vivo*.** (A) Schematic of the experimental procedure (B) Representative pictures of metastatic lungs of CL-treated and control mice; from left to right: photograph of whole lung *ex-vivo*, MRI of lung *in vivo* and H&E staining of lung sections (C) macroscopic nodules on extracted lung and (D) in H&E stainings (E) Survival curve expressed as a percentage of total mouse number (F) Representative pictures of IHC-sections stained for F4/80 in tumor bearing and healthy lungs and (G) Quantification of F4/80^{+}-cells compared to total cells. White arrows indicate positive cells. All data represents mean ± SEM; n = 6-10; * p≤0.05, ** p≤0.01, *** p≤0.001

4.1.3 MΦ depletion in the MaFIA mouse model

The effects of MΦ depletion on primary tumor growth described in Section 4.1.1 were confirmed with a second, mechanistically different model of MΦ depletion *in vivo,* the MaFIA (**M**acrophage **F**as **i**nduced **a**poptosis) mouse. In these mice, the c-fms promoter controls the expression of a suicide gene, which transcribes for a fusion protein of the cytoplasmic Fas-domain and the FK506-binding protein and administration of the chemical compound AP20187 causes dimerization of the suicide protein and results in Fas-mediated apoptosis of c-fms-expressing cells, mainly MΦ and Monocytes (Burnett et al., 2006) (*Figure 13A*). Importantly, the c-fms promoter is usually controlling the transcription of CSFR, the receptor for M-CSF. Recent data suggests, that M-CSF is a M2-polarizing cytokine, which implies that CSFR-expressing cells are most probably M2-polarized MΦ (Fleetwood et al., 2009). So in this model, a more specific targeting of M2-MΦ and with this more benefit for the mice is expected.

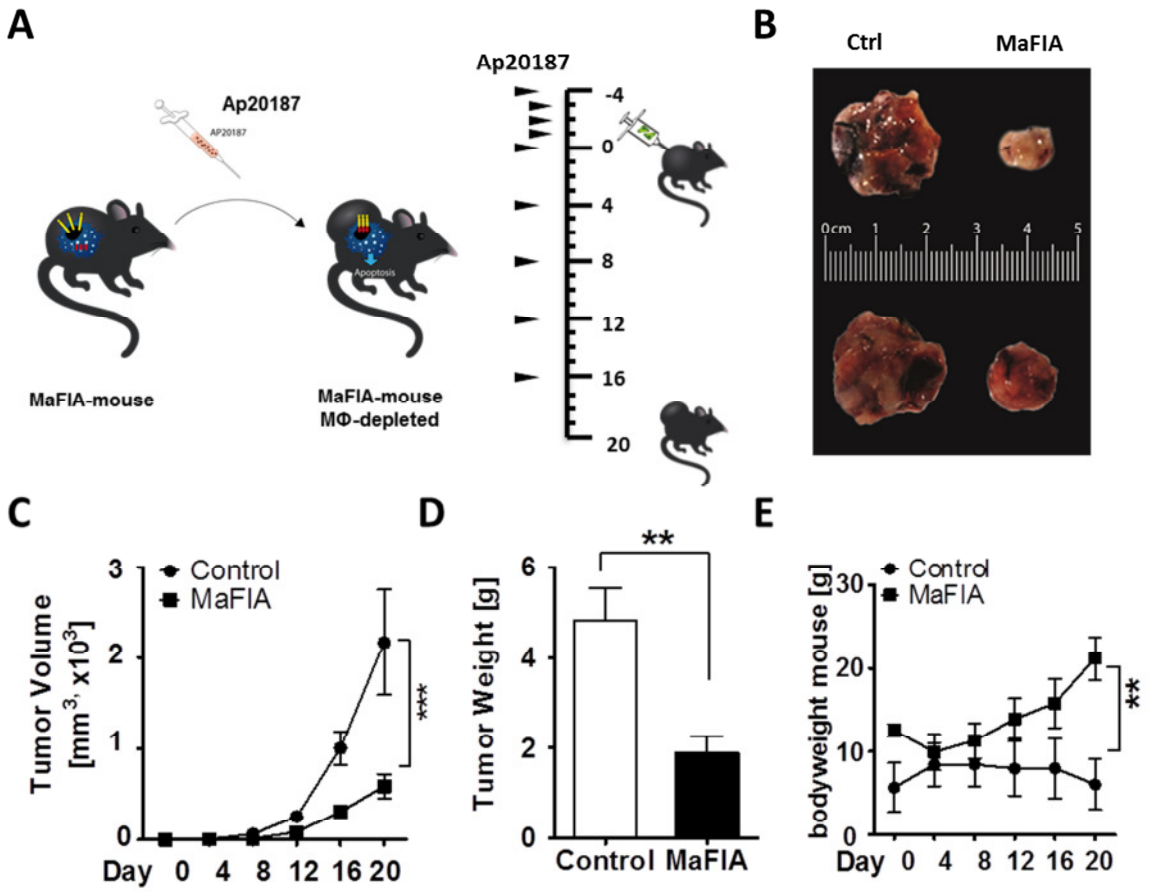

Figure 13 **Primary tumor growth is inhibited *in vivo* in MΦ-depleted MaFIA Mice.** (A) Schematic of the principle and experimental procedure (B) Representative pictures of extracted tumors (C) Tumor volume (measured with digital calipers on indicated time points) and (D) Tumor weight. (E) Mice bodyweight. All data represents mean ± SEM; n = 6-10; * p≤0.05, ** p≤0.01, *** p≤0.001, compared to control.

Indeed, the observed decrease of primary tumor growth was more pronounced with an earlier significance as soon as day 12 compared to the CL-depleted model. These findings were supported by a decrease of primary tumor volume and weight. In contrast to the CL-depleted model, the MaFIA-mice gained weight under the treatment, compared to controls (*Figure 13B-E*).

Moreover, IHC analysis of sections from these s.c. revealed a reduced number of $PCNA^+$ cells in the tumor from MaFIA mice, as an index of proliferation *(Figure 14A-B*). To quantify MΦ accumulation, first, tumor sections were stained for $F4/80^+$ cells and second, digested tumors were analyzed with flow cytometry. In line with a stronger inhibition of tumor growth compared to the CL-depleted mice, more MΦ were depleted (approximately 91.9%) in the tumor microenvironment. To verify the systemic depletion, total intraperitoneal cells were isolated and analyzed with flow cytometry, and MΦ were decreased over 90%. Taken these both results together, a successful systemic long-term depletion of MΦ can be assumed (*Figure 14C-E*).

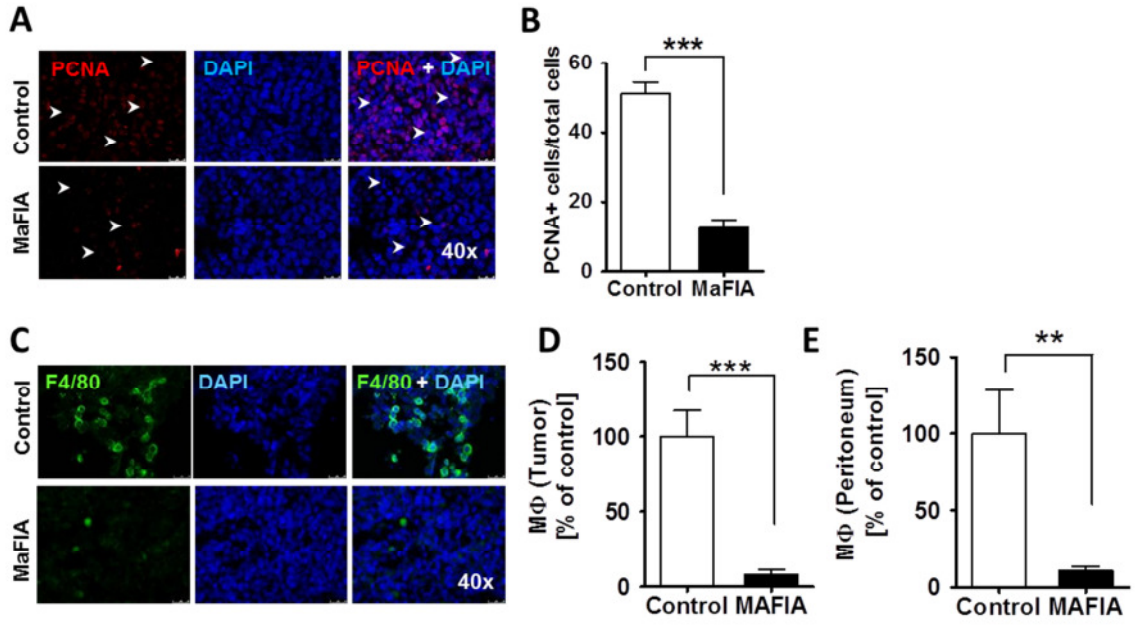

***Figure 14* Ap20187-treated MaFIA mice displays fewer $PCNA^+$ cells and MΦ in the tumor microenvironment.** (A) Immunohistochemistry for PCNA and (B) Quantification (C) Immunohistochemistry for $F4/80^+$ cells (D) Flow cytometric analysis of MΦ accumulation in s.c. tumor tissue and (E) in the peritoneal cave. White arrows indicate positive cells. All data represent mean ± SEM, n = 6-10, * $p \leq 0.05$, ** $p \leq 0.01$, *** $p \leq 0.001$.

Interestingly, the MΦ depletion of over 90% is accompanied by a very significant decrease of M2-markers in the tumor microenvironment with a simultaneous increase of M1-markers,

indicating that MaFIA mediated MΦ-depletion shifts the balance from M2- MΦ to tumor-fighting M1-MΦ, which may provide a basis for the impressive tumor decrease (*Figure 15A*). The gain of weight and strong shift from M1 to M2 markers show that a more specific M2-targeting via the M-CSF receptor, like in the MaFIA mice, is more beneficial for cancer-bearing mice compared to a general depletion with CL. At the same time, we were unable to detect the membrane expressed chemokine receptor CCR2 in the microenvironment. Additionally CX3CR1 expression was strongly decreased in the tumor stroma (*Figure 15B).* These findings strongly support the involvement of chemokine receptors in tumor development and progression.

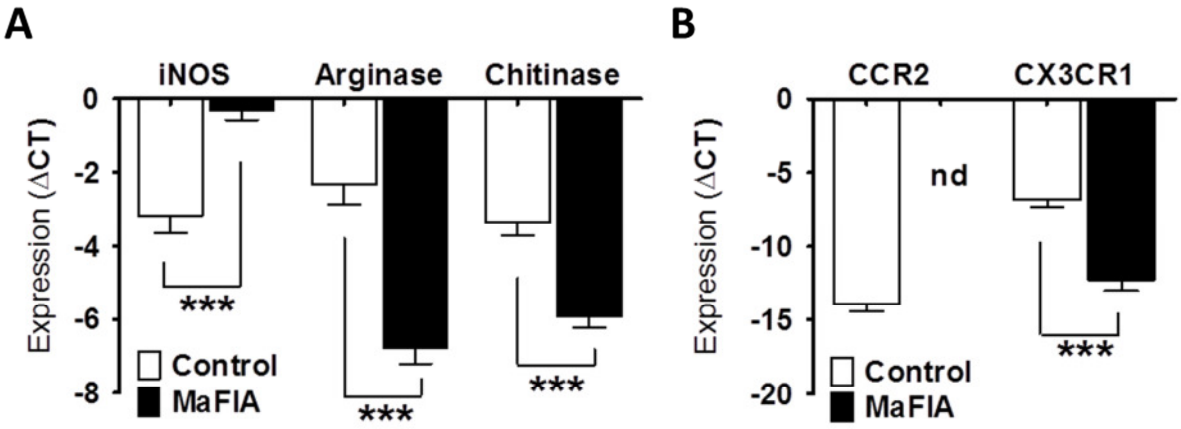

Figure 15 **Phenotype marker and chemokine-receptor expression in the tumor microenvironment of MaFIA-mice**. (A) Relative mRNA levels of M1- and M2-marker (B) relative mRNA-levels of chemokine receptors. All data represent mean ± SEM, n=6, * p≤0.05, ** p≤0.01, *** p≤0.001.

4.2 In vitro co-culture of bone-marrow derived WT MΦ with murine lung adenocarcinoma cells (LLC1)

4.2.1 Characterization of bone-marrow derived macrophages (BM- MΦ)

After isolation and 10 days of culture in the presence of rmM-CSF, MΦ were subjected to ICC, to confirm the expression of common MΦ-marker like F4/80 and MoMa1 (*Figure 16A*). To verify the purity of the isolated MΦ against granulocyte or DC contamination, MΦ were analyzed with flow cytometry for the markers CD45, F4/80, CD11c, CD11b and GR-1 before experimental use. The purity of the isolation process was over 97% in all experiments (*Figure 16B*).

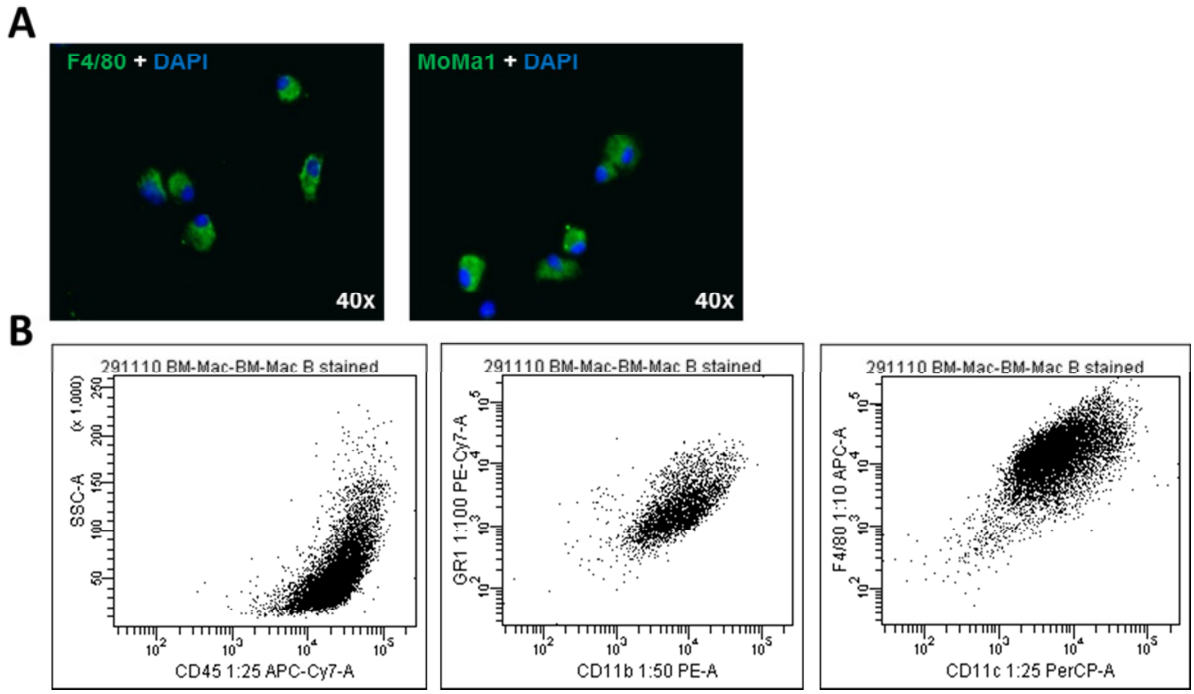

***Figure 16* MΦ -marker expression and purity after generation of BM-MΦ.** (A) Immunocytochemistry for F4/80 (left) and MoMa1 (right) (B) Flow cytometric analysis of bone marrow derived MΦ.

4.2.2 Effect of co-culture on MΦ polarization

MΦ can adopt different phenotypes, which are defined by functionality and expression patterns of intracellular markers as well as cytokine secretion patterns and TAMs are known to display a M2-phenotype (Hamilton, 2008; Mantovani et al., 2002), but the exact underlying mechanisms of this polarization-phenomena remain unclear. To test, if co-culture with cancer cells (LLC1) alone can induce an M2-phenotype, control and co-cultured MΦ were screened for typical M1markers (iNOS, IL-1β, IL-6 and TNFα) and M2-markers (arginase, chitinase, IL-10 and IL-1RA) and relative mRNA expression of these markers revealed that MΦ polarize into M2-MΦ after co-culture, with a significant reduction of the M1-marker iNOS and TNFα (*Figure 17*A) and a strongly significant upregulation of all screened M2-markers, such as arginase, chitinase, IL-10 and IL-1RA (*Figure 17*B).

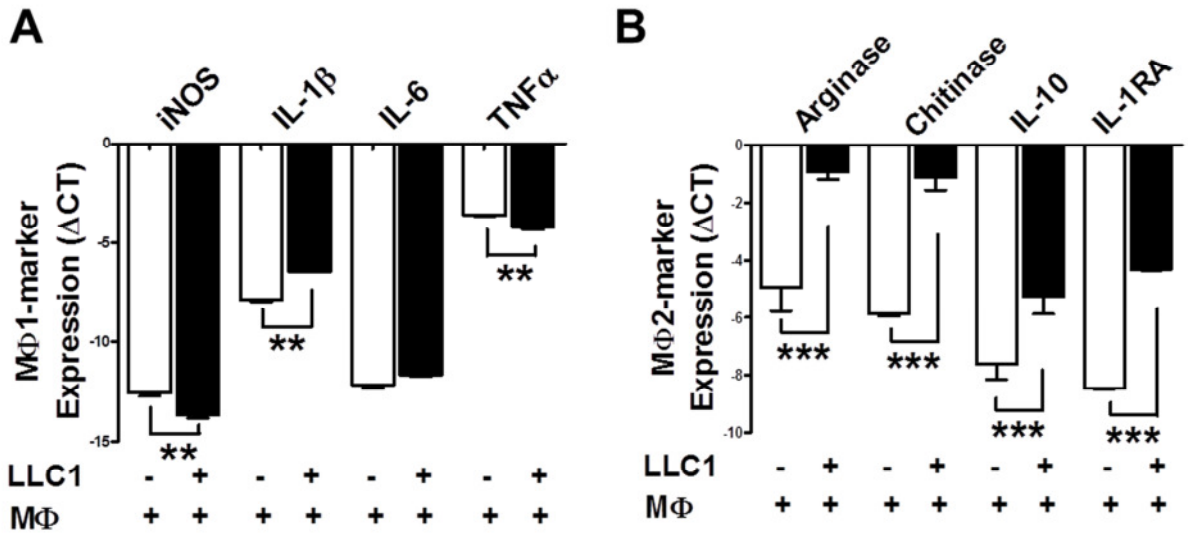

Figure 17 **MΦ polarization after co-culture with LLC1.** (A) relative mRNA-levels of M1-polarization markers iNOS, IL-1β, IL-6, TNFα and (B) of M2-polarization marker arginase, chitinase, IL-10 and IL-1RA. All data represent mean ± SEM, n=6, * p≤0.05, ** p≤0.01, *** p≤0.001.

4.2.3 Characterization of the cytokine profile in co-culture supernatants

To gain an overview of the differentially secreted cytokines of LLC1 and MΦ after co-culture, an antibody-based cytokine-array for 40 different cytokines was performed using CM from co-culture-CM or LLC1 and MΦ CM alone (*Figure 18).* The cytokine array coordinates and entire list of cytokines are listed in the table in the appendix.

Among the 36 cytokines, 19 were either higher or newly secreted in the co-culture CM. Interestingly, we found already 7 cytokines constitutively secreted by LLC1 alone. *Figure 19* lists the strongest regulated or most abundant secreted cytokines. Notably, LLC1 appear to secrete abundant amounts of the MΦ and MC attracting CCL2 and the mitogen and neutrophil attracting CXCL1, compared to other cytokines. Various cytokines such as IL-1RA, IL-23, CCL5, CCL12, CXCL10 and MIP-2 are constitutively secreted by M-CSF-generated MΦ and are therefore found on a similar level in co-cultured CM.

Although the cytokine array has a maximum detection capacity of approximately 6000 arbitrary units, as seen with the positive control, the mentioned cytokines still may be expressed higher in co-cultured CM, but the difference would not be detectable with the cytokine array. Cytokines that were secreted at significantly higher levels in the co-cultured CM include IL-1α, IL-23, M-CSF and TNFα, and those only secreted in the co-culture CM include IL-6, IL-10, CCL1, MIP-1α, MIP-1β, G-CSF and siCAM-1. Notably,

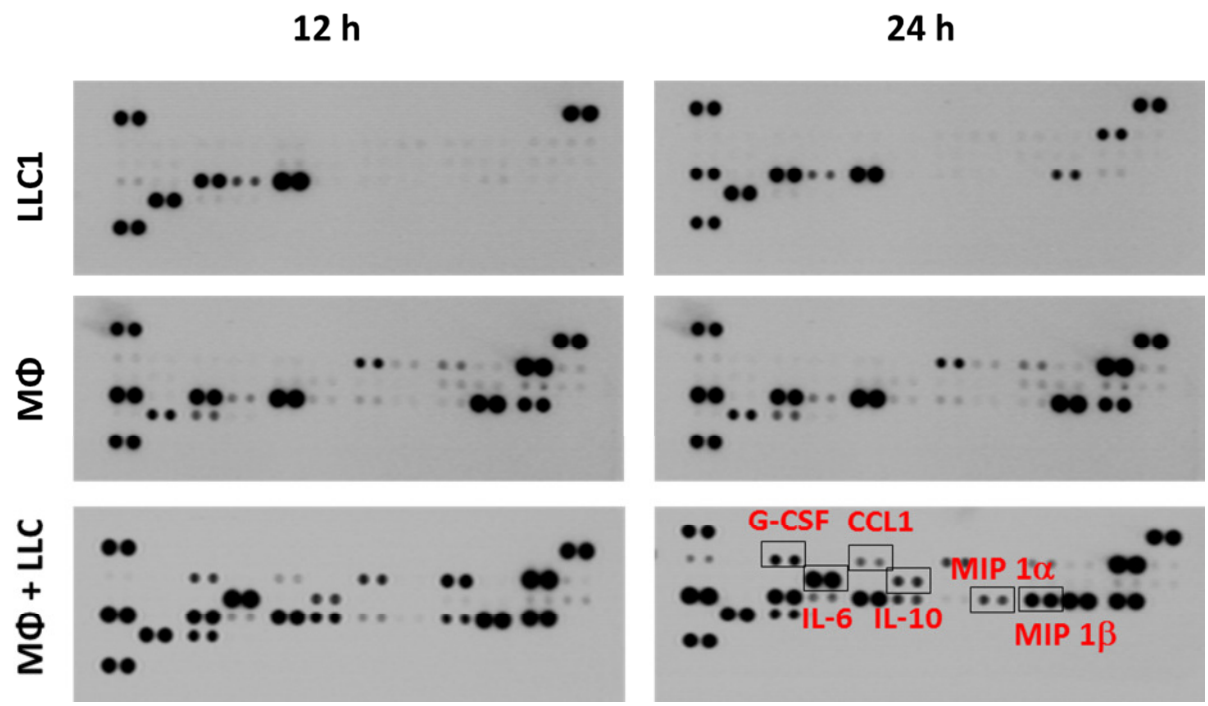

Figure 18 **Cytokine-Array** Visualization of antibody spotted membranes after incubation with different CM and time points as indicated. ***CCL1*** C-C motif chemokine 1; ***G-CSF*** granulocyte-colony stimulating factor; *IL-6* interleukin-6; ***IL-10*** interleukin-10; ***MIP-1α*** macrophage inflammatory protein-1 alpha; ***MIP-1β*** macrophage inflammatory protein-1 beta

eotaxin, the ligand for CCR3 was not detectable in any setting. CCR3 levels were also unchanged in MΦ-depleted tumor microenvironments (*Figure 19*).

The remarkable effect of MΦ depletion on tumor growth and metastasis, reduction in expression of chemokine receptors CCR2 and CX3CR1 in the tumor microenvironment and the extremely high levels of the MΦ chemoattractant CCL2 detected with the cytokine array suggests a chemokine mediated interplay between lung cancer cells and MΦ.

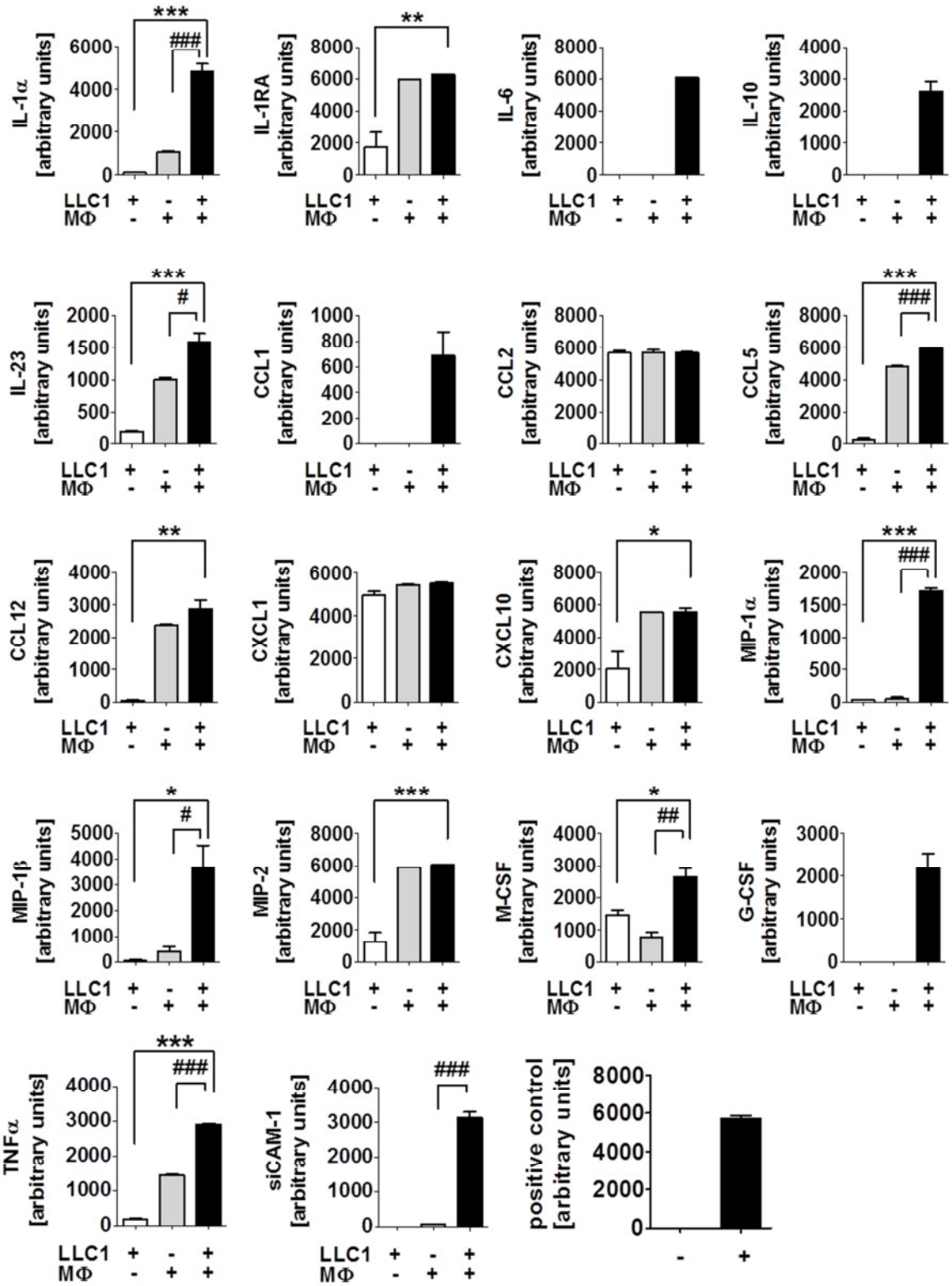

Figure 19 **Co-culture-regulated and constitutively secreted cytokines** All data represent mean ± SEM, * p≤0.05, ** p≤0.01, *** p≤0.001. * compares LLC1-CM vs. co-culture-CM, # compares LLC1-CM vs. MΦ-CM.

Thus, first the CCL2 secretion observed in the co-cultured CM was assigned to one cell type. Relative mRNA levels of CCL2 in control and co-cultured LLC1 clearly show LLC1 as a major source of CCL2. CCL2 transcription was significantly upregulated in LLC1 after co-culture at every time point (*Figure 20A*). As the cytokine array can only detect relative levels, CCL2 secretion was further confirmed and quantified via ELISA (*Figure 20B*).

Since not only CCR2 was significantly less expressed in the tumor microenvironment, but also CX3CR1 (*Figure 15*B) the secretion of CX3CL1 ligands was investigated. Results were similar to those of CCL2-secretion. CX3CL1 mRNA level was significantly upregulated in co-cultured LLC1 (*Figure 20C*) and CX3CL1 was significantly secreted at higher levels in co-culture CM (*Figure 20D*).

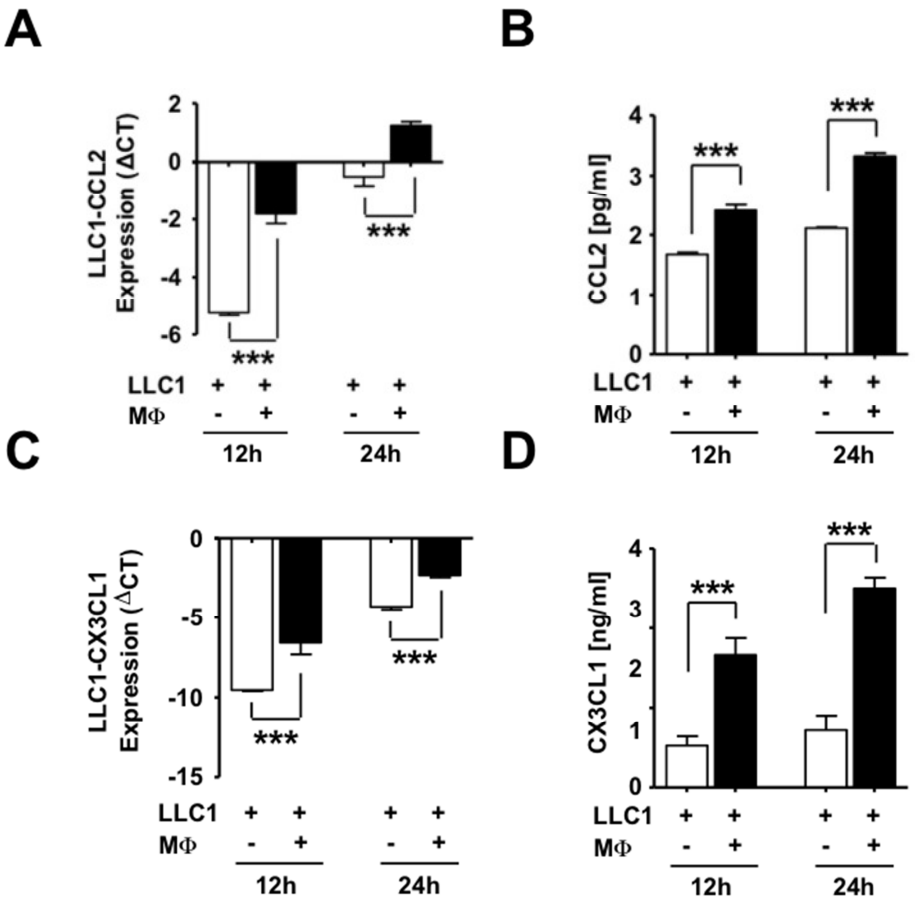

***Figure 20* CCL2 and CX3CL1-secretion of LLC1.** (A) Relative CCL2 mRNA expression in control (white bars) or co-cultured LLC1 (black bars) (B) CCL2 secretion (ELISA) (C) relative CX3CL1 mRNA expression in control or co-cultured LLC1 (D) CX3CL1-secretion (ELISA) All data represent mean ± SEM, n=6, * $p \leq 0.05$, ** $p \leq 0.01$, *** $p \leq 0.001$.

4.2.4 Expression profile of chemokine receptors in LLC1

Since LLC1 abundantly secret chemotactic working peptides like CCL2 and CX3CL1, they also might express the according receptors, CCR2 and CX3CR1. Interestingly, a screen of LLC1 revealed weak basal expression of CX3CR1, but not CCR2 or CCR3.

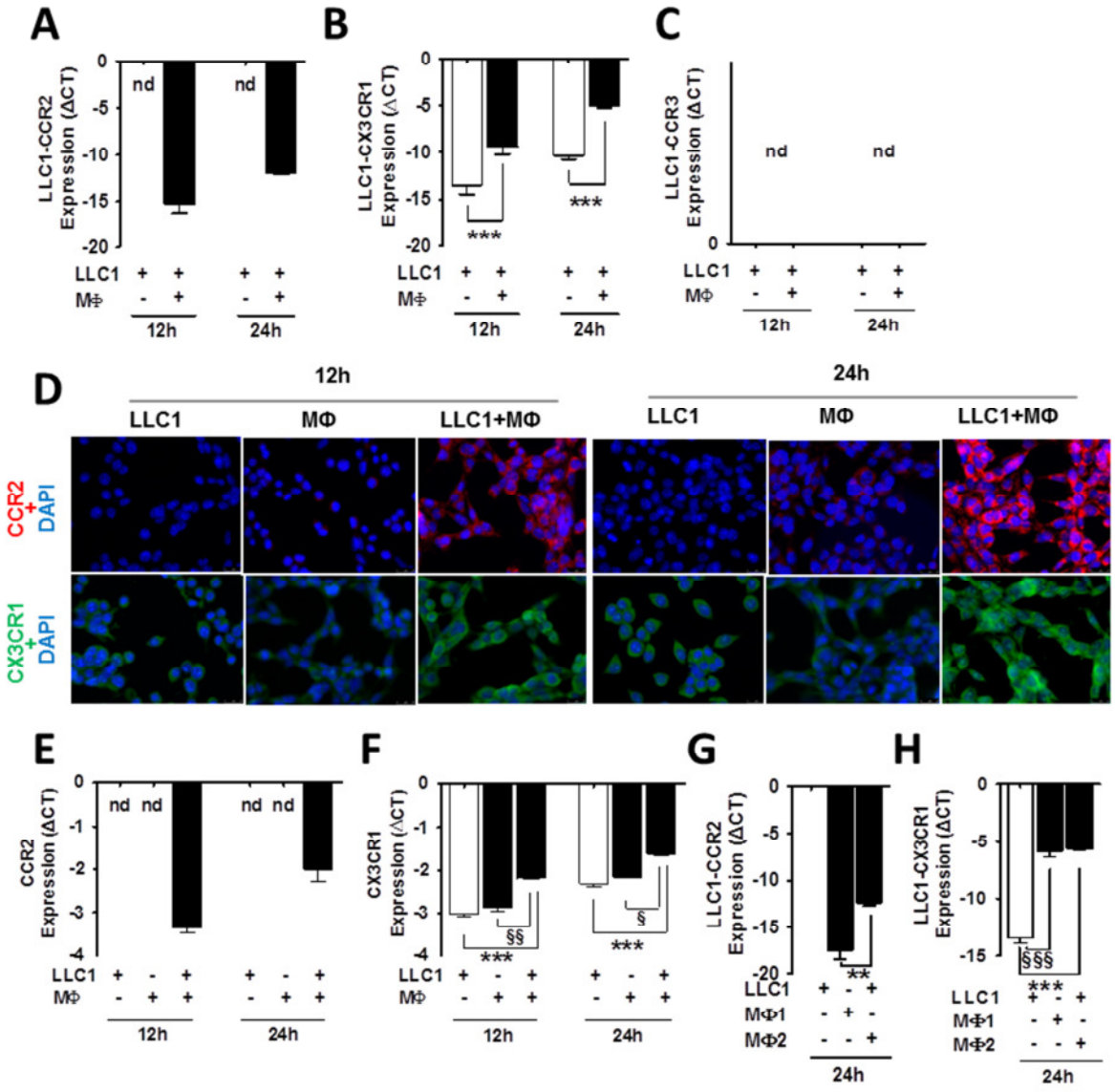

Figure 21 **CCR2 and CX3CR1 expression on LLC1.** (A) relative mRNA expression of CCR2, (B) CX3CR1 and (C) CCR3 in directly co-cultured LLC1. (D) CCR2 or CX3CR1 expression on LLC1 after stimulation with the indicated conditioned media from indicated co-culture time points (E) relative mRNA expression of CCR2 and (F) CX3CR1 on CM stimulated LLC1 (G) relative mRNA expression of CCR2 or (H) CX3CR1 in LLC1 after co-culture with MΦ of different phenotype. All data represent mean ± SEM, n=6, * $p \leq 0.05$, ** $p \leq 0.01$, *** $p \leq 0.001$. * compares LLC1 vs. co-cultured LLC1, § compares MΦ-CM stimulated LLC1 vs. co-cultured LLC1

More importantly, CCR2 and CX3CR1 receptors were significantly upregulated in LLC1 after co-culture with MΦ (*Figure 21A-C*).

To analyze if the CCR2 onset or CX3CR1 upregulation is only dependent on MΦ secreted factors or the result of the communication of both cell types, fresh LLC1 were stimulated with CM derived from co-cultures. This experiment confirmed that the chemokine-receptor upregulation is dependent on the exchange of secreted factors between LLC1 and MΦ, since the upregulation is absent after stimulation with only MΦ-CM, but present after stimulation with co-culture CM (*Figure 21D-F*).

To test if the described chemokine-receptor upregulation by LLC1 might be dependent on the MΦ-phenotype, LLC1 were co-cultured with either M1 or M2-MΦ. Importantly, we observed a significantly stronger upregulation of CCR2 after co-culture with M2-MΦ, whereas the CX3CR1 upregulation was overall independent of the MΦ phenotype (*Figure 21G-H*).

Taken together, these results suggest an active attraction of MΦ by LLC1 and a subsequent biomimicking of MΦ receptor expression by LLC1 after interaction with MΦ. This loop is enforced by M2-polarization of MΦ.

4.2.5 Expression profile of MMPs and VEGFs on LLC1 and BM-MΦ

Levels of VEGFs and several MMPs were decreased in the tumor microenvironment of MΦ-depleted mice. To study if, inversely, co-culture with MΦ can upregulate these effector molecules, mRNA from control and co-cultured LLC1 samples was screened for VEGF expression, and MΦ mRNA was screened for MMP expression, since MΦ are the typical source of MMPs. VEGFa and VEGFc, but not VEGFb were significantly upregulated after co-culture with MΦ (*Figure 22A*).

Furthermore, the entire group of stromelysins (MMP-3, -10 and -11) was upregulated in MΦ after co-culture, which is well in line with our *in vivo* observation, where this group of MMPs was entirely downregulated in MΦ-depleted mice. In addition MMP-8, -9 and -13 were significantly upregulated in co-cultured MΦ, with the strongest induction of MMP-13 expression *(Figure 22B-D).*

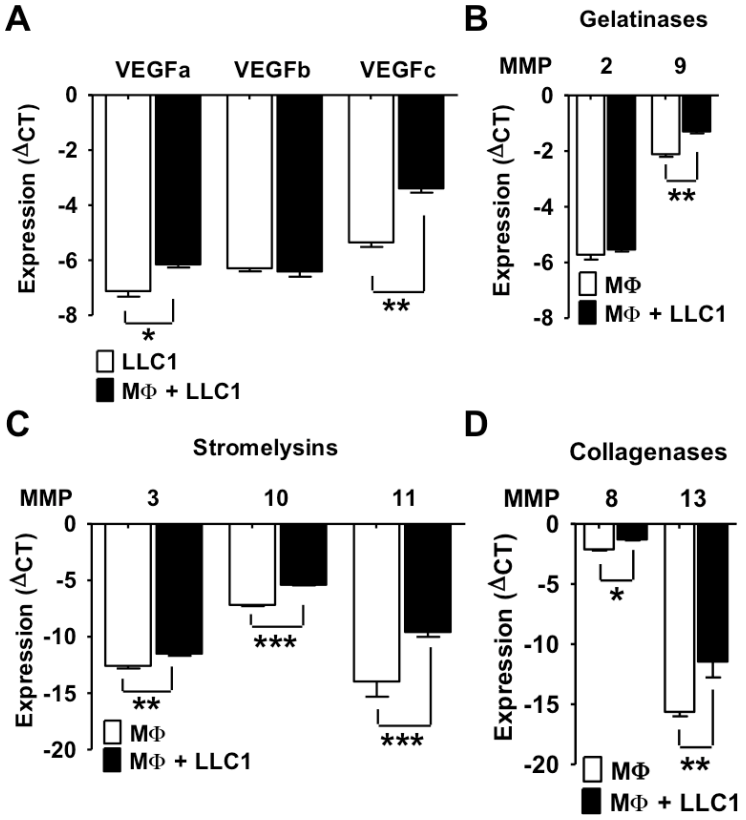

***Figure 22* VEGF expression LLC1 and MMP expression in macrophages.** (A) Relative mRNA level of VEGFa-c in control (white bars) or co-cultured LLC1 (B) relative mRNA-expression levels of gelatinases (C) stromelysins and (D) collagenases in control and co-cultured MΦ. All data represent mean ± SEM, n = 6, *p≤0.05, **p≤0.01, *** p≤0.001.

4.3 Functional characterization of co-culture CM

4.3.1 Effect on LLC1 proliferation

After observing upregulation of chemokine receptors CCR2 and CX3CR1, usually expressed on immune cells, LLC1 were examined by several functional assays, e.g. to investigate functional alterations in proliferation of LLC1 from co-culture with MΦ (*Figure 23A*-B). Proliferation, measured by BrdU-incorporation, was slightly but significantly increased in LLC1 exposed to CM from 12 h co-cultures. An even higher significance was seen in LLC1 cultured with CM from 24 h co-cultures. Notably, the LLC1 proliferation was increased after treatment with CM from MΦ alone, which is in line with the observation that M-CSF generated MΦ display a slight M2-phenotype compared to GM-CSF-generated MΦ *(Figure 23C).*

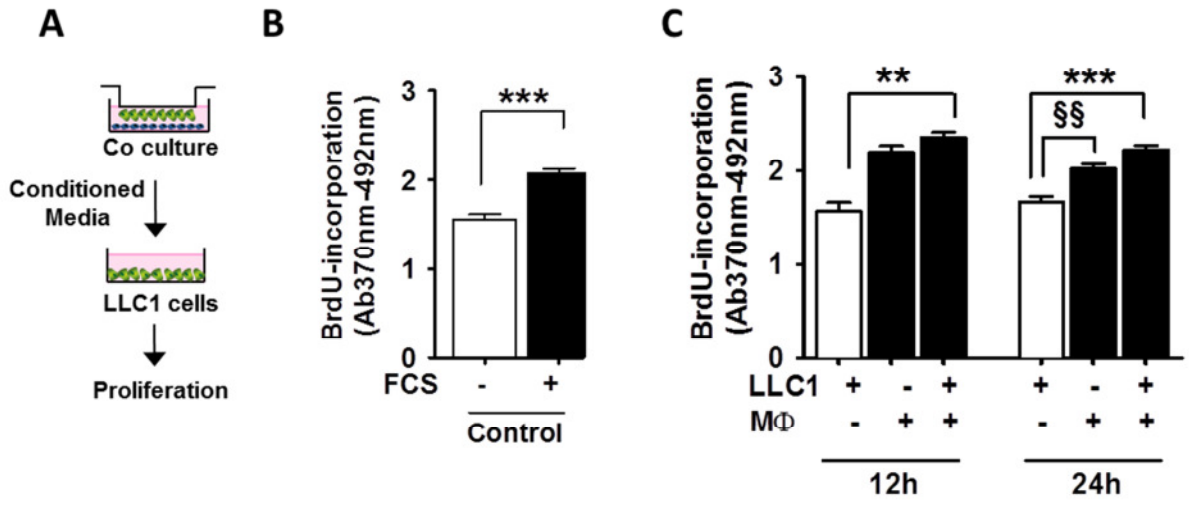

Figure 23 **Effect of CM on LLC1 proliferation.** (A) Schematic of experimental procedure (B) Positive (+) and negative (-) control (C) Proliferation of LLC1 stimulated with the indicated co-culture CM harvested on the indicated co-culture time points All data represent mean ± SEM, n = 6, *p≤0.05, **p≤0.01, *** p≤0.001. * compares LLC1 vs. co-culture, # compares LLC1 vs. MΦ.

4.3.2 Effect on LLC1 migration

After the moderate effect on LLC1 proliferation, LLC1 were examined using a boyden-chamber-based migration assay (*Figure 24A*). The migration of LLC1 towards CM of MΦ alone was already increased 9 fold, suggesting that MΦ secrete either chemotactic working peptides or other soluble factors, which are able to prime cancer cells directly into a more metastatic phenotype. However, the migration toward co-culture CM was remarkably high at 20 fold. Overall, the migration significantly increased after 12 h and 24 h towards CM from MΦ alone, as well as from co-cultures (*Figure 24B-C).*

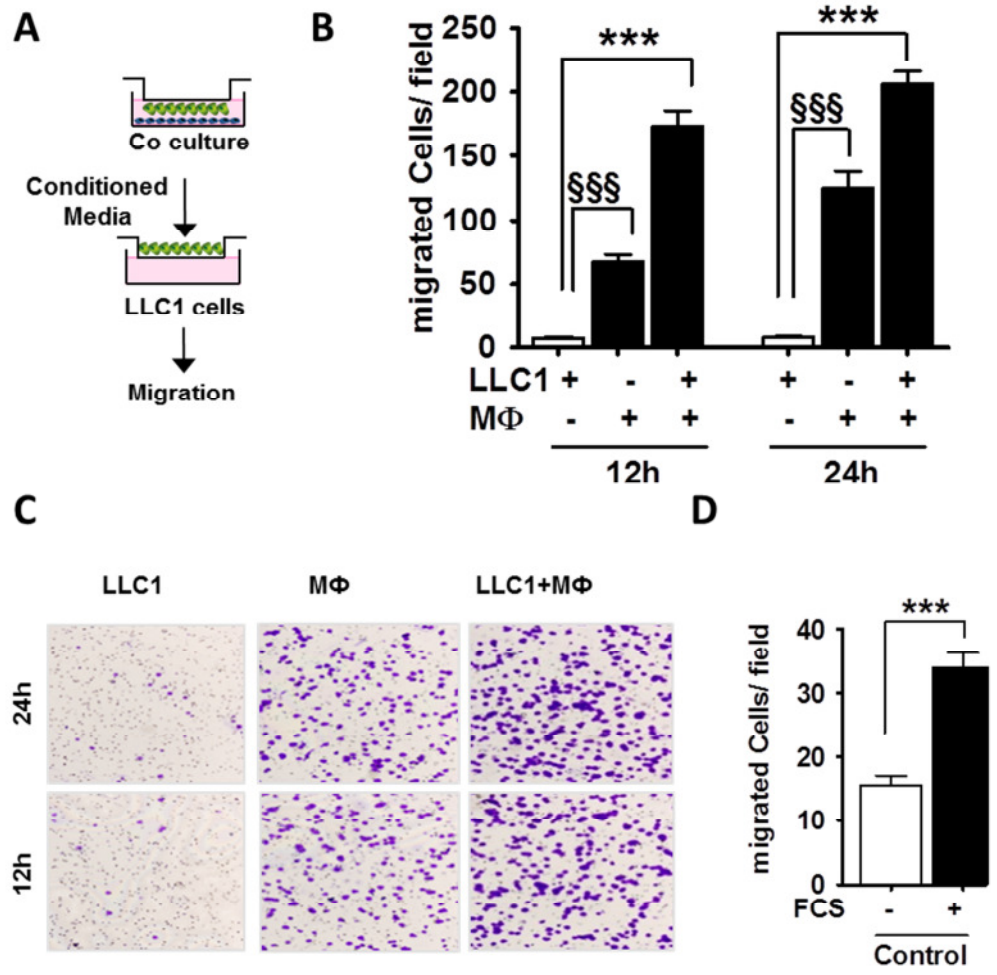

***Figure 24* Effect of CM on LLC1 migration.** (A) Schematic of experimental procedure (B) Migration of LLC1 stimulated with the indicated co-culture CM harvested on the indicated co-culture time points (C) Representative pictures of migrated LLC1 (D) Positive (+) and negative (-) control. All data represent mean ± SEM, n = 4, *p≤0.05, **p≤0.01, *** p≤0.001. * compares LLC1 vs. co-culture, § compares LLC1 vs. MΦ

4.4 Knockdown of CCR2 and CX3CR1 in LLC1

4.4.1 Effect on CCR2 and CX3CR1 expression

To evaluate, if the observed CCR2 and CX3CR1 upregulation has any functional consequences for cancer cells, LLC1 were transduced with empty vector (EV), scramble shRNA (SCR) or shRNA against murine CCR2 or CX3CR1. Additional controls were performed with untransfected cells (UT). Transduced LLC1 were stimulated with either CM from LLC1 alone or co-culture CM, and screened for CCR2 *(Figure 25A)* and CX3CR1 expression (*Figure 25B*). Stimulation with co-culture CM was necessary, since CCR2 is not

basally expressed in LLC1. Analysis of mRNA expression confirmed successful knockdown of CCR2 in shCCR2 transduced cells, and no effects in UT, EV, SCR or shCX3CR1 transduced cells. shCX3CR1 transduced cells did not express CX3CR1 and the upregulation was abolished as well.

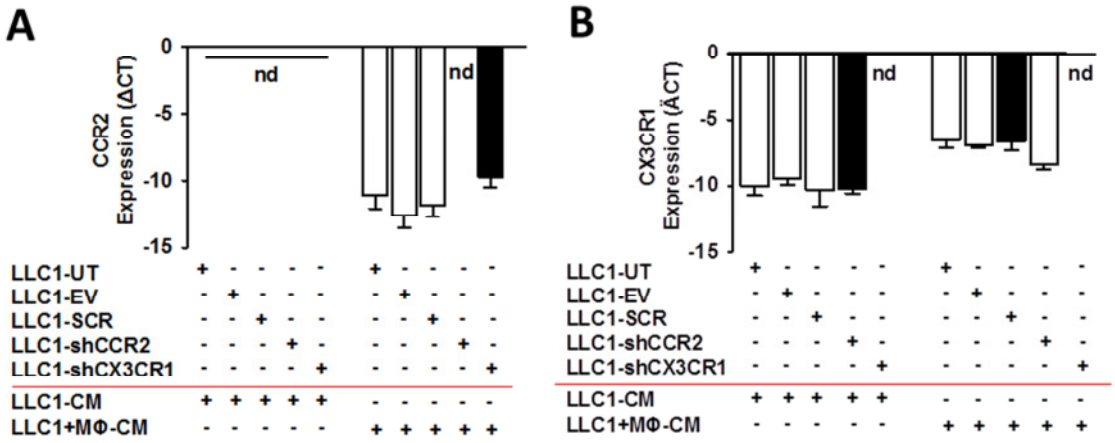

Figure 25 **Knockdown of CCR2 and CX3CR1 in LLC1.** (A) relative mRNA-expression of CCR2 and (B) CX3CR1 after shRNA-mediated KnockDown All data represent mean ± SEM, n = 3, *p≤0.05, **p≤0.01, *** p≤0.001.

4.4.2 Effect on LLC1 proliferation and migration

Transduced LLC1 were then examined using proliferation (*Figure 26A)* and migration assays *(Figure 26B*) to analyze the functional consequences of CCR2 and CX3CR1 upregulation, respectively, on cancer cells. LLC1 were stimulated with CM from either LLC1 or MΦ alone or co-culture. The transduction itself had no effect on LLC1-proliferation. The MΦ CM and co-culture CM induced proliferation was partially, but significantly prevented in shCCR2-transduced cells. The knockdown of CX3CR1 had no influence on proliferation. However, the effects on the migratory response to CM were notable. Interestingly, the migration of shCCR2-transduced cells was already significantly impaired towards MΦ CM. Migration of LLC1 with either CCR2- or CX3CR1-knockdown towards co-culture CM was reduced to less than 30% of any of the controls.

In summary, if the MΦ-induced chemokine receptor upregulation is inhibited with CCR2 or CX3CR1 shRNA, LLC1 lose their ability to response to CM from MΦ and co-cultures, which is an important hint to a functional relevance of the co-culture-induced CCR2 and CX3CR1 upregulation on cancer cells.

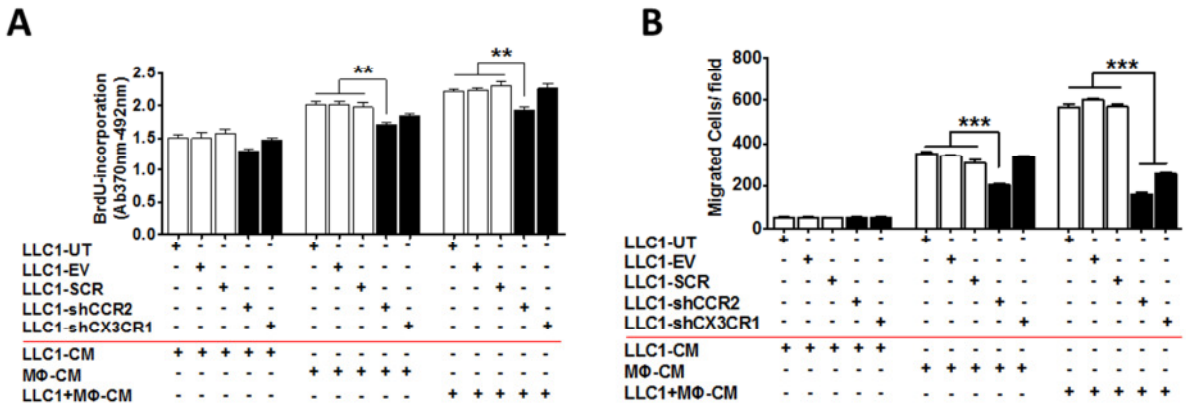

Figure 26 **Knockdown of CCR2 impairs LLC1-proliferation and migration**. (A) Proliferation and (B) Migration of LLC1 after shRNA-mediated Knockdown of CCR2 or CX3CR1 in response to indicated co-culture- or control CM (harvested at 24 h) All data represent mean ± SEM, n = 3, *p≤0.05, **p≤0.01, *** p≤0.001.

4.5 In vitro co-culture of bone-marrow derived CCR2$^{-/-}$ or CX3CR1$^{-/-}$ MΦ with LLC1

4.5.1 Characterization of CCR2$^{-/-}$ and CX3CR1$^{-/-}$ MΦ

Altogether these observations imply a crucial involvement of the CCR2-CCL2 and CX3CR1 axis in lung cancer progression, and raised question as to whether the CCR2 and CX3CR1 receptors have only unipolar involvement in lung cancer cell proliferation and migration or if they also play a role in their original host, MΦ. For this purpose, MΦ were isolated and generated from CCR2$^{-/-}$ or CX3CR1$^{-/-}$ mice and co-cultured with LLC1 as described above. The expression of the classical MΦ-marker F4/80, CD11b, MoMa1 and CD68 were compared to the WT MΦ using ICC. Overall, no difference in quantity or quality of the knockout MΦ was detected (*Figure 27*).

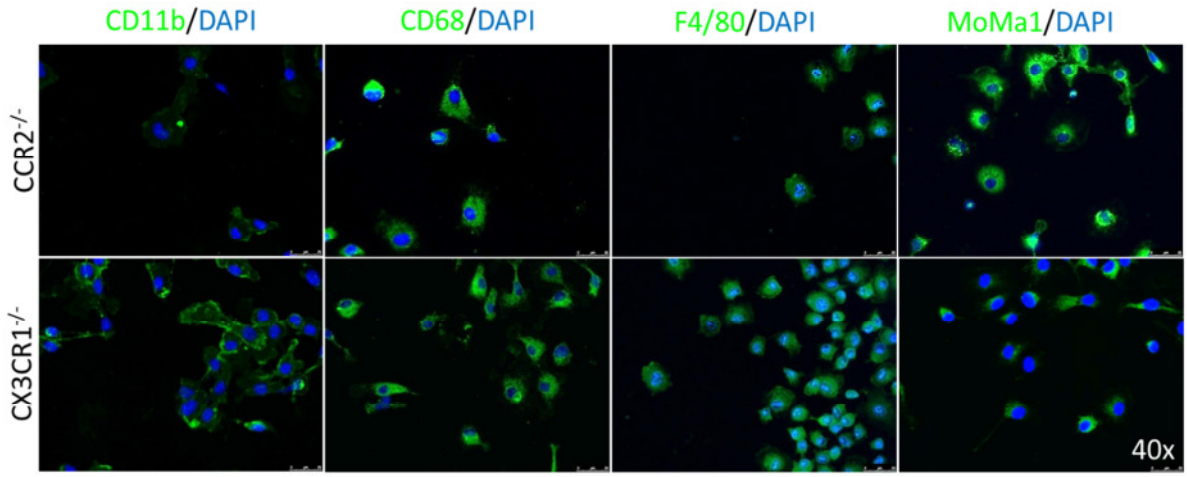

***Figure 27* CCR2$^{-/-}$ and CX3CR1$^{-/-}$ macrophages.** Immunocytochemistry for MΦ-marker CD11b, CD68, F4/80 and MoMa1 (from left to right)

4.5.2 Effect on MΦ polarization

Since MΦ adopt a very potent M2-phenotype after co-culture with LLC1, CCR2$^{-/-}$ MΦ and CX3CR1$^{-/-}$ MΦ were screened for polarization after co-culture with LLC1 as well. Surprisingly, CCR2$^{-/-}$ and CX3CR1$^{-/-}$ control MΦ already displayed a more M1-like phenotype as compared to WT MΦ simply due to the according knockout, with significantly lower expression of arginase and IL-10 and a significantly higher expression of IL-1β in CCR2$^{-/-}$ MΦ compared to WT MΦ. CX3CR1$^{-/-}$ MΦ showed a comparable expression pattern as WT MΦ, but with a significantly higher expression of the M1-marker IL-1β and the M2-marker IL-1RA.

Interestingly, the CCR2 knockout in MΦ significantly prevented co-culture induced MΦ-polarization and the upregulation of all M2-markers was inhibited. Conversely, the downregulation of M1-marker iNOS and TNFα was not prevented. A similar effect was observed in CX3CR1$^{-/-}$ MΦ. The upregulation of M2-marker arginase, chitinase, IL-10 and IL1-RA was significantly abolished, whereas the downregulation of M1-markers iNOS and TNFα was not changed (*Figure 28A-B*). In conclusion, CCR2$^{-/-}$ and CX3CR1$^{-/-}$ MΦ are more resistant to cancer cell-induced M2-polarization and might function in restricting lung cancer cell growth and migration.

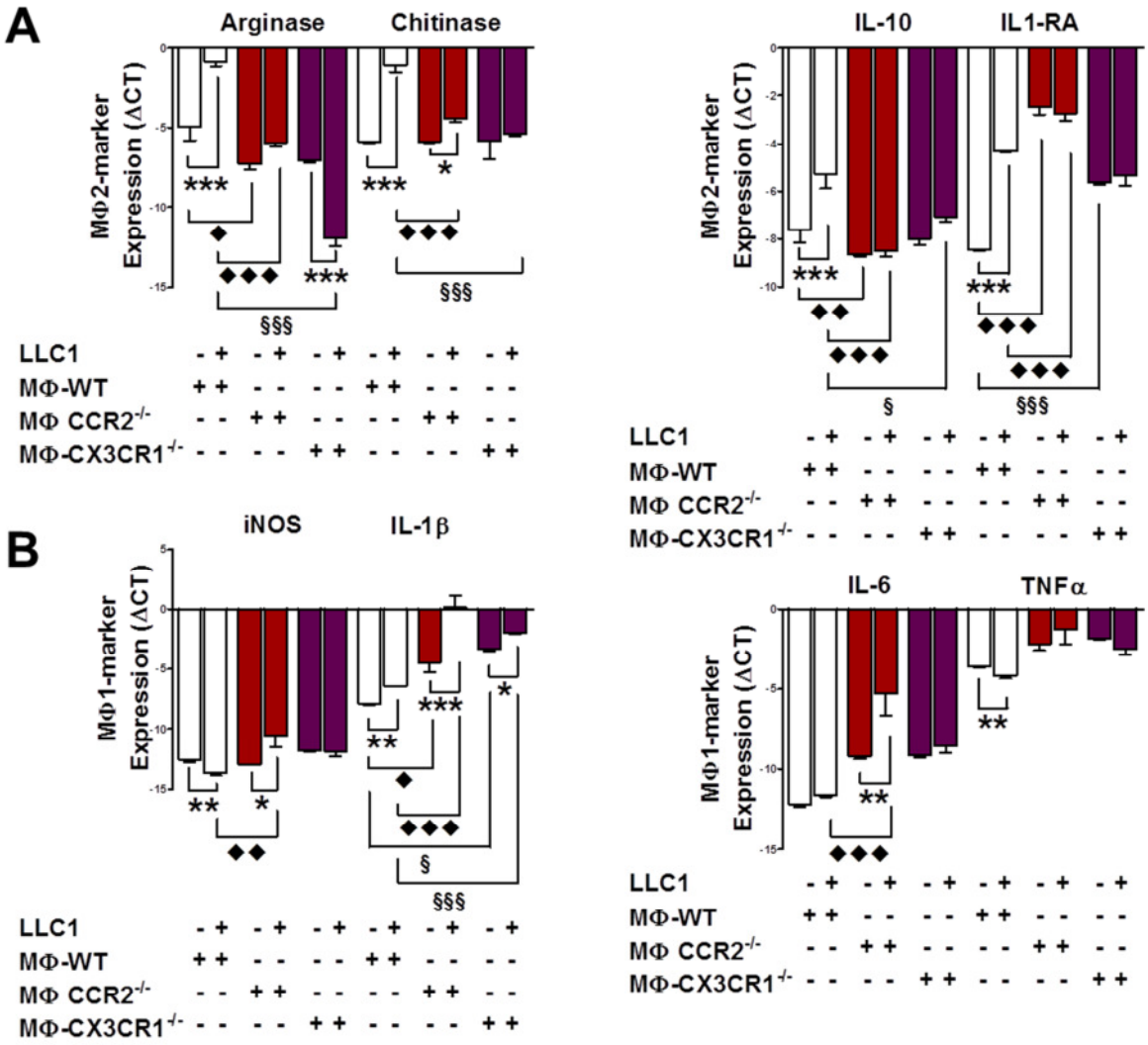

Figure 28 **Effect of CCR2- and CX3CR1-knockout on macrophage polarization.** (A) Relative mRNA levels of M2-marker arginase, chitinase, IL-10 and IL-1RA (B) M1-marker iNOS, IL-1β, IL-6 and TNFα and in WT (white bars), $CCR2^{-/-}$ (red bars) and $CX3CR1^{-/-}$ (purple bars) MΦ before and after co-culture. All data represent mean ± SEM, n = 3, *p≤0.05, **p≤0.01, *** p≤0.001, * WT Control vs. WT Co-culture, ♦ WT vs. $CCR2^{-/-}$,§ WT vs. $CX3CR1^{-/-}$.

4.5.3 Effect on CCR2 and CX3CR1 expression on LLC1

After co-culture of LLC1 with either $CCR2^{-/-}$ or $CX3CR1^{-/-}$ MΦ, LLC1 were isolated and screened for relative mRNA expression levels of CCR2, CCL2, CX3CR1 and CX3CL1.

Interestingly, the expression of CCR2 in LLC1 was no longer detected after co-culture with $CCR2^{-/-}$ MΦ, indicating that the expression of CCR2 is obligatory for the interplay with LLC1. In contrast, the expression of the ligand CCL2 was even higher than compared to WT-co-culture, to compensate for the loss of CCR2 *(Figure 29A-B*). Surprisingly, the induction of

CX3CR1 expression by co-culture was significantly decreased after CCR2$^{-/-}$ co-culture, whereas higher levels of the ligand CX3CL1 were expressed (*Figure 29C-D*).

As seen after CCR2$^{-/-}$ co-culture, the upregulation of CX3CR1 was reduced after CX3CR1$^{-/-}$ co-culture, though not completely abolished. In contrast, the upregulation of the ligand CX3CL1 was highly impaired after CX3CR1$^{-/-}$ co-culture compared to WT co-culture (*Figure 29C-D*).

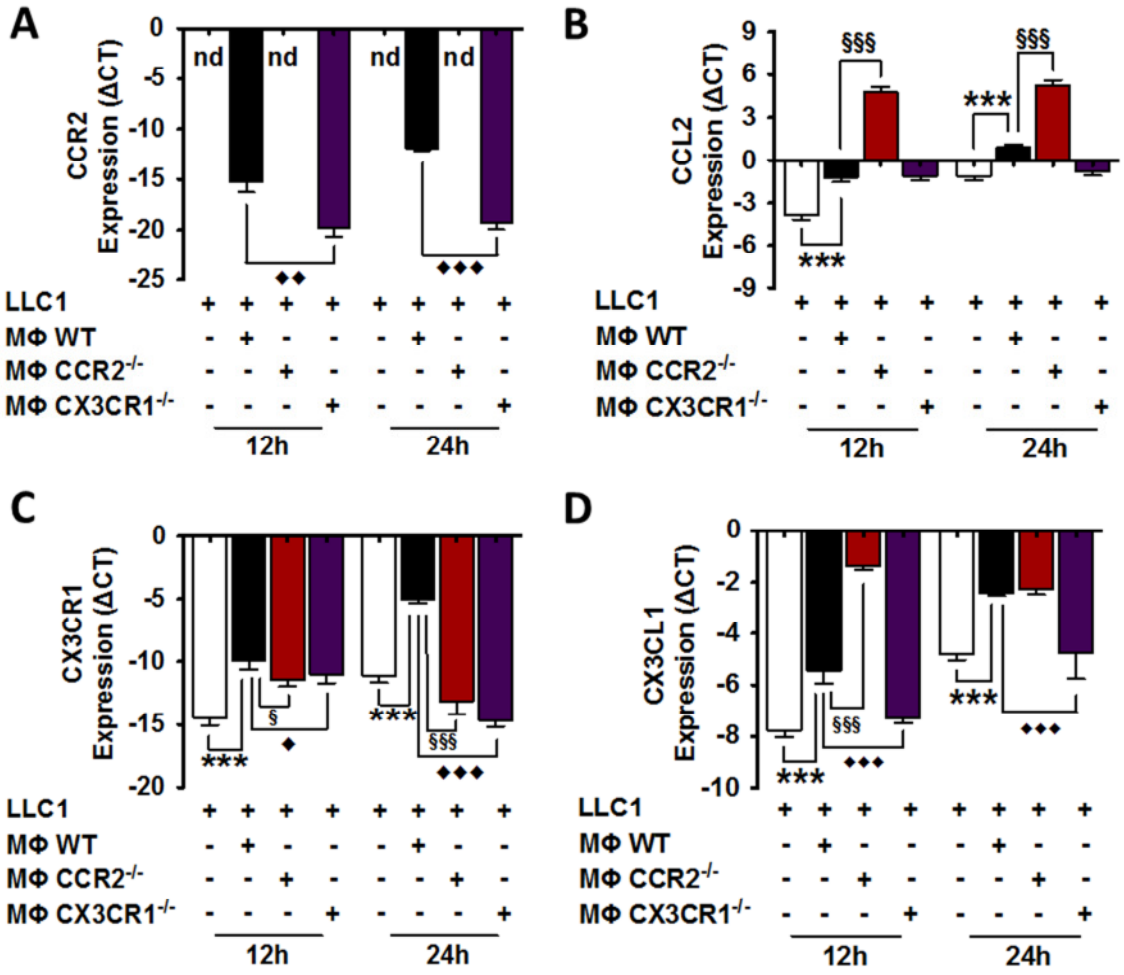

***Figure 29* CCR2 and CX3CR1 expression on LLC1 after co-culture with CCR2$^{-/-}$ and CX3CR1$^{-/-}$ MΦ.** (A) Relative mRNA-expression levels of CCR2, (B) CLL2, (C) CX3CR1 and (D) CX3CL1 on LLC1 after stimulation with indicated CM derived from co-cultures of CCR2$^{-/-}$ or CX3CR1$^{-/-}$ MΦ. All data represent mean ± SEM, n = 3, *p≤0.05, **p≤0.01, *** p≤0.001. * WT Control vs. WT Co-culture, ♦ WT vs. CCR2 $^{-/-}$,§ WT vs. CX3CR1$^{-/-}$.

Interestingly, as observed after CCR2$^{-/-}$ co-culture, the induced upregulation of the second receptor CCR2 was significantly diminished, in CX3CR1$^{-/-}$ co-cultures (*Figure 29C-D*). These observations suggest a synergistic interaction between CCR2 and CX3CR1.

4.5.4 Effect on LLC1 proliferation

Proliferation of LLC1 subjected to CM derived from co-culture with either CCR2$^{-/-}$ or CX3CR1$^{-/-}$ MΦ was significantly reduced after CCR2$^{-/-}$ MΦ and CCR2$^{-/-}$ co-culture CM, though not strongly. Contrary to the observations in the CCR2 knockout, the proliferation of LLC1 after exposure to CX3CR1$^{-/-}$ CM was strongly impaired, with the maximum inhibited proliferation after co-culture CM of 24 h (*Figure 30*).

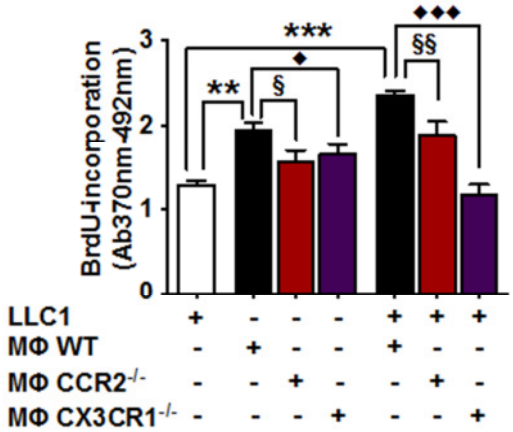

Figure 30 Effect of MΦ-CCR2$^{-/-}$ or MΦ-CX3CR1$^{-/-}$ co-culture CM on LLC1 proliferation. **All data represent mean ± SEM, n = 3, *p≤0.05, **p≤0.01, *** p≤0.001. * WT Control vs. WT Co-culture, ♦ WT vs. CCR2$^{-/-}$,§ WT vs. CX3CR1$^{-/-}$.**

4.5.5 Effect on LLC1 migration

Surprisingly, LLC1 migration was significantly abolished after treatment with CCR2$^{-/-}$ CM compared with WT CM. In particular, the migratory response to CCR2$^{-/-}$ co-culture CM was markedly decreased. The migration of LLC1 after exposure to CX3CR1$^{-/-}$ CM was not impaired after 12 h in both conditions (*Figure 31A).* After 24 h the migration of LLC1 subjected to CX3CR1$^{-/-}$ MΦ-CM and CX3CR1$^{-/-}$ co-culture CM was significantly inhibited, although not as dramatically as exposure to CCR2$^{-/-}$ CM. (*Figure 31*B-C).

Taken together, these results show a substantial impact of MΦ on lung cancer cells in enhancing their proliferation and migration as well changing the basal expression profile of

chemokine receptors. The effects of MΦ on LLC1 are significantly mediated via the CCR2-CCL2 and CX3CR1-CX3CL1 axis.

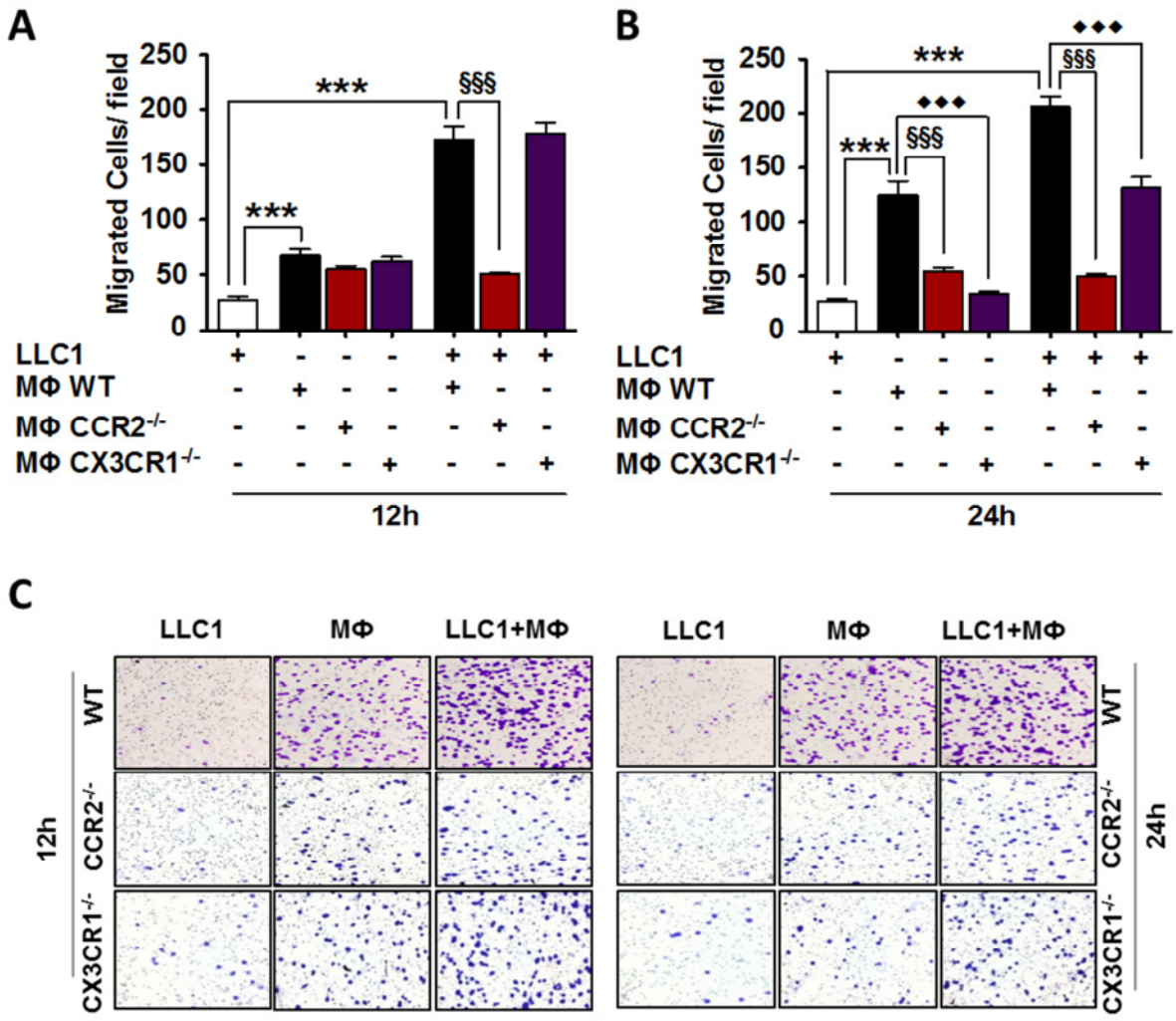

***Figure 31* Effect of MΦ CCR2$^{-/-}$ or MΦ-CX3CR1$^{-/-}$ co-culture CM on LLC1 migration.** (A) LLC1 migration towards CM as indicated after 12 h and (B) 24 h (C) Representative pictures of migrated LLC1. CCR2$^{-/-}$ and CX3CR1$^{-/-}$ are indicating the genotype of co-cultured MΦ. All data represent mean ± SEM, n = 3, *p≤0.05, **p≤0.01, *** p≤0.001, * WT vs. control, § WT vs. CCR2$^{-/-}$, ♦ WT vs. CX3CR1$^{-/-}$.

4.5.6 Effect on MMP and VEGF expression on MΦ

The CCR2- or CX3CR1-knockout in co-cultured MΦ not only affected the LLC1, but also influenced the MMP expression in MΦ. After co-culture with CCR2$^{-/-}$ as well as CX3CR1$^{-/-}$ MΦ the upregulation of the in ovarian and neck cancer progression involved collagenase MMP-8 (Moilanen et al., 2002; Stadlmann et al., 2003) as seen after co-culture with WT MΦ was inhibited, although the upregulation of other MMPs was not influenced. Furthermore,

MMP-8 promotes infiltration of polymorphonuclear cells (Khatwa et al., 2010), which exerts a direct influence on the tumor microenvironment composition.

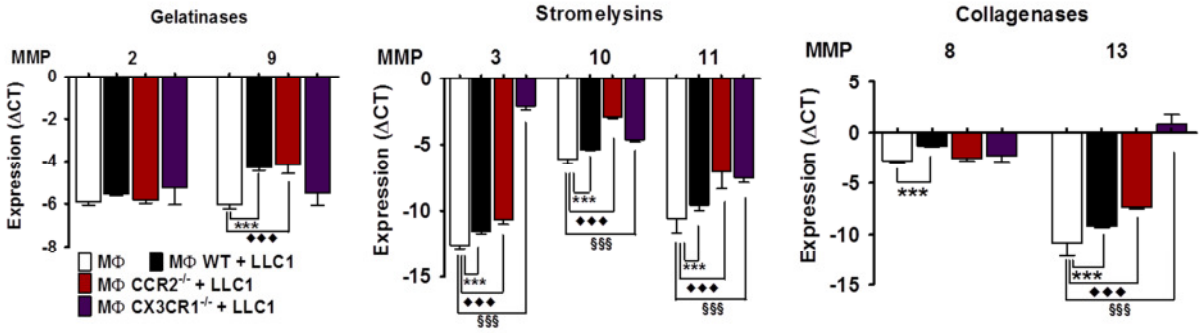

Figure 32 MMP mRNA expression of control or co-cultured MΦ-CCR2$^{-/-}$ or MΦ-CX3CR1$^{-/-}$. All data represent mean ± SEM, n = 3, *p≤0.05, **p≤0.01, *** p≤0.001, * WT vs. control, § WT vs. CCR2$^{-/-}$, ♦ WT vs. CX3CR1$^{-/-}$.

4.6 Primary tumor growth and metastasis in CCR2$^{-/-}$ and CX3CR1$^{-/-}$ mice

4.6.1 Primary tumor growth

To confirm the important role of CCL2 and CX3CL1 in cancer growth, LLC1 were injected s.c. in control and WT mice. After confirmation of tumor growth for 21 days, mice were sacrificed and plasma levels of CCL2 and CX3CL were evaluated using ELISA. As expected, CCL2 and CX3CL1 plasma levels were significantly elevated in tumor bearing mice. This data implies CCL2 and CX3CL1 are released in the blood circulation and are able to administrate systemic effects (*Figure 33A-B*).

To further translate the *in vitro* observations to a living organism, LLC1 were injected s.c. in CCR2$^{-/-}$ and CX3CR1$^{-/-}$ mice and primary tumor growth was monitored over 21 days (*Figure 34A*). As expected, the primary tumor growth was significantly reduced after day 16, with 51% reduction of the final tumor volume and 59% reduction of the tumor weight in CCR2$^{-/-}$ mice compared to WT tumors (*Figure 34*). The measurements with digital calipers were confirmed with µCT scans (*Figure 34)*. The tumor size in CX3CR1$^{-/-}$ mice was markedly reduced compared to the primary tumor growth in CCR2$^{-/-}$ mice, with a decrease of 65% in tumor volume and 60% in tumor weight in CX3CR1$^{-/-}$ compared to WT tumors. These results were confirmed by µCT scans. Notably, µCT pictures of whole resected tumors show a lack of surface vessels (*Figure 34B-D*). Both knockout-mice show a better weight gain by trend

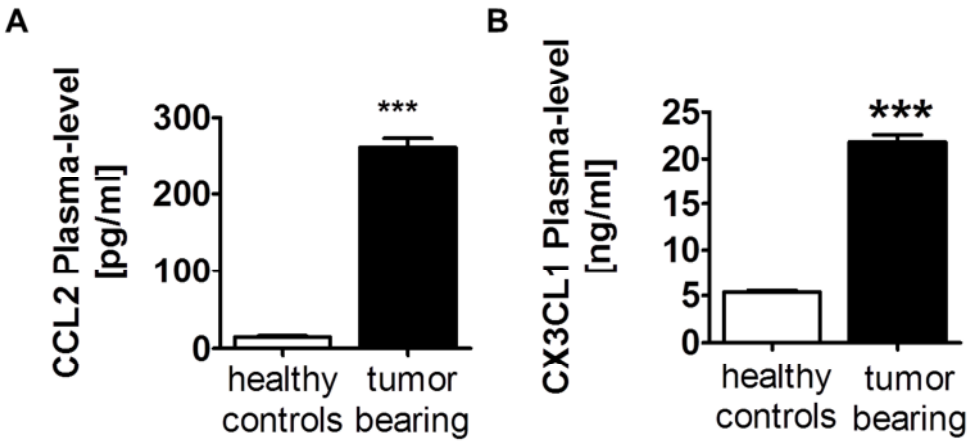

Figure 33 **CCL2 and CX3CL1 plasma level in tumor bearing mice.** (A) Plasma levels of CCL2 and (B) CX3CL1 in lung cancer syngraft models as estimated with ELISA. All data represent mean ± SEM, n = 6, *p≤0.05, **p≤0.01, *** p≤0.001.

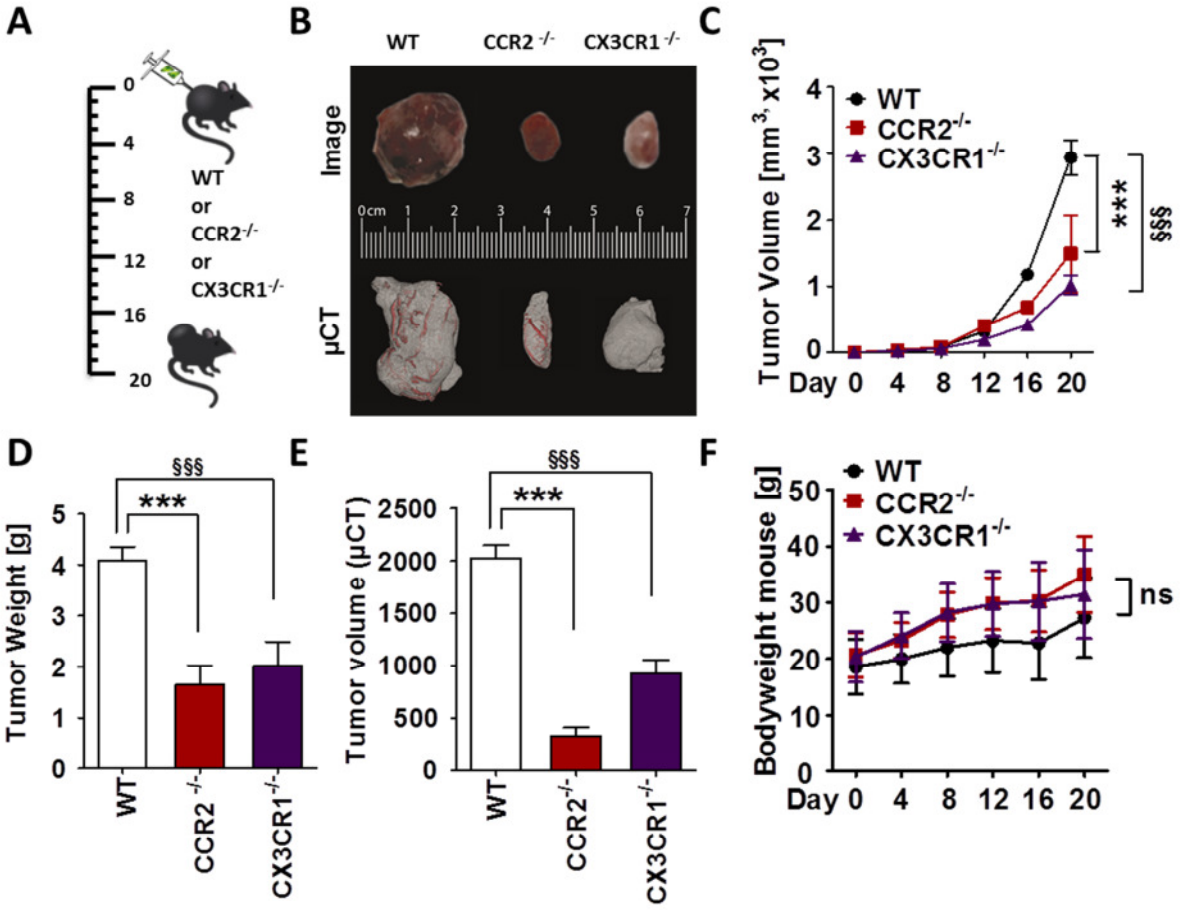

Figure 34 **Primary tumor growths in CCR2$^{-/-}$ and CX3CR1$^{-/-}$ mice.** (A) Schematic of experimental procedure (B) Representative pictures of resected tumors (C) Volume as measured with digital calipers at indicated time points (D) Tumor weight of extracted tumors (E) Tumor Volume as assessed with µCT (F) Bodyweight. All data represent mean ± SEM, n = 15, *p≤0.05, **p≤0.01, *** p≤0.001 * WT vs. CCR2$^{-/-}$,§ WT vs. CX3CR1$^{-/-}$.

than WT mice. However, this effect might be due to the strongly decreased tumor size and does not necessarily reflect a better health condition of the mice (*Figure 34E*).

Immunohistochemical analysis of primary tumor sections showed a significant decrease of $PCNA^+$ tumor cells in $CCR2^{-/-}$ and $CX3CR1^{-/-}$ derived tumors, supporting the observed effects on primary tumor volume and weight (*Figure 35A-B*). To further examine the correlation of infiltrated MΦ with primary tumor growth, accumulated TAMs in the tissue were stained with F4/80 in primary tumor sections. Quantification of MΦ by flow cytometry detected a highly significant reduction of 61% less MΦ in $CCR2^{-/-}$ tumors. Surprisingly, MΦ accumulation in the tumor environment of $CX3CR1^{-/-}$ only decreased by 44%, and was not as marked as in $CCR2^{-/-}$ mice, although the reduction was still very significant (*Figure 35C-D*).

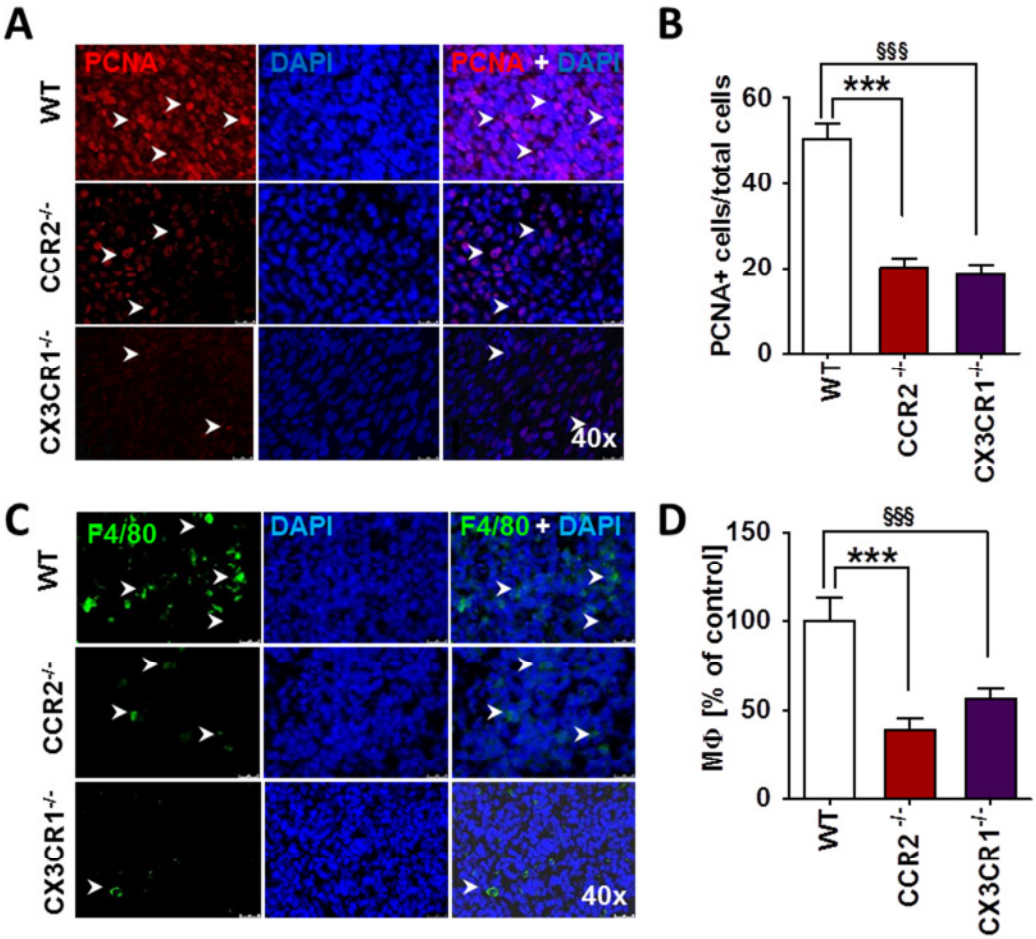

***Figure 35* CCR2$^{-/-}$ and CX3CR1$^{-/-}$ displays less PCNA$^+$ cells and macrophages in the tumor microenvironment.** (A) Immunohistochemistry for PCNA and (B) Quantification (C) Immunohistochemistry for F4/80$^+$ cells (D) Flow cytometric analysis of Macrophage-accumulation in s.c. tumor tissue. White arrows indicate positive cells. Data represent mean ± SEM, n = 6-10, * p≤0.05, ** p≤0.01, *** p≤0.001. 001 * WT vs. CCR2$^{-/-}$,§ WT vs. CX3CR1$^{-/-}$.

Interestingly, the MΦ marker profile of tumors of CCR2$^{-/-}$ mice suggests lower amounts of M2-MΦ in the tumor compared to WT, as the mRNA levels of M2 markers arginase and chitinase are significantly decreased. No changes were detected in the M1 marker iNOS. The MΦ marker profile in CX3CR1$^{-/-}$mice derived tumors was not shifted to M2 markers, as seen in the CCR2$^{-/-}$ tumor tissue, in which none of the MΦ markers were expressed (*Figure 36A*). Furthermore, the chemokine receptor CX3CR1 was strongly decreased in CCR2$^{-/-}$ tumors, whereas the mRNA expression of CCR2 was no longer detected.

These results confirm in vivo that LLC1 require contact with CCR2 expressing MΦ to gain CCR2 expression. CX3CR1 was significantly down regulated in CX3CR1$^{-/-}$ tumors, while CCR2 expression was not changed (*Figure 36B).*

Taken together, these observations in the CCR2$^{-/-}$ and CX3CR1$^{-/-}$ model provide clear evidence, that cancer cells gain CCR2 expression, since the number of the main CCR2 expressing cell population, MΦ, is significantly reduced in the CX3CR1$^{-/-}$ tumors, but CCR2 expression in the tumor microenvironment did not changed. The same observation is true for CX3CR1, since CX3CR1 is detected at the mRNA level in CX3CR1$^{-/-}$ tumors, the only CX3CR1-expressing population can be the LLC1.

To investigate further consequences of impaired MΦ trafficking on the tumor microenvironment, the tumor tissue was screened for VEGF and MMP expression on mRNA level. VEGFs are important for neoangiogenesis and neolymphangiogenesis, two processes that build the foundation for tumor progression and metastasis to distant organs. In CCR2$^{-/-}$ tumors, mRNA expression of VEGFa and VEGFb was significantly decreased, whereas VEGFc levels did not change. None of the VEGF levels were affected in the CX3CR1$^{-/-}$ tumor microenvironment (*Figure 36C*).

Screening for MMP expression revealed a significant decrease of MMP-2, MMP-3, MMP-8 and MMP-10 expression in tumors derived from CCR2$^{-/-}$ mice. In contrast, only MMP-2 and MMP-3 showed reduced expression in CX3CR1$^{-/-}$ tumor tissue compared to WT. Conversely, MMP-9 was upregulated in the CX3CR1$^{-/-}$ tumor microenvironment (*Figure 36D-F*). To unravel a possible mechanism of MΦ action on tumor growth, contrast fluid filled tumors were scanned with μCT and nanoCT to visualize the vascularization. The primary interest was if the total vessel volume in relation to the total volume was impaired in the knockout animals, compared with vessel volume/total volume ratios of the WT tumors. The macroscopic vasculature evaluated with μCT, showed a trend of alteration in CCR2$^{-/-}$ mice,

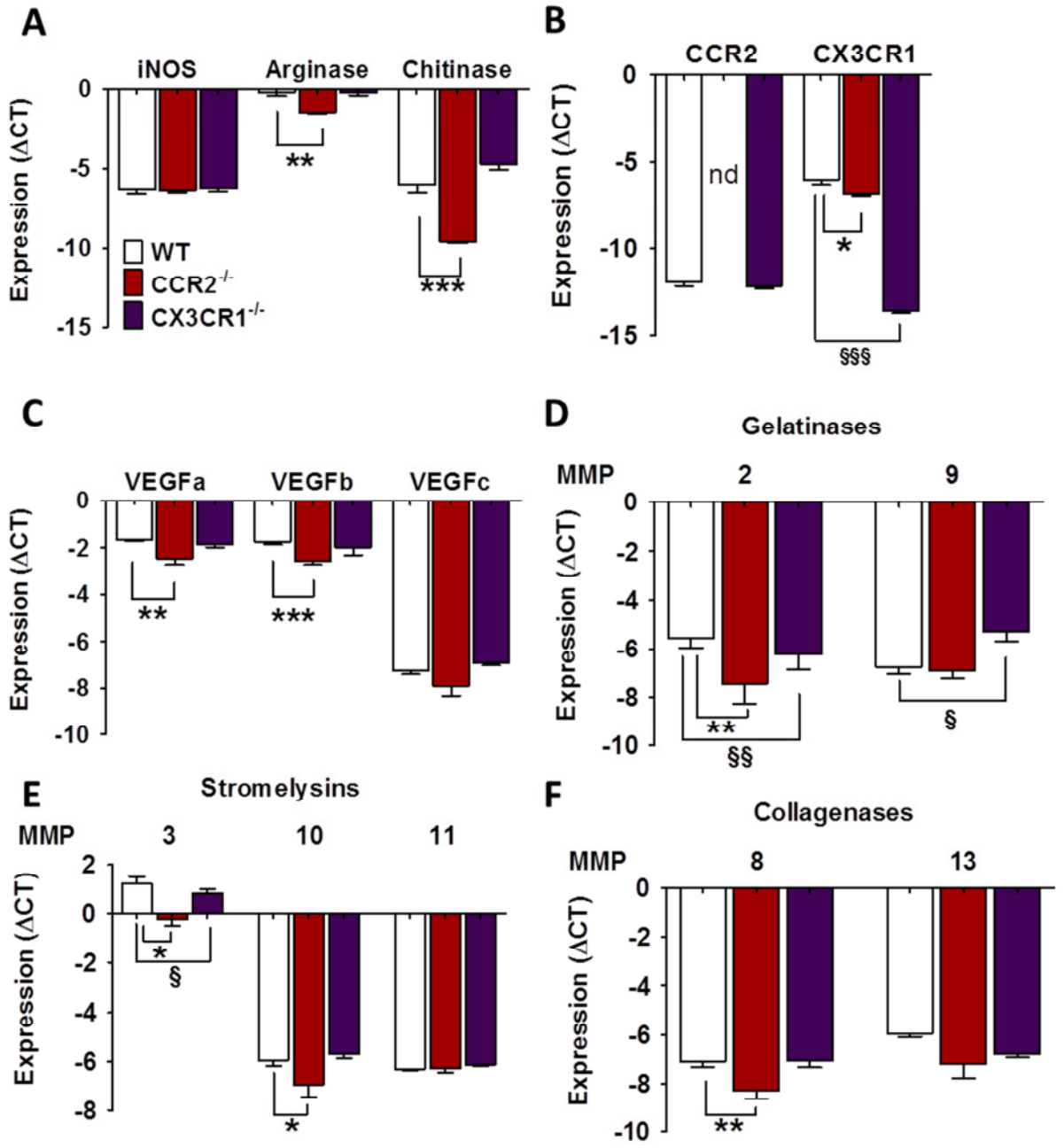

Figure 36 **mRNA expression profile in tumors derived from CCR2$^{-/-}$ and CX3CR1$^{-/-}$ mice reflects a less invasive tumor microenvironment.** (A) Relative mRNA expression levels of MΦ-polarization marker (B) Chemokine receptors (C) VEGFs (D) Gelatinases (E) Stromelysins and (F) Collagenases. All data represent mean ± SEM, n = 6, *p≤0.05, **p≤0.01, *** p≤0.001. 001 * WT Control vs. CCR2$^{-/-}$,§ WT vs. CX3CR1$^{-/-}$.

but changes were significant in CX3CR1$^{-/-}$ mice, in which the vessel network was overall poorly developed (*Figure 37A-B*). A far more drastic effect was found after analysis with the nanoCT. The microvessel supply, given as a ratio of the total vessel volume/total volume, was massively decreased in CCR2$^{-/-}$ and CX3CR1$^{-/-}$ derived tumors, compared to WT-derived tumors (*Figure 37A-C).* This resulted in a broader vessel distribution, as represented by the

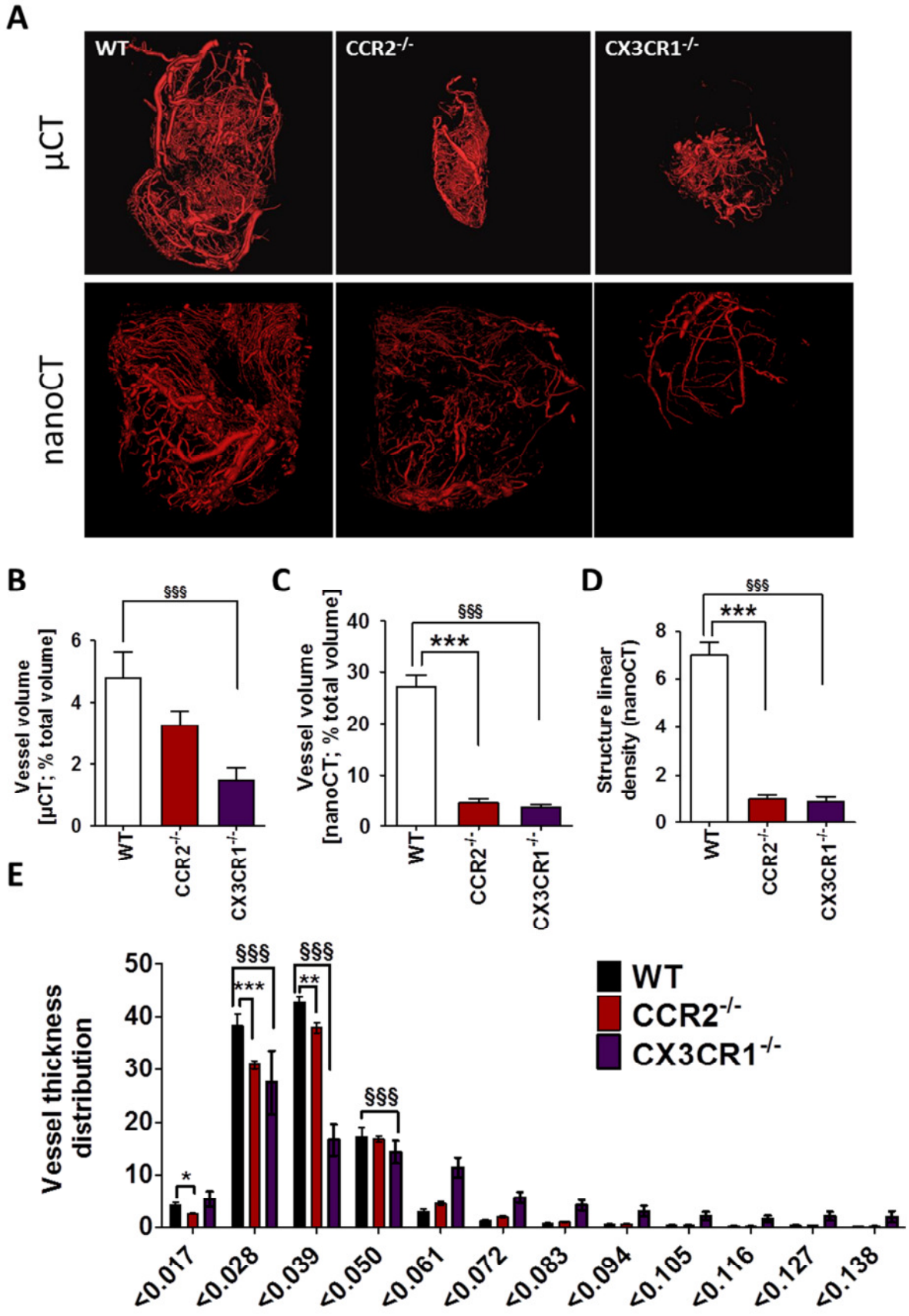

Figure 37 **Vascularization in CCR2$^{-/-}$ and CX3CR$^{-/-}$mice derived tumors**

***Figure 38* Vascularization in CCR2$^{-/-}$ and CX3CR$^{-/-}$mice derived tumors:**

(A) 3D-reconstructions of the vessel network in WT, CCR2$^{-/-}$ and CX3CR1$^{-/-}$ derived tumors. Upper panel: µCT-scans, representing macrovasculature, lower panel: nanoCT, representing microvasculature (B) Total vessel volume as assessed with µCT and (C) nanoCT (D) structure linear density, represents vessel distribution within the tumor (E) Vessel fractions according to their size. All data represent mean ± SEM, n = 3-8, *p≤0.05, **p≤0.01, *** p≤0.001, * WT vs. CCR2$^{-/-}$; § WT vs. CX3CR1$^{-/-}$.

parameter "structure linear density", which leads to a higher probability of inadequately supplied tumor areas, which in turn leads to an inhibited tumor growth (*Figure 37D).* In line with the findings described above in the CL-depleted model, mainly the vessels of sizes of 0.017-0.039 mm^2 are significantly decreased in the microenvironment of CCR2$^{-/-}$ mice and vessels of sizes of 0.017-0.050 mm^2 in the CX3CR1$^{-/-}$ tumors, suggesting that MΦ have mainly impact on the nurturing microvasculature (*Figure 37E*).

Altogether, these results show a clear involvement of MΦ in tumor growth. Remarkably, the interruption of chemotactic pathways such as CCR2 and CX3CR1 results in an effect comparable to the complete systematic depletion of MΦ. Given that CCR2 and CX3CR1 can serve as potential new drug targets for lung cancer, this knowledge is very criticle, as a systemic depletion of MΦ in patients is not practicable.

4.6.2 Lung metastasis formation in CCR2$^{-/-}$ and CX3CR1$^{-/-}$ mice

The massive effect of CCR2 or CX3CR1 knockout on tumor vessel supply suggests a similar effect on metastasis formation, since intravasation of cancer cells into the tumor supplying vasculature is one of the initial steps of distant metastasis. To investigate the effects of CCR2$^{-/-}$ or CX3CR1$^{-/-}$ on lung metastasis, the tumor relapse model was used after s.c. LLC1 injection in the according knockout mice (*Figure 39A*). In both knockouts, lung metastasis derived from the primary s.c. tumor was significantly decreased. This was reflected in the number of macroscopic, peripheral nodules on the lung surface, as well as the total metastasis as analyzed in H&E stained sections. The vessel structure in metastatic nodules appeared worse compared to healthy tissue as visualized with µCT. A similar worse vessel structure was already observed in the according primary tumors, thus these results again confirm the influence of CCR2$^{-/-}$ and CX3CR1$^{-/-}$ on the tumor vessel supply (*Figure 39B-D*). The reduced metastasis leads to a significantly better survival of the CCR2$^{-/-}$ and CX3CR1$^{-/-}$ mice compared to WT mice. The median survival for WT mice was 22 ± 1.3 days, compared to CCR2$^{-/-}$ with 29 ± 2.6 days and CX3CR1$^{-/-}$ mice with 33 ± 0.88 days (*Figure 39E*).

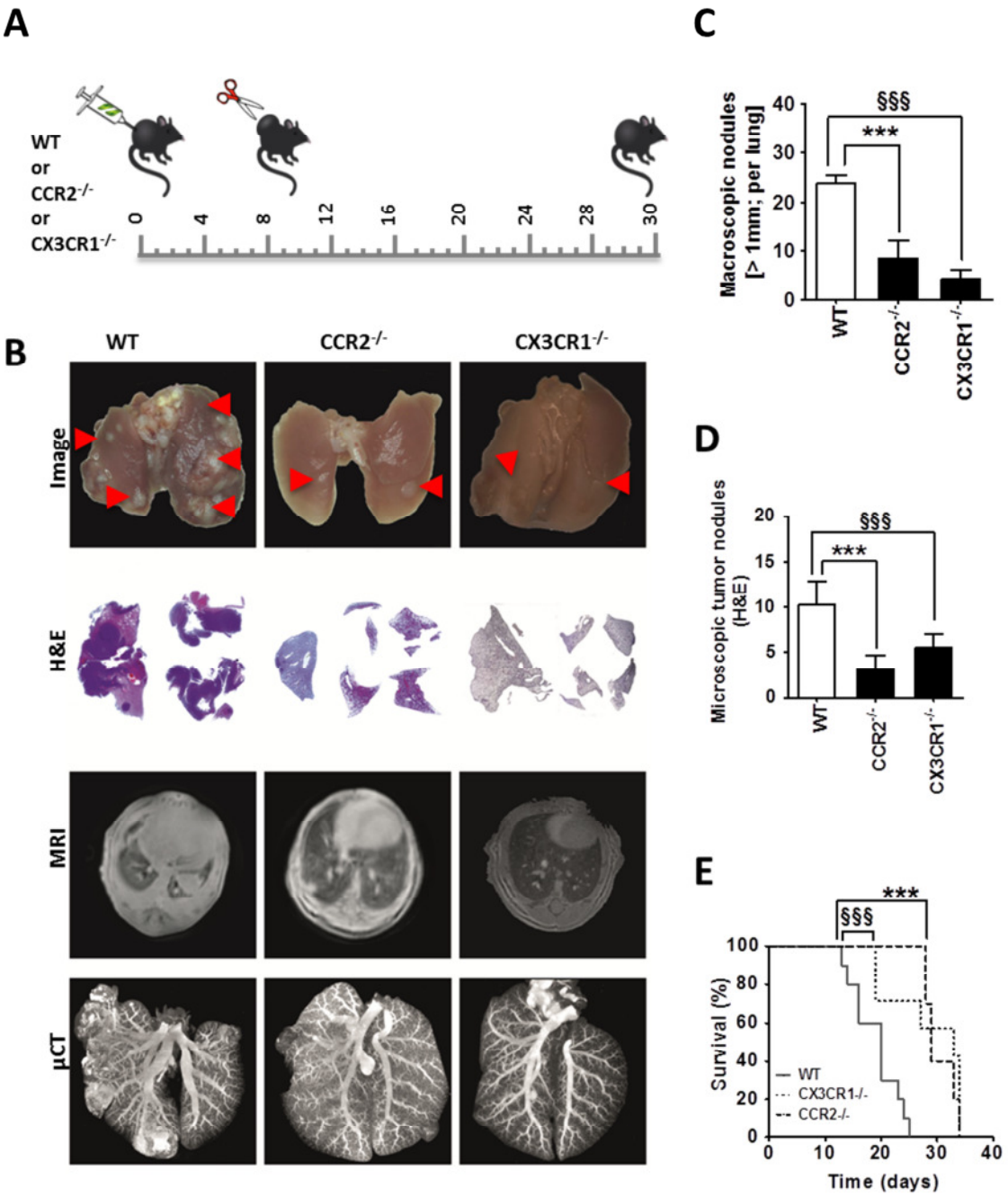

Figure 39 **Impaired lung metastasis formation in CCR2$^{-/-}$ and CX3CR1$^{-/-}$ mice.**

(A) Schematic of the experimental procedure (B) Representative picture of extracted lungs, H&E stained lung sections, MRI assessed lungs and 3D-reconstructions from µCT-scanned lungs (from up to down) (C) Number of macroscopic nodules found on the lung surface (D) Microscopic and Macroscopic nodules detected in H&E stained lung sections (E) Survival of CCR2$^{-/-}$, CX3CR1$^{-/-}$ and WT mice. All data represent mean ± SEM, n = 3-8, *p≤0.05, **p≤0.01, *** p≤0.001, * WT vs. CCR2$^{-/-}$; § WT vs. CX3CR1$^{-/-}$.

To evaluate the connection between lung metastasis formation and MΦ accumulation, MΦ were quantified in healthy lungs, and tumor sections from WT, CCR2-/- or CX3CR1-/- lungs. MΦ infiltration is represented as the ratio of F4/80+ to total cells, and the ratio was

significantly less in metastatic lung nodules in CCR2-/- and CX3CR1-/- lungs. Notably, the MΦ accumulation in CCR2-/- was again more marked in CX3CR1-/- mice, although overall not as strong as in the primary tumor model, due to already existing resident alveolar MΦ (Figure 40A-B).

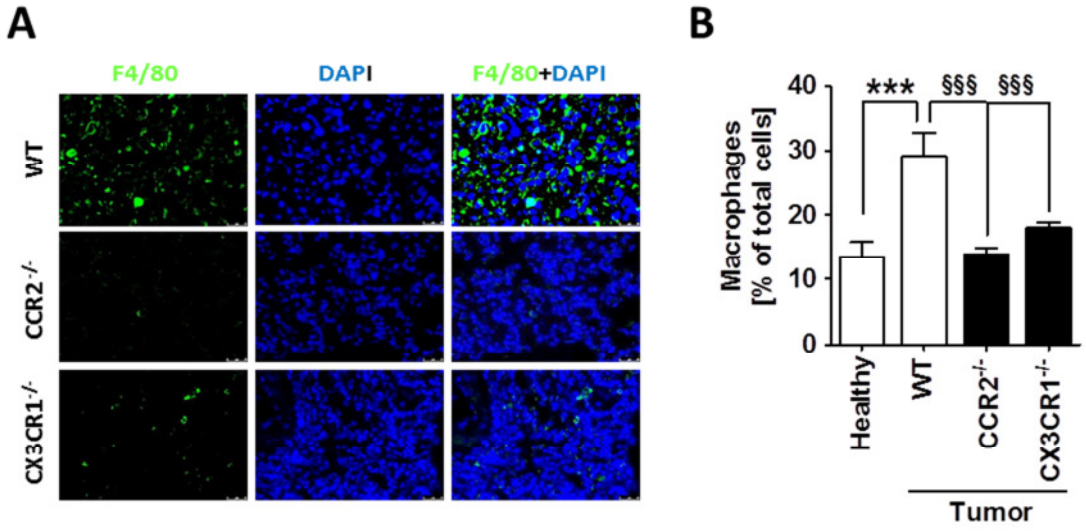

***Figure 40* MΦ accumulation in metastatic lung nodules.** (A) Immunohistochemistry for F4/80 in metastatic nodules in lungs derived from the indicated genotype and (B) Quantification. All data represent mean ± SEM, n ≥ 8, *p≤0.05, **p≤0.01, *** p≤0.001, * Healthy vs. WT, § WT vs. $CCR2^{-/-}$ or $CX3CR1^{-/-}$.

4.7 CCR2 and CX3CR1 expression on human lung cancer cell lines and correlation with tumor stage and metastasis in human lung cancer patients

4.7.1 CCL2 and CX3CL1 expression on human lung cancer cell lines

To evaluate the relevance of CCR2/CX3CR1-upregulation for lung cancer in general, we screened 10 human lung cancer cell lines for CCR2-CCL2 and CX3CR1-CX3CL1 expression. Importantly, CCR2 was not detected in any cell line, CX3CR1 was detected on very low levels (data not shown), whereas all cell lines expressed both ligands, CCL2 and CX3CL1 on different levels. This actuality supports the transferability of the observations made with mouse cell lines and models. Notably, squamous cell carcinomas (H520, H226) show overall the highest and large-cell lung cancers (H66a1, H460) the lowest CCL2-expression (*Figure 41A*). No major differences of CX3CL1 expression were observed between histological lung cancer subtypes (*Figure 41B*).

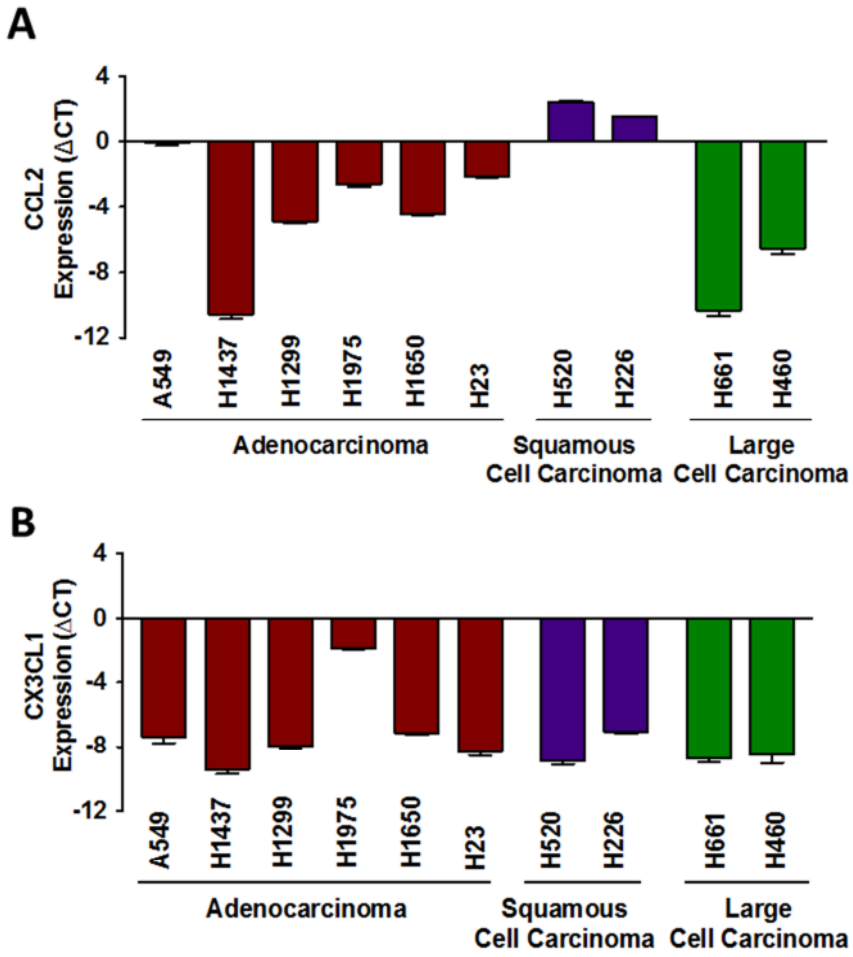

Figure 41 CCL2 and CX3CL1 expression on human lung cancer cell lines. (A) relative mRNA levels of CCL2 and (B) CX3CL1

The four cell lines with the highest CCL2-expression (two adenocarcinomas: A549, H23; and two squamous cell carcinomas: H226, H520), were chosen for further experiments. All cell lines were co-cultured with human MC-derived MΦ and a substantial, co-culture-mediated induction of CCR2-expression was detected in all cell lines, with the overall strongest induction in A549. Notably, mRNA-levels of CCL2 were significantly upregulated after co-culture in all cell lines compared to control (*Figure 42A and B*). Though, CX3CR1-expression was significantly upregulated in H23 and H520 but not in H226 and A549. The according ligand CX3CL1 was significantly upregulated in A549, H23 and H520 but not H226 (*Figure 42C and D*).

These results confirm the importance of CCR2-CCL2 and CX3CR1-CX3CL1 axes for human lung cancer.

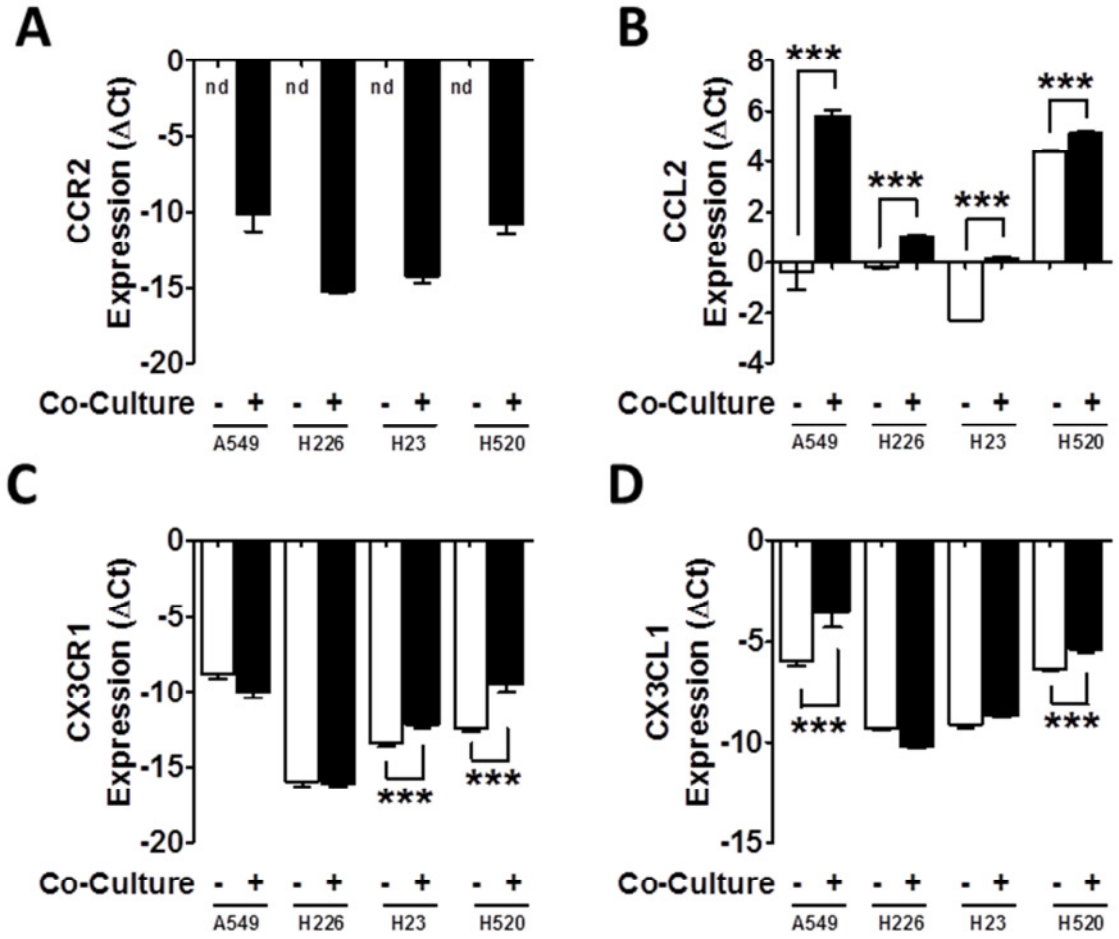

Figure 42 CCR2 onset and CX3CR1 upregulation after co-culture with MΦ. (A) Relative mRNA expression of CCR2, (B) CCL2, (C) CX3CR1 and (D) CX3CL1 on different human lung cancer cell lines. All data represent mean ± SEM, n = 3, *p≤0.05, **p≤0.01, *** p≤0.001.

4.7.2 MΦ accumulation in tumor sections of lung cancer patients

To assess the significance of our results for human lung cancer patients, 72 samples of human adenocarcinoma and squamous cell carcinoma sections were stained with CD68. Positive cells were counted and normalized to the total cell number. In adenocarcinoma and squamous cells carcinoma, the number of $CD68^+$ cells strongly correlates with the tumor stage. As early as stage I carcinoma, more MΦ accumulated compared to healthy lungs. In contrast, there was no significant MΦ accumulation in the tumor tissue suggesting that MΦ seem to play a minor role in small cell lung cancer (*Figure 43A-B*). Importantly, the amount of $CD68^+$ cells in the primary tumor also correlated with the metastastic stage, confirming the *in vivo* observations in the mouse models (*Figure 43C*).

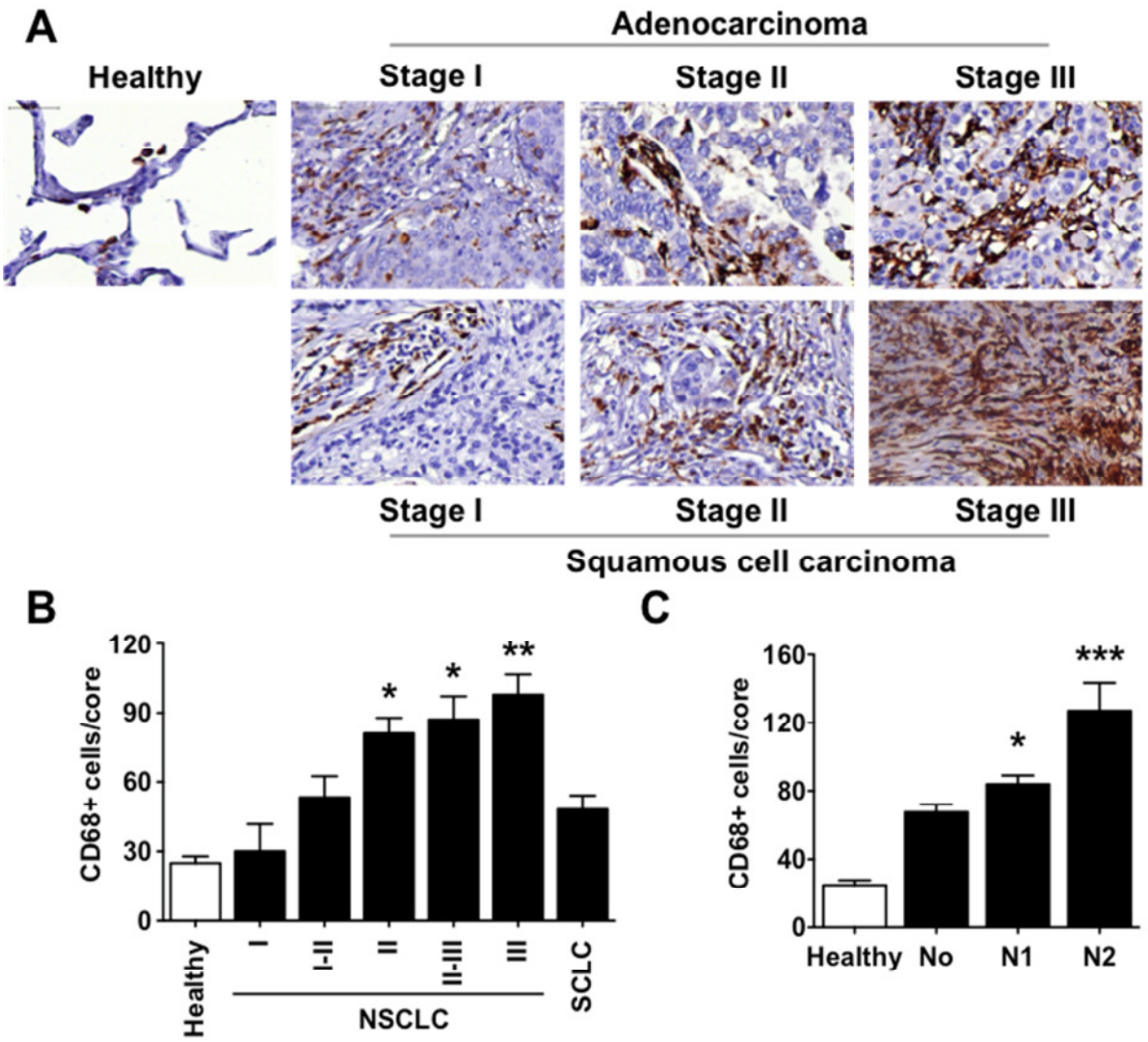

Figure 43 **Tumor infiltration of MΦ in lung cancer patients.** (A) Immunohistochemistry for $CD68^+$ cells in lung cancer sections with different state (B) MΦ-accumulation in relation to the lung cancer stage (C) and to the metastatic stage. All data represent mean ± SEM, n = 12, *p≤0.05, **p≤0.01, *** p≤0.001.

4.7.3 MΦ become $CCR2^+$ depending on lung cancer stage and metastatic status

Furthermore, the accumulated MΦ in the tumor tissue become more $CCR2^+$ in depending on the stage of adenocarcinoma and squamous cell carcinomas underlying the importance of this signaling pathway. Again this mechanism appears to play no role in SCLC (*Figure 44A-B*). Additionally, the MΦ in the primary tumor stroma become more $CCR2^+$ in correlation with the metastatic stage (*Figure 44C*). Importantly, in advanced lung cancer stages, lung cancer cells also become $CCR2^+$. Altogether these results show the importance and negative involvement of MΦ and $CCR2^+$ cells in lung cancer development.

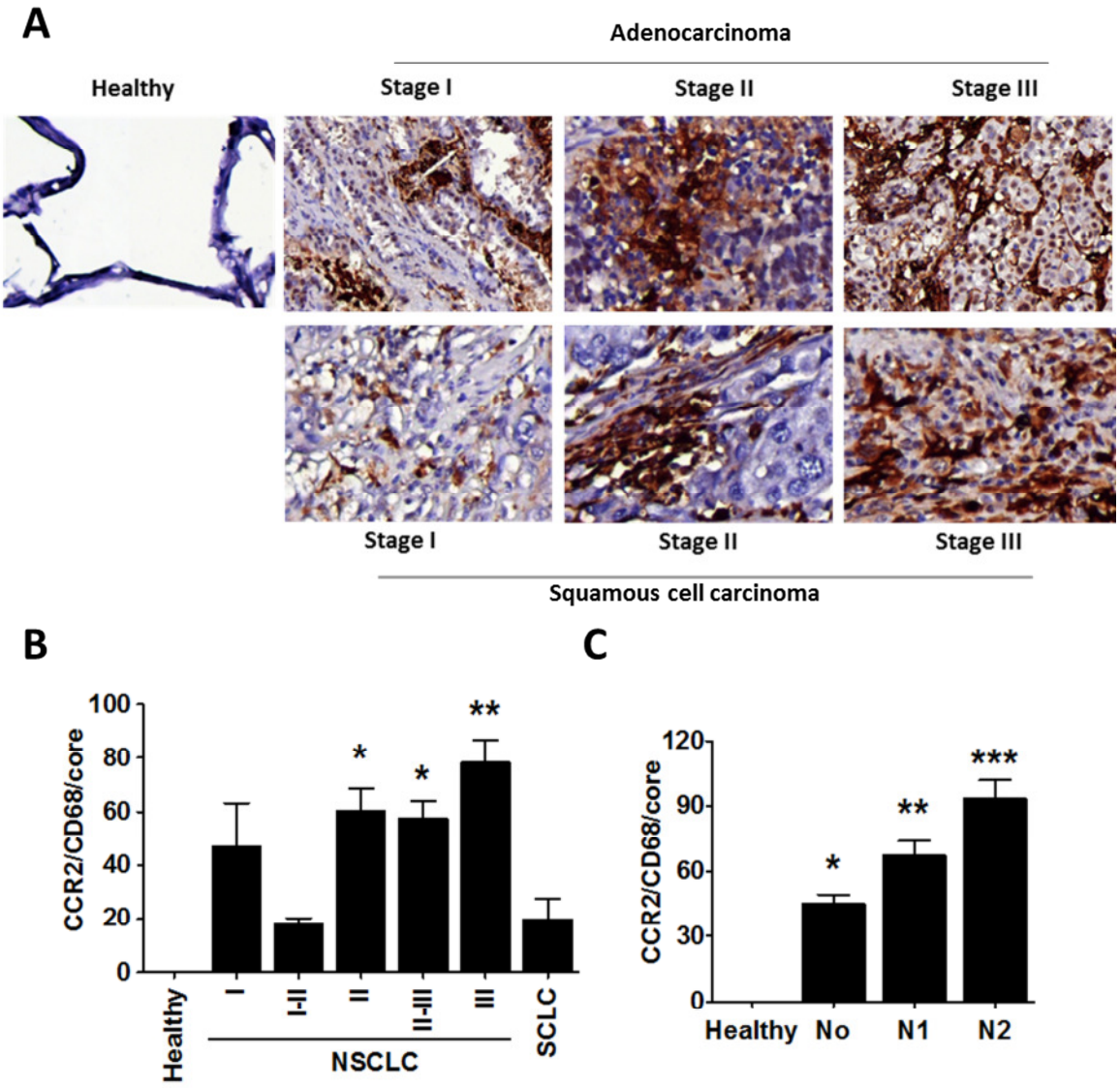

***Figure 44* CCR2 expression on tumor infiltrating MΦ.** (A) Immunohistochemistry for $CCR2^+$ cells in lung cancer sections with different state (B) $CCR2^+$ MΦ in relation to total MΦ in relation to the lung cancer stage (C) and to the metastatic stage. All data represent mean ± SEM, n = 12, *p≤0.05, **p≤0.01, *** p≤0.001.

5 Discussion

5.1 MΦ depletion in primary tumor growth and metastasis

This study reports an outstanding involvement of MΦ in lung cancer development and metastasis. A highly significant correlation between MΦ infiltration in areas with primary tumor growth and metastasis was demonstrated in two independent models of systemic MΦ depletion. These observed effects were associated with a changed microvasculature and a highly damaged vessel structure. Moreover, dramatic changes in the tumor microenvironmental expression patterns of MMPs, VEGFs and MΦ-markers were observed. MΦ have been reported to be one of the most prevalent cell types in the tumor microenvironment (Kelly et al., 1988). Their influence on cancer progression was previously demonstrated for several cancer types such as breast cancer, colon cancer, melanoma and urethane-induced cancer (Gazzaniga et al., 2007; Zaynagetdinov et al., 2011), but only little is known regarding their role in lung tumor formation. In the present study, the crucial role of MΦ in lung cancer development and metastasis was confirmed.

The model of MΦ-depletion with CL-administration is well-established but is strongly dependent on the injection route. The chosen intraperitoneal application depletes phagocytosing MΦ derived from bone marrow, in the spleen, liver, some lymph nodes, in the peritoneal cavity and the circulation (van Rooijen et al., 1997; van Rooijen and van Kesteren-Hendrikx, 2002). Since CL cannot cross intact vessel barriers, CL was additionally injected directly into the tumor to sustain a very successful MΦ depletion. However, in the tumor microenvironment, the expression of the typical M1-polarization marker iNOS was increased, indicating that the remaining MΦ are M1-MΦ with tumor-restrictive activity. Further, iNOS can be expressed by other cell types such as lymphocytes and vascular endothelial cells (Leifeld et al., 2002). To conclude, whether M1-phenotype MΦ are responsible for increased iNOS expression in the tumor microenvironment or other iNOS-expressing cells are elevated further analysis is required (e.g. IHC for F4/80 and iNOS double positive cells). A high expression of arginase-1 in MΦ is associated with an anti-inflammatory and angiogenetic activities and thus a tumor promoting M2-phenotype (De Palma et al., 2005; Pucci et al., 2009). Another high arginase-expressing cell population are fibroblasts, in which arginase functions in collagen synthesis (Kitowska et al., 2008). Since fibroblasts are not affected by

CL-administration, the lower arginase expression in the tumor microenvironment might support the finding of a higher percentage of M1-MΦ of the remaining MΦ-population.

In addition to the strong restriction of primary tumor growth in CL-depleted mice, a strong decrease of metastatic nodules in the lung was observed in the metastatic model. The reduced number of lung metastasis could be a secondary effect to the reduced primary tumor growth. Although the tumor size measured on day 10 (the day of primary tumor removal in the metastatic model) showed no difference between control and CL-treated groups, the tumor microenvironment of control mice could be already in a different state of activation compared to the CL-treated tumor microenvironment. In this context, the significant downregulation of several MMPs, as observed in the CL-depleted primary tumor model, may have contributed to the strongly impaired formation of metastatic nodules in the lung. In particular, expression of the stromelysins was impaired in primary tumors of CL-treated mice, an MMP subgroup that functions in the breakdown of basement membranes and extracellular matrix proteins, was impaired in primary tumors of CL-treated mice. MMP-3, -10 and -11 are strongly associated with metastasis (Delebecq et al., 2000; Gill et al., 2004; Justilien et al., 2012). Both MMP-9 and MMP-13 were also downregulated, and MMP-13 is the only MMP that is known to be able to break down triple helical collagen structures, such as those found in cartilage and bones. Together with the fact that after the brain, bones are the second-most frequent site of metastasis for all lung cancer subtypes (Quint et al., 1996), this suggests a crucial role of MMP-13 in lung cancer progression and metastasis. Thus far, the role of MMP-13 was described in the development of breast-to-bone metastasis, and interestingly, the bone metastasis-promoting activity of MMP-13 involves the activation of MMP-9, which is significantly downregulated in CL-treated primary tumors as well (Morrison et al., 2011; Nannuru et al., 2010; Pivetta et al., 2011).

Analysis of vessel supply and density revealed a remarkable decrease in macro- and microvasculature in CL-treated mice. The lack of a proper vessel supply, and thus adequate oxygen and nutrition, is important for primary tumor growth as well as for metastasis formation, since the intravasation of cancer cells in the systemic vasculature is the initiating step of metastatic spread. Angiogenesis is induced by members of the VEGF family (placental growth factor (PIGF), VEGFa-VEGFd), four members of the angiopoietin family (Ang1-Ang4) and at least one member of the ephrin family (Ephrin B2). Further tumor neoangiogenesis can be induced by less-specific growth factors, such as PDGFβ, TNFα, IL-8 and bFGF (Rehman and Jayson, 2005; Yancopoulos et al., 2000). Tumors of the CL-treated

mice exhibited significantly lower expression of VEGFc, which might be directly related to the decreased number of accumulated MΦ, since MΦ are a source for VEGFs and angiogenesis is triggered by a loop in which VEGF itself acts as a chemoattractant for monocytes, which in response secrete further VEGF. The correlation between VEGF expression in tumors and MΦ accumulation was previously demonstrated for breast cancer (Barleon et al., 1996; Grunewald et al., 2006; Leek et al., 2000). Moreover, VEGFc was shown to be important for lymph angiogenesis and importantly, like VEGFa, VEGFc binds to VEGFR-2 (Flk1, vascular endothelial growth factor receptor 2), which is the main receptor responsible for VEGF-mediated actions such as endothelial cell migration and angiogenesis. Furthermore, VEGFc was recently described to be the main angiogenetic factor in cancer. A properly developed microvessel density (MVD) promotes tumor progression and gives rise to metastatic spread (Carroll et al., 2013; Terme et al., 2013). However, other members of the VEGF family are not altered, so the screening should be extended to include the previously mentioned vascular growth factors. Furthermore, cancer cells secrete abundant levels of VEGF as well, which might adjust the lack of MΦ-secreted VEGF (Murdoch et al., 2004).

It is known that tumor vessels can be leaky with heterogeneous flow profiles, since the stabilizing maturation phase is missing (Dewhirst, 1998; McDonald and Choyke, 2003). This effect on the vessel structure was even worse in the CL-depleted model. Nevertheless, in relation to tumor growth properties, the more drastic impact was the overall decrease of vessels in CL-depleted mice. Angiogenesis, which delivers optimal oxygen and nutrition supply, is required for tumors to grow beyond 500 µm in diameter. Heterogeneity in tumor perfusion results in hypoxia, an acidic microenvironment and a shift from an aerobic to an anaerobic metabolism of cells (Hanahan and Folkman, 1996; Vaupel et al., 1989). Hypoxia triggers cell apoptosis in a p53-dependent manner, and additionally HIF-1α was shown to mediate anti-proliferative and pro-apoptotic effects in embryonic stem cells (Carmeliet et al., 1998; Graeber et al., 1996). In particular, the MVD could be correlated with prognosis in patients with solid tumors, such as head and neck, colorectal, breast and prostate cancers, and furthermore with the metastatic state of breast cancer (Cernea et al., 2004; Couvelard et al., 2005; Fernandez-Aguilar et al., 2006; Lackner et al., 2004; Li et al., 2000; Lindmark et al., 1996)

A reduced number of accumulated MΦ was observed in both the MaFIA mice and CL-depleted mouse models. Importantly, a significant shift of M2 to M1 polarization-marker was prominently observed only in tumor-bearing MaFIA mice. This shift might be influenced by

the model, since the suicide gene in MaFIA mice is driven by the cfms-promoter. The cfms gene encodes the M-CSF receptor CSFR1. Several *in vitro* studies demonstrated that MΦ-polarization is dependent on GM-CSF vs. M-CSF-generation, whereas M-CSF stimulation facilitates the M2-phenotype (Fleetwood et al., 2009; Sierra-Filardi et al., 2010; Verreck et al., 2004). Hence, in the MaFIA mice MΦ are preferentially depleted, although the process of MΦ-polarization is dynamic and reversible and not strictly dependent on only one stimulus. Nevertheless, these observations present the CSFR1 as a potential target for therapeutic intervention in lung cancer. Although the tumor size was decreased in both models compared to the control, the tumor-bearing MaFIA-mice benefitted more from the MΦ depletion as indicated by the gain of body weight over the time compared to controls. The CL-depleted tumor-bearing mice did not gain bodyweight. These observations indicate that the entire MΦ population has an impact on lung cancer growth, but that selective M2 MΦ-depletion in the MaFIA mouse model results in an enhanced improvement during the disease. These results confirm the importance of MΦ–polarization in lung cancer and emphasize the importance of M2-polarized tumor associated MΦ as a major promoter of tumor growth.

In summary, the current study demonstrates and confirms that MΦ support lung cancer cell progression and metastasis formation, as reported previously for other cancer cell types such as colon and breast cancer. In addition, possible mechanisms underlying the changes in the tumor microenvironment induced by MΦ-cancer cell interactions, such as effects on the expression of several MMPs and VEGF, which could be associated with lung cancer progression, were identified (Fakhoury et al., 2012; Zheng et al., 2010)

5.2 LLC1-MΦ co-culture mediated effects on CCR2 and CX3CR1 regulation and functional consequences

To elucidate the underlying molecular mechanisms of MΦ action on lung cancer cells, we established an *in vitro* model for a lung cancer cell/MΦ co-culture. LLC1 were chosen to represent lung cancer cells. LLC1 are classified as adenocarcinoma, which is the most prevalent subtype of all lung cancers and the subtype with the lowest relationship to smoking (Chen et al., 2009; Kenfield et al., 2008). Both of these reasons support the use of adenocarcinoma in lung cancer research. Since human cancer cell lines require immunodeficient mice as a host in which cancer cell-host cell interactions might be influenced, using LLC1 with the syngeneic C57/Bl6 mice as a host remains the ideal model to study cancer cell-immune cell interactions within primary tumor growth and metastasis.

Nevertheless, it is crucial to show relevance to the human situation, so this study was not only extended to human cancer cell lines but also to other lung cancer subtypes, such as squamous cell carcinoma and large-cell carcinoma.

The co-culture was established without applying MΦ-like cell lines such as RAW264.7 or AMJ2 (Palleroni et al., 1991; Raschke et al., 1978) since these cell lines are immortalized by virus and/or oncogene transfection and thus exhibit cancer-like properties. The disadvantages of using primary cells are the more laborious and challenging culture as well as the need to apply the specific growth factors GM-CSF and M-CSF that already promote a pre-polarization (Sierra-Filardi et al., 2010). Therefore, BM-MΦ were generated with M-CSF to mimic the M2-phenotype of TAMs. Nevertheless, M-CSF-generated MΦ displayed enough flexibility to respond to co-cultures with cancer cells adapting an even stronger M2-phenotype with high arginase, chitinase, IL-1RA and IL-10 expression.

Interaction of cancer cells with MΦ lead to an increased proliferation and a potently increased migration of cancer cells, when stimulated with CM. MΦ are known to produce several growth factors such as TGF-β, epidermal growth factor (EGF) and PDGF (Lewis and Pollard, 2006). A constitutive PDGF and EGF secretion of MΦ that was even increased after co-culture was as well observed within this study (data not shown). The increased migration toward CM is most likely mediated via secreted cytokines. MΦ as well as cancer cells secrete abundantly chemokines such as CCL2, CCL5, CCL12, CXCL1, CX3CL1, MIP-1α and CXCL10, which mediate a chemotactic response of cells that express the according receptor. One possible mechanism would be the chemotactic response to CCL2 and CX3CL1, which are abundantly secreted in co-culture CM from MΦ- as well as cancer cells. The same CM induces an upregulation of CCR2 and CX3CR1 on cancer cells (see section below) that thus become able to respond to the CCL2- and CX3CL1-mediated chemotactic signal. However, only MΦ-CM induced already a migratory response of cancer cells but failed to induce chemokine-receptor upregulation, suggesting multiple mechanisms responsible for cancer cell migration in parallel to CCR2/CX3CR1-upregulation. Additionally to the cytokines and chemokines detected in this study MΦ as well as CAF are moreover able to secrete CXCL12 (SDF-1, stromal cell-derived factor), whose involvement in cancer cell chemotaxis *in vitro* and metastasis *in vivo* could be demonstrated for several cancer types such as breast cancer, prostate cancer as well as NSCLC (Koshiba et al., 2000; Oonakahara et al., 2004; Orimo et al., 2005). Moreover, several inhibitors of the SDF-1/CXCR4 pathway, namely MDX-1338 and plerixafor are currently in phase I/II or phase III trials (DiPersio et al., 2009; Kuhne et al.,

2013), underlying the importance of chemotactic pathways for cancer progression and metastasis formation. Another chemotactic response of cancer cells could be demonstrated for CCL19/CCL21-CCR7 interactions in breast cancer and leukemia or upon CCL22 binding to CCR4 in lung cancer (Li et al., 2009; Muller et al., 2001; Picchio et al., 2008). Moreover, directed movement of cancer cells can take place in the presence of growth factors such as EGF, PDGF, FGF and IGF, which all can be secreted by MΦ. The migratory response of cancer cells towards growth factor was demonstrated for various cancer types including breast, lung, and pancreatic cancer as well as glioblastoma and melanoma (Roussos et al., 2011).

Interestingly, increased chemokine-receptor expression (CCR2 and CX3CR1) on LLC1 after co-culture with MΦ was observed. The upregulation was associated with enhanced proliferation and migration of LLC1. Importantly, the CCR2/CX3CR1 upregulation and the according functional consequences were strictly dependent on interaction with MΦ. Moreover, this effect was dependent on the expression of CCR2 or CX3CR1 in co-cultured MΦ. Suppression of CCR2 or CX3CR1 expression in either MΦ or LLC1 led to attenuated proliferation and migration.

The present study is the first to report the upregulation of chemokine receptors on cancer cells in response to MΦ and the functional consequences from this upregulation. These findings imply that lung cancer cells can adapt to an expression and secretion profile that is similar to immune cells. Importantly, upregulations of CCR2 and CX3CR1 in LLC1 could enable possible response and migration towards chemotactic gradients of CCL2 and CX3CL1, which implies a crucial role in metastatic spread of lung cancer. The ligands CCL2 and CX3CL1 were constitutively expressed by LLC1, yet significantly upregulated after MΦ co-culture. Abundant secretion of CCL2 by cancer cells was already previously reported for breast, prostate and pancreatic cancers, as well as gliomas (Brown et al., 2007; Monti et al., 2003; Qian et al., 2011; Zhang et al., 2010) and the major task is the recruitment of MΦ into the tumor microenvironment. Conversely, in pancreatic cancer, CCL2-mediated attraction of TAM was described as beneficial. However, the role of CX3CL1 in cancer progression has not been well investigated. Recent studies report the involvement of CX3CL1 in chemotaxis of TAM in breast cancer and lymphocytic leukaemia (Ferretti et al., 2011; Reed et al., 2012). Notably, CCR2 induction in LLC1 was connected to the MΦ-phenotype used for co-culture. This fact emphasizes the important role of CCR2 upregulation in cancer progression.

Importantly, the upregulation of CCR2/CCL2-axis was confirmed in several human lung cancer cell lines (A549, H23, H226, H520), emphasizing the relevance of this pathway for lung cancer in general. Furthermore, CX3CR1/CX3Cl1 axis was elevated in 50% of the used human cancer cell lines. Based on the fact that xenograft models with human cancer cells lines provide no information about metastatic behavior, it is difficult to elucidate the functional consequences of CCR2/CX3CR1 upregulations on human cancer cells. However, the strong association of CCR2 with the tumor stage and metastatic stage could be confirmed.

In line with the observed upregulation of CCR2 and CX3CR1 on cancer cells after co-culture with MΦ, is reversely the significantly lower expression of CCR2 and CX3CR1 in the tumor stroma of MΦ-depleted mice. This downregulation does partly reflect the MΦ-depletion itself, since CCR2 as well as CX3CR1 are abundantly expressed on MΦ. However, although other MΦ –marker are still well detectable, CCR2 is not detectable at all in the tumor stroma of MΦ-depleted mice, which suggest an outstanding role of $CCR2^+$ subpopulations for cancer growth. Recent publications demonstrated that $CCR2^+$ MΦ-subpopulations are important for breast cancer metastasis, and siRNA-mediated knockdown of CCR2 in monocytes was shown to reduce tumor growth in mice models of lymphoma and colorectal cancer (Cortez-Retamozo et al., 2012; Leuschner et al., 2011; Qian et al., 2011). However, the role of $CX3CR1^+$ cell populations in cancer growth and metastasis has not been investigated.

The same group of genes (VEGFs, MMPs) as in the *in vivo* models was screened. In contrast to the decrease of VEGF in MΦ-depleted tumor stroma, a significant upregulation of VEGFa and VEGFc after LLC1/MΦ interaction was detected. This fact directly connects the observed microenvironmental changes in CL-depleted and MaFIA mice directly to MΦ-infiltration. The same tendency was reflected by upregulation of MMP-8, -9 and -13. The importance of MMP-9 and MMP-13, especially in invasiveness of solid tumors and metastasis, was previously described for various cancer types (Nannuru et al., 2010). However, the reported induction of MMPs in MΦ directly after interaction with lung cancer cells is novel. In contrast to the CL-depleted model in which MMP-8 was not decreased in primary tumors, it is upregulated after the LLC1/MΦ co-culture. MMP-8 was shown to correlate with the disease course in colorectal cancer and was directly associated with metastasis (Vayrynen et al., 2012). Moreover, expression of proMMP as well as active MMP-8 was higher in breast cancer tissue compared to healthy controls (Kohrmann et al., 2009).

That lung cancer cells and MΦ exhibit a strong interaction and exchange multiple secreted factors is evident. Yet the question remains as to how these interactions lead to upregulation

of the typical immune cell receptors CCR2 and CX3CR1 on cancer cells. Possible mediators of the MΦ-cancer cell interactions include the secreted cytokines, as several are either newly secreted or enhanced after co-culture. LLC1 abundantly secrete CCL2 and CX3CL1, but fail to autoregulate CCR2/CX3CR1 expression in response to their own CCL2/CX3CL1. Moreover, they fail to express CCR2/CX3CR1 in response to stimulation with MΦ-CM, although MΦ secrete CCL2/CX3CL1 as well. The missing piece to this puzzle might be one of the cytokines enhanced or newly secreted after co-culture, namely IL-1α, IL-6, IL-10, CCL1, IL-23, MIP-1α, MIP-1β, G-CSF, TNFα or siCAM-1. One possible candidate is IL-10, since it is upregulated in WT co-cultures, but not in MΦ-CCR2$^{-/-}$ co-cultures. Moreover, CCR2$^{-/-}$MΦ display a more M1-like phenotype, and are less likely to secrete anti-inflammatory cytokines such as IL-10. This is in line with the observation that CCR2 upregulation on cancer cells is dependent on the phenotype of MΦ, with a stronger upregulation in response to M2-MΦ. CCR2/CCL2 was also highly upregulated in IL-10-overexpressing mice compared to WT in the context of fibrosis (Sun et al., 2011). Furthermore, IL-10 was shown to upregulate CCR2-expression on human MC and thus increase their chemotactic response (Sozzani et al., 1998). Other cytokines, such as IL-6, were shown to upregulate CCL2-secretion, but had no influence on CCR2 expression (Arendt et al., 2002). Thus far, no influence of CCL1, IL-23, MIP-1α on CCR2 expression has been described in the literature. Another candidate involved in co-culture-induced CCR2 upregulation is G-CSF. G-CSF upregulated CCR2 transcription 86-fold after 8 hours of stimulation in the myeloid cell line FDN-1 (Iida et al., 2005). Whether the same effect would be observed in epithelial or cancer cells is not yet known. IL-2 is a well-known cytokine that enhances CCR2 expression on a transcriptional and translational expression level (Polentarutti et al., 1997). However, IL-2 was not secreted in either the control-CM or co-culture-derived CM, which is well in line with the fact that IL-2 is the major growth factor for T-lymphocytes but not for MΦ. Hence, these observations suggest an even higher CCR2-induction *in vivo*, with a well-established interplay among several cell types, such as cancer cells, MΦ and IL-2-secreting lymphocytes. Eventually, CCR2 expression on LLC1 is regulated by a distinct group of cytokines and the interaction and activation of several pathways finally leads to CCR2/CX3CR1 upregulation on cancer cells. A previous study demonstrated that an inflammatory pattern of cytokines, including IL-6, IL-1β and TNFα, causes CCR2 downregulation to maintain recruited MΦ at the site of inflammation or disease and prevent reverse migration (Sica et al., 2000). In line with these observations, the CCR2$^{-/-}$ MΦ and CX3CR1$^{-/-}$ MΦ show an M1-phenotype with a pro-inflammatory cytokine profile.

The observation that several cytokines, instead of only one cytokine, show changes in expression implies that the CCR2/CX3CR1 is connected to a certain cytokine secretion profile of MΦ that mediates MΦ actions on cancer cells. Interestingly, both receptors seem to influence the expression of the other, as CX3CR1 expression had an effect on CCR2 expression. CCR2 was downregulated in $CX3CR1^{-/-}$ MΦ. The exact molecular signaling patterns between MΦ and cancer cells that lead to upregulation of CCR2 and CX3CR1 requires further investigation.

5.3 *In vivo* influence of CCR2 and CX3CR1 on tumor growth and metastasis

We uncovered a MΦ-dependent CCR2-CCL1 and CX3CR1-CX3CL1 upregulation in cancer cells *in vitro*. Furthermore, we demonstrated that the adapted expression of the chemokine-receptors CCR2 and CX3CR1 on lung cancer cells is dependent on the expression of the receptors in MΦ. If MΦ lack CCR2 expression, they lose the ability to enhance cancer cell proliferation, migration and, most important, to induce CCR2 expression on cancer cells.

Previous studies reported that hypoxia is mostly responsible for MΦ attraction to the tumor microenvironment (Murdoch et al., 2004). In this attempt an additional, excessive chemotactic attraction of MΦ to the tumor via CCL2 and CX3CL1 became evident. The systemic plasma levels of both cytokines were elevated during tumor progression in a grafted model. Once these axes are interrupted, tumor growth is impaired.

Consistent with the *in vitro* data, $CCR2^{-/-}$ and $CX3CR1^{-/-}$ mice demonstrated decreased primary tumor growth, metastasis and improved survival compared to WT mice. Decreased primary tumor growth in $CCR2^{-/-}$ mice is well in line with previous reports in liver cancer and colon cancer (Wolf et al., 2012; Yang et al., 2006), whereas little is known regarding tumor growth in $CX3CR1^{-/-}$ mice. The decrease in tumor growth and metastasis correlated well with the MΦ infiltration and changes in the microvasculature in the tumor microenvironment. The impaired microvasculature might be a result of fewer accumulated MΦ in the tumor microenvironment. Moreover, $CCR2^{+}$ MΦ in particular seem to be involved in angiogenesis, as shown in wound healing (Willenborg et al., 2012). Interestingly, the MΦ marker profile in tumor tissue derived from $CCR2^{-/-}$ was shifted to M1-phenotype markers, confirming the *in vitro* results of M1-polarization of $CCR2^{-/-}$-MΦ. Furthermore, CCR2 expression was not induced on cancer cells *in vivo*. In addition to the dramatically reduced metastasis in $CCR2^{-/-}$ mice, these results indirectly confirm our *in vitro* results showing that CCR2 expression is

connected to a distinct cytokine expression profile and/or MΦ phenotype, which induces CCR2 expression in cancer cells, and in turn primes these for metastasis.

In contrast, the reduced tumor growth and metastasis in CX3CR1$^{-/-}$ mice were more likely caused by profound vessel changes not only in the microvasculature but also everywhere, implying that severe malnutrition is responsible for the impaired tumor growth and metastasis. Since CX3CR1 is not specifically expressed only on MΦ, but on all leukocyte subsets, other cell populations might be involved in the marked tumor impairment. Supporting this finding, CX3CL1- CX3CR1 was shown to induce endothelial cell dependent angiogenesis (Lee et al., 2006).

Despite these differences in the cause for impaired tumor growth in CCR2$^{-/-}$ or CX3CR1$^{-/-}$ mice, overall the reduction in both mice is remarkable. This is to some extent surprising, since CCR2^{+} and CX3CR1^{+} MΦ are described as two different subpopulations. In the murine organism, within several MC-subpopulations, two either CCR2- or CX3CR1-expressing MC-subtypes are described: (1) Ly6C^{high}, CD11b^{+}, CCR2^{high}, CX3CR1^{low} MC (MΦ-CCR2) and (2) Ly6C^{low}, CD11b^{+}, CCR2^{low}, CX3CR1^{high} (MΦ-CX3CR1) (Palframan et al., 2001; Serbina et al., 2008; Shi and Pamer, 2011). Since CCR2 and CX3CR1 seem to be expressed on MC in a contrary way, one might expect different or even opposite functions of these different subpopulations. However, MΦ-CCR2 are characterized as inflammatory MΦ, which accumulate abundantly upon infection with various bacteria, fungi, protozoa and viruses (Shi and Pamer, 2011). In contrast, decreased accumulation of MΦ-CCR2 was associated with a milder progression of influenza virus-provoked pneumonia, and thus with decreased mortality (Aldridge et al., 2009; Dawson et al., 2000). In the context of HIV, CCR2 could be associated with a response to anti-inflammatory cytokines (M2-phenotype) (Sozzani et al., 1998). This study could confirm this, since CCR2$^{-/-}$ MΦ displayed a more M1-like phenotype. This fact might once more support the finding of decreased tumor growth in CCR2$^{-/-}$, since not just less MΦ are accumulated in the tumor microenvironment but additionally the remaining (resident) MΦ are tumor restrictive M1- MΦ.

In contrast, the function of MΦ-CX3CR1 is much less investigated. These MC are described as vessel-patrolling MC. However, they also accumulate upon bacterial infection (Auffray et al., 2007; Auffray et al., 2009; Landsman et al., 2009). CX3CR1 expression was not associated with a certain MΦ-phenotype yet, and CX3CR1$^{-/-}$ MΦ could not be assigned to a phenotype in the current study. However, CX3CR1-signaling facilitates prolonged survival of

MC (Landsman et al., 2009), which might result in shorter life span and thus less operative time within the tumor microenvironment of $CX3CR1^{-/-}$ MΦ.

Eventually, in various diseases the accumulation of both MΦ-CCR1 and MΦ-CX3CR1 could be described, and inhibition of the accumulation of one of them turned out beneficial, so that altogether both MΦ-subpopulations are not acting as differently as expected but rather synergistically. Moreover, transfer of the separation in MΦ-CCR2 and MΦ-CX3CR1 in the human organisms proves to be difficult. Based on functional similarity, MΦ-CCR2 in humans are $CD14^+$, $CD16^-$ and $CCR2^+$. Patrolling, MΦ-CX3CR1-similar MΦ are $CD14^+$, $CD16^+$ (Cros et al., 2010; Geissmann et al., 2003; Ziegler-Heitbrock, 2007). In consequence, CCR2 or CX3CR1 expression cannot be strictly associated with a certain subpopulation, since the expression on MC in the human organism is not as exclusive as in the mouse. Importantly, in this study CCR2 and CX3CR1 expression and not only MΦ-accumulation, could be correlated with worse disease progression and metastasis.

Summarized, our findings therefore suggest that CCL2-CCR2 and CX3CR1-CX3CL1 chemokines represent potential anti-cancer therapies that bidirectionally target MΦ and cancer cells in the tumor microenvironment. Thus, blocking CCR2/CX3CR1 (1) targets cancer cells directly, reduces proliferation and impairs the migratory response to CCL2/CX3CL1 and (2) targets MΦ trafficking into the tumor microenvironment.

5.4 Patient data

To assess the human relevance of the described results, MΦ infiltration was estimated in 72 lung tissue sections from cancer patients. The sections covered NSCLC, especially adenocarcinoma and squamous cell carcinoma, in different stages and with different metastatic lymph node involvement and SCLC sections. MΦ accumulation, as represented by $CD68^+$ cells, strongly correlates with stage and metastatic stage. However, MΦ polarization was not considered in this study, but several published studies describe a M2-polarization for TAM. Moreover, correlation of MΦ-infiltration and stages in SCLC was not feasible, since SCLC is only classified in extensive or limited disease (Kalemkerian and Gadgeel, 2013; Micke et al., 2002), although attempts are made to extend the (for NSCLC usual) TNM staging system to SCLC. Overall, MΦ-accumulation seems to play a minor role in the progression of SCLC. This might be related to the neuroendocrine origin of SCLC and its abundant secretion of ectopically produced hormones such as adrenocorticotropic hormone

(ACTH) and anti-diuretic hormone (ADH), rather than cytokines (Gandhi and Johnson, 2006; Pelosof and Gerber, 2010; Raftopoulos, 2007).

Furthermore, evaluation of $CD68^+CCR2^+$ cells showed a correlation to tumor stage and metastatic spread as well. Notably, these immunohistochemical stainings identified $CCR2^+$ tumor cells, especially in advanced stages. These observations need to be quantified with appropriate adenocarcinoma and squamous cell carcinoma markers. However, adenocarcinoma or squamous cell carcinoma markers are not completely specific; most lung cancer subtypes show heterogeneous expression profiles and some markers are also expressed on healthy epithelial cells (Molina et al., 2003; Tacha et al., 2012). This makes a quantification of $CCR2^+$ tumor cells challenging. Interestingly, no $CCR2^+$ cells were detected in healthy lungs. This approach needs to be extended to $CX3CR1^+$ cells in correlation with the lung cancer stage.

5.5 Conclusion

Tumor cells and MΦ exhibit an extensive communication network via several secreted mediators and receptors within the tumor microenvironment. Based on the observed results, the following critical steps for tumor progression and metastasis can be summarized: (1) Tumor cell-host cell interactions are not limited to the tumor microenvironment but include the systemic pool of immune cells such as MC. Tumor cells actively attract monocytes via CCL2 and CX3CL1 from the blood stream. Systemic plasma levels of CCL2 and CX3CL1 in tumor-bearing mice are constantly high. (2) After migration into the tumor stroma, MC differentiate and polarize into M2-MΦ in response to tumor-cell-secreted M-CSF (among other factors) (3) In return, MΦ-secreted-factors (e.g. IL-10, Il-1α, IL-1β, CCL5, CXCL10 amongst others), in particular IL-10 might play a key role and induce CCR2 and CX3CR1 expression in tumor cells. (4) Expression of CCR2 and CX3CR1 supports the proliferation and migration of the tumor cells. Simultaneously, MΦ and tumor cells secrete MMPs, VEGFs and growth factors (GF; PDGFa, PDGFb, EGF etc), which cause microenvironmental changes and promote tumor progression. (5) The enhanced migration of tumor cells finally results in metastasis formation.

Several for crucial steps for tumor development can be blocked by knocking out CCR2 and CX3CR1 in MΦ, and thereby blocking connected signaling events such as IL-10 secretion and CCR2 and CX3CR1 up regulation in tumor cells.

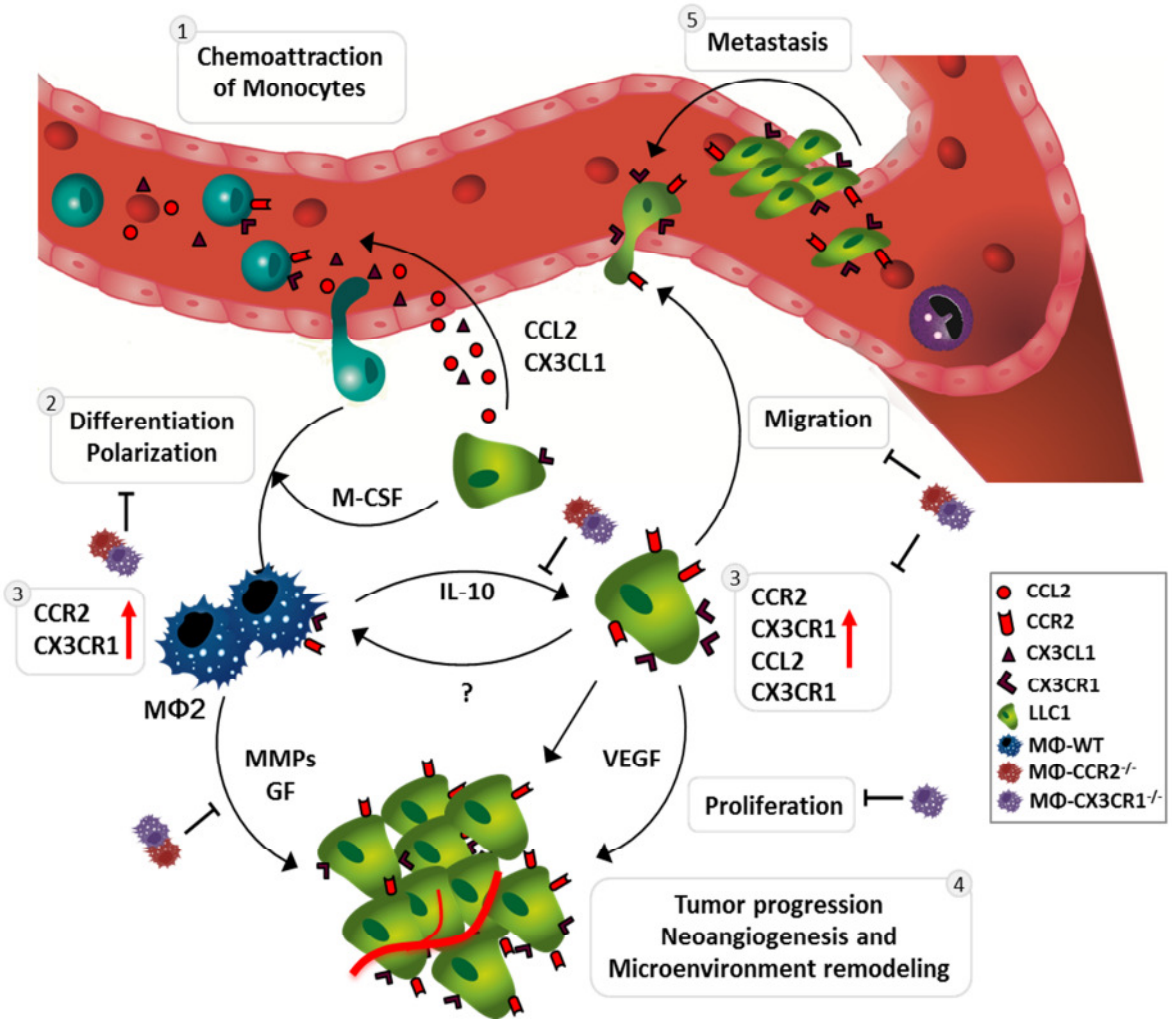

Figure 45 **Diagram of signaling events in the tumor microenvironment involving CCR2 and CX3CR**. 1) Tumor cells attract monocytes via CCL2 and CX3CL1 from the blood stream. 2) After migration into the tumor stroma, MΦ are differentiated and polarized into M2-MΦ via M-CSF (amongst others). 3). In return they secrete factors (e.g. IL-10) that induce CCR2 and CX3CR1 expression in tumor cells. 4). Expression of CCR2 and CX3CR1 support the proliferation and migration of the tumor cells. Simultaneously MΦ and tumor cells secret MMPs, VEGF and growth factors (GF; PDGFa, PDGFb, EGF etc), which cause microenvironmental changes and promote tumor progression. 5). The enhanced migration of tumor cells finally results in metastasis formation. The described signaling loop can be attenuated by inhibition of CCR2/CX3CR1 signaling on either MΦ or cancer cells.

5.6 Outlook

- Further investigations should focus on the underlying mechanisms of CCR2 and CX3CR1 regulation of cancer cells. IL-10 might be a key player in CCR2 and CX3CR1 regulation, but several other cytokines are newly or more abundantly secreted after co-culture, such as IL-6, IL-1α, IL-23, M-CSF, TNFα, IL-6, CCL1, MIP-1α, MIP-1β, G-CSF and soluble ICAM-1. Furthermore, initiation and termination of inflammatory reactions is frequently orchestrated by a distinct pattern or group of cytokines; therefore, overlapping and interacting pathways are expected. Additionally, the detection of cytokines with antibody arrays or RT-PCR is very limited, and thus signaling proteins such as enzymes, growth factors, further cytokines and chemokines involved in and regulated by cancer cell-MΦ co-cultures might not be yet detected in this study. The entire secretome of MΦ and cancer cells with or without co-culture could be determined with a proteomic approach. This approach could also be extended to the proteome of cancer cells/MΦ.
- Other possibilities include investigations of the transcriptome with microarrays or miR-expression profiles in cancer cells/MΦ. The elucidation of dysregulated pathways specific to cancer cell-MΦ interactions opens up research to new and better targets for lung cancer treatment.
- Additional studies should be performed to validate CCR2 and CX3CR1 as suitable targets for lung cancer intervention. In particular, treatment of tumor-bearing mice with CCR2/CX3CR1-blocking antibodies or chemical receptor antagonists is necessary to evaluate the pharmacological characteristics and possibilities of a xenobiotic intervention. A 100% receptor blockade as achieved with a genetic knockout is unlikely to achieve the general pharmakodynamic and kinetic properties from xenobiotics.
- Finally, CCR2 should be considered as a diagnostic marker for staging and metastatic states, since the expression in primary tumors correlated clearly with the primary tumor stage and metastasis. For this purpose, more extensive patient studies need to be performed.

6 Summary

Recent studies indicate that tumor-associated macrophages with an M2 phenotype can play a critical role in tumor growth and metastasis. However, the regulatory pathways remain poorly characterized. Using macrophage (MΦ)-depleted mice, the present study confirms a major contribution of MΦ to primary lung cancer growth and metastatic spread. Furthermore, the data demonstrates that M2-polarized MΦ play a critical role in establishing the vessel structure and microvasculature associated with tumors. Depletion of MΦ restricts the expression of matrix metalloproteinases and vascular endothelial growth factor and thus results in an overall regressive tumor microenvironment.

Co-culture experiments of MΦ with lung carcinoma cells revealed cancer-cell-mediated M2-polarization and subsequent M2-MΦ-induced proliferation, migration and CCR2/CX3CR1 expression on carcinoma cells. Importantly, adenocarcinoma cells initiate a vicious circle with an abundant secretion of tumor-associated MΦ-attracting CCL2/CX3CL1, and then recruited MΦ polarize into M2, enhance CCL2/CX3CL1 secretion and induce CCR2/CX3CR1 expression of cancer cells with the functional consequence of enhanced cancer cell proliferation and migration. The co-culture-induced cytokines interleukin-10, interleukin-6, interleukin-1α, and interleukin-23, CCL1, macrophage-colony stimulating factor, tumor necrosis factor α, macrophage inflammatory proteins 1α and 1β, granulocyte-colony stimulating factor and soluble intercellular adhesion molecule 1 may play a crucial role in this cycle. Inhibition of CCR2/CX3CR1 signaling on either lung cancer cells or MΦ attenuates co-culture induced proliferation and migration. In conclusion, lung adenocarcinoma cells hijack CCR2/CX3CR1^{+} MΦ to support their own proliferation and migration.

Consistent with these observations, both CX3CR1$^{-/-}$ and CCR2$^{-/-}$ mice had reduced primary tumor size, lung metastasis and numbers of M2-polarized MΦ compared to WT mice. With the absence of CCR2^{+} or CX3CR1^{+} MΦ, induction of CCR2/CX3CR1 on cancer cells also failed *in vivo*. These results support a model whereby TAMs play a critical, chemokine dependent role in the regulation of lung cancer progression. Furthermore, studies with CX3CR1$^{-/-}$ and CCR2$^{-/-}$ reveal a similar reduction of tumor-associated neoangiogenesis with in particular targeted microvasculature and moreover a similar restriction of matrix metalloproteinases and vascular endothelial growth factor expression compared to total MΦ-depleted mice. Consequently, this study indicates CCR2 and CX3CR1 as promising drug

targets to inhibit cancer progression and metastasis by directly manipulating the tumor microenvironment. The enhanced concentration of CCR2 and CX3CR1 expression in the tumor microenvironment provides ideal conditions for this purpose.

Finally, not only MΦ infiltration but also the ratio of $CCR2^+$ MΦ within human lung adenocarcinoma and squamous cell carcinoma correlate with lung cancer stage and metastasis. These observations confirm the human relevance of TAM-associated CCR2/CX3CR1-signaling cascades.

Altogether, these results provide a mechanism for the regulation of lung tumor growth and metastasis by tumor-associated macrophages, and targeting M2-macrophage expressed receptors provides a new strategy for the development of lung cancer therapeutics.

7 Zusammenfassung

Neueste Studien belegen eine entscheidende Rolle von Tumor-assoziierten Makrophagen mit M2-Phenotyp innerhalb von Tumorentstehung, Fortschritt der Erkrankung und letzten Endes Metastasierung. Dennoch verbleiben dieser Beobachtung zugrunde liegende Signalwege und Regulationsmechanismen besonders in Bezug auf Lungenkarzinome weitestgehend unbekannt. Die vorliegende Studie bestätigt diese Schlüsselrolle der Makrophagen in Primärtumorwachstum der Lunge und Entstehung von peripheren Metastastasen, unter zu Hilfenahme zwei verschiedener Makrophagen-depletierter Maus-modelle. Im Weiteren wird nachgewiesen, dass M2-polarisierte Makrophagen eine tragende Rolle bei der Ausbildung von Tumor-assoziierten Gefäßstrukturen, insbesondere Mikro-zirkulation spielen. Die Depletion von Makrophagen führt weiterhin zu einer verringerten Expression von Matrix-Metalloproteinasen und vascular endothelial growth factor (VEGF) und damit zu einem insgesamt überwiegend Tumor-restriktiv agierenden Tumor-Stroma.

Die durchgeführten Experimente mit in einer Co-Kultur befindlichen Makrophagen und Lungenkarzinom-Zellen offenbaren eine Krebszellen-vermittelte M2-Polarisation der Makrophagen mit nachfolgender M2-Makrophagen induzierter Proliferation, Migration und CCR2-/CX3CR1 Expression von/auf Krebszellen. Im Wesentlichen wird hierbei ein Teufelskreis ausgelöst, beginnend mit der mit der beträchtlichen CCL2/CX3CL1-Sekretion von Adenokarzinomzellen, um direkt Makrophagen in das Tumor-Stroma zu rekrutieren, die daraufhin einen M2-Phenotypen ausbilden um anschließend wiederum die CCL2/CX3CL1-Sekretion zu verstärken und eine CCR2/CX3CR1-Expression auf Adenokarzinomzellen zu induzieren. Dies führt funktionelle Konsequenzen für die Krebszellen herbei, insbesondere eine verstärkte Proliferation und Migration. Weitere Schlüsselfunktionen in diesem Teufelskreis könnten dabei von Co-Kultur induzierten Zytokinen und Chemokinen wie Interleukin-10, -6, -1α, und -23, CCL1, macrophage-colony stimulating factor (M-CSF), tumor necrosis factor α (TNFα), macrophage inflammatory proteins-1α and -1β, granulocyte-colony stimulating factor (G-CSF) und soluble intercellular adhesion molecule 1 (siCAM-1) übernommen werden. Wird die CCR2/CX3CR1-übermittelte Signaltransduktion nun auf Makrophagen oder Lungenkrebszellen inhibiert, werden folglich auch die durch Co-Kultur erzeugte gesteigerte Proliferationsrate sowie Migrationsverhalten stark abgeschwächt. Somit

missbrauchen Lungenadenokarzinomzellen im Speziellen CCR2/CX3CR1^{+} Makrophagen um ihre eigene Proliferation und Migration zu fördern.

Im Einklang mit diesen Beobachtungen, wurden in CX3CR1$^{-/-}$ und CCR2$^{-/-}$-Mäusen ein reduziertes Primärtumorwachstum, eine geringere Anzahl an Lungenmetastasen sowie weniger M2-polarisierte Makrophagen im Vergleich mit WT-Mäusen festgestellt. Durch den Mangel an CCR2/CX3CR1^{+} Makrophagen, ist auch *in vivo* die Induktion von CCR2/CX3CR1-Expression auf Krebszellen fehlgeschlagen. Diese Ergebnisse unterstützen das Model von Tumor-assoziierten Makrophagen als ausschlaggebende, Chemokin-abhängige Regulatoren im Voranschreiten einer Lungenkrebserkrankung. Des Weiteren konnte in CX3CR1$^{-/-}$ und CCR2$^{-/-}$-Mäusen ein ähnlicher Einfluss auf die Neoangiogenese, mit besonders beeinträchtigter Mikrozirkulation, sowie eine gleichermaßen verringerte Expression/Sekretion von Matrix- Metalloproteinasen und vascular endothelial growth factor (VEGF) im Vergleich zu den Maus-Modellen mit totaler Depletion von Makrophagen beobachtet werden. Folglich konnten in dieser Studie CCR2 und CX3CR1 als vielversprechende Zielrezeptoren für Medikamente präsentiert werden, mit deren Inhibition oder Blockade es möglich wäre, Lungenkrebs durch direkte Manipulation des Tumor-Stroma zu therapieren.

Letztendlich korreliert nicht nur die gesamte Makrophagen-Infiltration, sondern auch der Prozentsatz an CCR2^{+} Makrophagen mit dem Schwere- und Metastasierungsgrad von pulmonalen Adenokarzinomen und Plattenepithelkarzinomen im Patienten. Damit konnte eine Relevanz für TAM-assoziierte CCR2- und CX3CR1-Signalkaskaden für den Patienten gezeigt werden.

Zusammengefasst wird in dieser Arbeit ein möglicher Mechanismus für Makrophagen-induziertes Primärtumorwachstum sowie Metastasen Bildung aufgezeigt, der Makrophagen-exprimierte Rezeptoren und Moleküle als neue Targets für die Entwicklung neuer Therapieansätze für Lungenkrebs aufdeckt.

8 List of Abbreviations

-/-	Knockout of indicated gene
ΔCt	Threshold-cycle difference (HPRT-GOI)
AC	Adenocarcinoma
ALK	Anaplastic lymphoma kinase
APC	Antigen presenting cell
BAC	Bronchoalveolar carcinoma
BM-MΦ	Bone marrow derived Macrophages
BRaf	v-Raf murine sarcoma viral oncogene homolog B1
Ca^{2+}	double positive calcium ion
CAF	Cancer associated fibroblast
cAMP	Cyclic adenosine monophosphate
CCL2/MCP-1	Chemokine (C-C motif)-Ligand 2/Monocyte chemotactic protein 1
CCR2/CD192	Chemokine (C-C motif)-receptor 2
CCR3/CD193	Chemokine (C-C motif)-receptor 3
CD	Cluster of differentiation
CEA	Carcinoembryonik antigen
CK	Cytokeratin
CL	Clodronate liposomes
CM	Conditioned media
CSFR1	Colony-stimulating factor receptor 1
CT	Computed tomographie

CX3CL1/FKN	Chemokine (C-X3-C motif)-ligand 2/Fractalkine
CX3CR1	Chemokine (C-X3-C motif)-receptor 1
CYFRA 21-1	Fragment of the cytokeratin 19
DC	Dendritic cell
DMSO	Dimethyl sulfoxide
ECM	Extracellular matrix
EGFR	Epidermal growth factor receptor
ETS	Environmental tobacco smoke
FAP	Fibroblast activation protein
FCS	Fetal calf serum
FGF	Fibroblast growth factor
FSP-1	Fibroblast specific protein 1
GM-CSF	Granulocyte-macrophage colony-stimulating factor
GOI	Gene of interest
HER1	Human epidermal growth factor receptor 2
HGF	Hepatocyte growth factor
IA	Invasive adenocarcinoma
IFNγ	Interferon γ
IL	Interleukin
IL-1RA	Interleukin 1 receptor antagonist
iNOS	Inducible nitric oxide synthases
JAK	Janus kinase
KO	Knockout

KRas	V-Ki-ras2 Kirsten rat sarcoma viral oncogene homolog
LKB-1	Liver kinase B1
LLC1	Lewis lung carcinoma 1
LPS	Lipopolysaccharide
MΦ	Macrophages
MΦ -CCR2$^{-/-}$	CCR2 knockout macrophage
MΦ -CX3CR1$^{-/-}$	CX3CR1 knockout macrophage
M1	Macrophage with M1-phenotype
M2	Macrophage with M2-phenotype
MaFIA	Macrophage FAS-induced apoptosis
MAPK	Mitogen-activated protein kinase
MC	Monocyte
MC-CCR2	Ly6C^{high}, CD11b^{+}, CCR2^{high}, CX3CR1^{low} monocyte
MC-CX3CR1	Ly6C^{low}, CD11b^{+}, CCR2^{low}, CX3CR1^{high} monocyte
M-CSF	Macrophage colony stimulating factor
MET	Proto-oncogene encoding for hepatocyte growth factor receptor
MHC-II	Major histocompatibility complex Class II
MIA	Minimally invasive adenocarcinoma
MMP	Matrix metalloproteinase
MUC-1	Mucin 1
MRI	Magnetic resonance imaging
MVD	Microvessel density
NF-κB	Nuclear factor kappa-light-chain-enhancer of activated B cells

NK-Cells	Natural killer cells
NSCLC	Non-small cell lung cancer
NSE	Neuron specific enolase
PBS	Phosphate buffered saline
PIK3CA	Class I PI 3-kinase catalytic subunit
PDGFR	Platelet-derived growth factor receptors
proGRP	Gastrin-releasing peptid-progenitor
SCC	Squamous cell carcinoma
SCLC	Small cell lung cancer
SMA	Smooth muscle actin
Sox2	Sex determining region Y-box 2
STAT	Signal transducers and activators of transcription
TAM	Tumor associated macrophage
TAN	Tumor associated neutrophil
TGFβ	Transforming growth factor β
T_H	T-helper cell
TTF-1	Thyroid transcription factor
TKI	Tyrosine-kinase inhibitor
TNFα	Tumor necrosis factor α
T_{REG}	Regulatory T-cell
VEGF	Vascular endothelial growth factor
WT	Wildtype

9 List of Figures and Tables

9.1 List of Figures

9.2 List of Tables

10 Literature

Aarntzen, E. H., Srinivas, M., Radu, C. G., Punt, C. J., Boerman, O. C., Figdor, C. G., Oyen, W. J., and de Vries, I. J. (2012). In vivo imaging of therapy-induced anti-cancer immune responses in humans. Cellular and molecular life sciences : CMLS.

Alberg, A. J., and Samet, J. M. (2003). Epidemiology of lung cancer. Chest *123*, 21S-49S.

Aldridge, J. R., Jr., Moseley, C. E., Boltz, D. A., Negovetich, N. J., Reynolds, C., Franks, J., Brown, S. A., Doherty, P. C., Webster, R. G., and Thomas, P. G. (2009). TNF/iNOS-producing dendritic cells are the necessary evil of lethal influenza virus infection. Proceedings of the National Academy of Sciences of the United States of America *106*, 5306-5311.

Anderberg, C., Li, H., Fredriksson, L., Andrae, J., Betsholtz, C., Li, X., Eriksson, U., and Pietras, K. (2009). Paracrine signaling by platelet-derived growth factor-CC promotes tumor growth by recruitment of cancer-associated fibroblasts. Cancer research *69*, 369-378.

Anderberg, C., and Pietras, K. (2009). On the origin of cancer-associated fibroblasts. Cell Cycle *8*, 1461-1462.

Arendt, B. K., Velazquez-Dones, A., Tschumper, R. C., Howell, K. G., Ansell, S. M., Witzig, T. E., and Jelinek, D. F. (2002). Interleukin 6 induces monocyte chemoattractant protein-1 expression in myeloma cells. Leukemia *16*, 2142-2147.

Arriagada, R., Bergman, B., Dunant, A., Le Chevalier, T., Pignon, J. P., and Vansteenkiste, J. (2004). Cisplatin-based adjuvant chemotherapy in patients with completely resected non-small-cell lung cancer. The New England journal of medicine *350*, 351-360.

Auffray, C., Fogg, D., Garfa, M., Elain, G., Join-Lambert, O., Kayal, S., Sarnacki, S., Cumano, A., Lauvau, G., and Geissmann, F. (2007). Monitoring of blood vessels and tissues by a population of monocytes with patrolling behavior. Science *317*, 666-670.

Auffray, C., Fogg, D. K., Narni-Mancinelli, E., Senechal, B., Trouillet, C., Saederup, N., Leemput, J., Bigot, K., Campisi, L., Abitbol, M.*, et al.* (2009). CX3CR1+ CD115+ CD135+ common macrophage/DC precursors and the role of CX3CR1 in their response to inflammation. The Journal of experimental medicine *206*, 595-606.

Azzoli, C. G., Krug, L. M., Miller, V. A., Kris, M. G., and Mass, R. (2002). Trastuzumab in the treatment of non-small cell lung cancer. Seminars in oncology *29*, 59-65.

Bailey, C., Negus, R., Morris, A., Ziprin, P., Goldin, R., Allavena, P., Peck, D., and Darzi, A. (2007). Chemokine expression is associated with the accumulation of tumour associated macrophages (TAMs) and progression in human colorectal cancer. Clinical & experimental metastasis *24*, 121-130.

Balkwill, F., Charles, K. A., and Mantovani, A. (2005). Smoldering and polarized inflammation in the initiation and promotion of malignant disease. Cancer cell *7*, 211-217.

Barleon, B., Sozzani, S., Zhou, D., Weich, H. A., Mantovani, A., and Marme, D. (1996). Migration of human monocytes in response to vascular endothelial growth factor (VEGF) is mediated via the VEGF receptor flt-1. Blood *87*, 3336-3343.

Barletta, J. A., Perner, S., Iafrate, A. J., Yeap, B. Y., Weir, B. A., Johnson, L. A., Johnson, B. E., Meyerson, M., Rubin, M. A., Travis, W. D.*, et al.* (2009). Clinical significance of TTF-1 protein expression and TTF-1 gene amplification in lung adenocarcinoma. Journal of cellular and molecular medicine *13*, 1977-1986.

Bertram, J. S., and Janik, P. (1980). Establishment of a cloned line of Lewis Lung Carcinoma cells adapted to cell culture. Cancer letters *11*, 63-73.

Bhowmick, N. A., Neilson, E. G., and Moses, H. L. (2004). Stromal fibroblasts in cancer initiation and progression. Nature *432*, 332-337.

Bianchi, F., Hu, J., Pelosi, G., Cirincione, R., Ferguson, M., Ratcliffe, C., Di Fiore, P. P., Gatter, K., Pezzella, F., and Pastorino, U. (2004). Lung cancers detected by screening with spiral computed tomography have a malignant phenotype when analyzed by cDNA microarray. Clinical cancer research : an official journal of the American Association for Cancer Research *10*, 6023-6028.

Biswas, S. K., and Mantovani, A. (2010). Macrophage plasticity and interaction with lymphocyte subsets: cancer as a paradigm. Nature immunology *11*, 889-896.

Bonomi, P., Kim, K., Fairclough, D., Cella, D., Kugler, J., Rowinsky, E., Jiroutek, M., and Johnson, D. (2000). Comparison of survival and quality of life in advanced non-small-cell lung cancer patients treated with two dose levels of paclitaxel combined with cisplatin versus etoposide with cisplatin: results of an Eastern Cooperative Oncology Group trial. Journal of clinical oncology : official journal of the American Society of Clinical Oncology *18*, 623-631.

Boring, L., Gosling, J., Chensue, S. W., Kunkel, S. L., Farese, R. V., Jr., Broxmeyer, H. E., and Charo, I. F. (1997). Impaired monocyte migration and reduced type 1 (Th1)

cytokine responses in C-C chemokine receptor 2 knockout mice. The Journal of clinical investigation *100*, 2552-2561.

Brown, C. E., Vishwanath, R. P., Aguilar, B., Starr, R., Najbauer, J., Aboody, K. S., and Jensen, M. C. (2007). Tumor-derived chemokine MCP-1/CCL2 is sufficient for mediating tumor tropism of adoptively transferred T cells. J Immunol *179*, 3332-3341.

Burke-Gaffney, A., Brooks, A. V., and Bogle, R. G. (2002). Regulation of chemokine expression in atherosclerosis. Vascular pharmacology *38*, 283-292.

Burnett, S. H., Beus, B. J., Avdiushko, R., Qualls, J., Kaplan, A. M., and Cohen, D. A. (2006). Development of peritoneal adhesions in macrophage depleted mice. The Journal of surgical research *131*, 296-301.

Burnett, S. H., Kershen, E. J., Zhang, J., Zeng, L., Straley, S. C., Kaplan, A. M., and Cohen, D. A. (2004). Conditional macrophage ablation in transgenic mice expressing a Fas-based suicide gene. Journal of leukocyte biology *75*, 612-623.

Butts, C., Murray, N., Maksymiuk, A., Goss, G., Marshall, E., Soulieres, D., Cormier, Y., Ellis, P., Price, A., Sawhney, R.*, et al.* (2005). Randomized phase IIB trial of BLP25 liposome vaccine in stage IIIB and IV non-small-cell lung cancer. Journal of clinical oncology : official journal of the American Society of Clinical Oncology *23*, 6674-6681.

Cagle, P. T., and Chirieac, L. R. (2012). Advances in treatment of lung cancer with targeted therapy. Archives of pathology & laboratory medicine *136*, 504-509.

Caporaso, N., Landi, M. T., and Vineis, P. (1991). Relevance of metabolic polymorphisms to human carcinogenesis: evaluation of epidemiologic evidence. Pharmacogenetics *1*, 4-19.

Carlini, M. J., Dalurzo, M. C., Lastiri, J. M., Smith, D. E., Vasallo, B. C., Puricelli, L. I., and Lauria de Cidre, L. S. (2010). Mast cell phenotypes and microvessels in non-small cell lung cancer and its prognostic significance. Human pathology *41*, 697-705.

Carmeliet, P., Dor, Y., Herbert, J. M., Fukumura, D., Brusselmans, K., Dewerchin, M., Neeman, M., Bono, F., Abramovitch, R., Maxwell, P.*, et al.* (1998). Role of HIF-1alpha in hypoxia-mediated apoptosis, cell proliferation and tumour angiogenesis. Nature *394*, 485-490.

Carroll, C. E., Liang, Y., Benakanakere, I., Besch-Williford, C., and Hyder, S. M. (2013). The anticancer agent YC-1 suppresses progestin-stimulated VEGF in breast cancer cells

and arrests breast tumor development. International journal of oncology *42*, 179-187.

Cavallo, F., De Giovanni, C., Nanni, P., Forni, G., and Lollini, P. L. (2011). 2011: the immune hallmarks of cancer. Cancer immunology, immunotherapy : CII *60*, 319-326.

Cernea, C. R., Ferraz, A. R., de Castro, I. V., Sotto, M. N., Logullo, A. F., Bacchi, C. E., and Potenza, A. S. (2004). Angiogenesis and skin carcinomas with skull base invasion: a case-control study. Head & neck *26*, 396-400.

Chang, G. C., Lan, H. C., Juang, S. H., Wu, Y. C., Lee, H. C., Hung, Y. M., Yang, H. Y., Whang-Peng, J., and Liu, K. J. (2005). A pilot clinical trial of vaccination with dendritic cells pulsed with autologous tumor cells derived from malignant pleural effusion in patients with late-stage lung carcinoma. Cancer *103*, 763-771.

Chaudhri, V. K., Salzler, G. G., Dick, S. A., Buckman, M. S., Sordella, R., Karoly, E. D., Mohney, R., Stiles, B. M., Elemento, O., Altorki, N. K., and McGraw, T. E. (2013). Metabolic alterations in lung cancer-associated fibroblasts correlated with increased glycolytic metabolism of the tumor. Molecular cancer research : MCR.

Chen, F., Jackson, H., and Bina, W. F. (2009). Lung adenocarcinoma incidence rates and their relation to motor vehicle density. Cancer epidemiology, biomarkers & prevention : a publication of the American Association for Cancer Research, cosponsored by the American Society of Preventive Oncology *18*, 760-764.

Chin, Y., Janseens, J., Vandepitte, J., Vandenbrande, J., Opdebeek, L., and Raus, J. (1992). Phenotypic analysis of tumor-infiltrating lymphocytes from human breast cancer. Anticancer research *12*, 1463-1466.

Cortez-Retamozo, V., Etzrodt, M., Newton, A., Rauch, P. J., Chudnovskiy, A., Berger, C., Ryan, R. J., Iwamoto, Y., Marinelli, B., Gorbatov, R.*, et al.* (2012). Origins of tumor-associated macrophages and neutrophils. Proceedings of the National Academy of Sciences of the United States of America *109*, 2491-2496.

Coukos, G., Benencia, F., Buckanovich, R. J., and Conejo-Garcia, J. R. (2005). The role of dendritic cell precursors in tumour vasculogenesis. British journal of cancer *92*, 1182-1187.

Coussens, L. M., Raymond, W. W., Bergers, G., Laig-Webster, M., Behrendtsen, O., Werb, Z., Caughey, G. H., and Hanahan, D. (1999). Inflammatory mast cells up-regulate angiogenesis during squamous epithelial carcinogenesis. Genes & development *13*, 1382-1397.

Coussens, L. M., and Werb, Z. (2002). Inflammation and cancer. Nature *420*, 860-867.

Couvelard, A., O'Toole, D., Turley, H., Leek, R., Sauvanet, A., Degott, C., Ruszniewski, P., Belghiti, J., Harris, A. L., Gatter, K., and Pezzella, F. (2005). Microvascular density and hypoxia-inducible factor pathway in pancreatic endocrine tumours: negative correlation of microvascular density and VEGF expression with tumour progression. British journal of cancer *92*, 94-101.

Crino, L., Scagliotti, G. V., Ricci, S., De Marinis, F., Rinaldi, M., Gridelli, C., Ceribelli, A., Bianco, R., Marangolo, M., Di Costanzo, F.*, et al.* (1999). Gemcitabine and cisplatin versus mitomycin, ifosfamide, and cisplatin in advanced non-small-cell lung cancer: A randomized phase III study of the Italian Lung Cancer Project. Journal of clinical oncology : official journal of the American Society of Clinical Oncology *17*, 3522-3530.

Cros, J., Cagnard, N., Woollard, K., Patey, N., Zhang, S. Y., Senechal, B., Puel, A., Biswas, S. K., Moshous, D., Picard, C.*, et al.* (2010). Human CD14dim monocytes patrol and sense nucleic acids and viruses via TLR7 and TLR8 receptors. Immunity *33*, 375-386.

Dawson, T. C., Beck, M. A., Kuziel, W. A., Henderson, F., and Maeda, N. (2000). Contrasting effects of CCR5 and CCR2 deficiency in the pulmonary inflammatory response to influenza A virus. The American journal of pathology *156*, 1951-1959.

De Palma, M., and Naldini, L. (2006). Role of haematopoietic cells and endothelial progenitors in tumour angiogenesis. Biochimica et biophysica acta *1766*, 159-166.

De Palma, M., Venneri, M. A., Galli, R., Sergi Sergi, L., Politi, L. S., Sampaolesi, M., and Naldini, L. (2005). Tie2 identifies a hematopoietic lineage of proangiogenic monocytes required for tumor vessel formation and a mesenchymal population of pericyte progenitors. Cancer cell *8*, 211-226.

de Visser, K. E., Eichten, A., and Coussens, L. M. (2006). Paradoxical roles of the immune system during cancer development. Nature reviews Cancer *6*, 24-37.

Delebecq, T. J., Porte, H., Zerimech, F., Copin, M. C., Gouyer, V., Dacquembronne, E., Balduyck, M., Wurtz, A., and Huet, G. (2000). Overexpression level of stromelysin 3 is related to the lymph node involvement in non-small cell lung cancer. Clinical cancer research : an official journal of the American Association for Cancer Research *6*, 1086-1092.

DeNardo, D. G., Andreu, P., and Coussens, L. M. (2010). Interactions between lymphocytes and myeloid cells regulate pro- versus anti-tumor immunity. Cancer metastasis reviews *29*, 309-316.

Deshmane, S. L., Kremlev, S., Amini, S., and Sawaya, B. E. (2009). Monocyte chemoattractant protein-1 (MCP-1): an overview. Journal of interferon & cytokine research : the official journal of the International Society for Interferon and Cytokine Research *29*, 313-326.

Devesa, S. S., Bray, F., Vizcaino, A. P., and Parkin, D. M. (2005). International lung cancer trends by histologic type: male:female differences diminishing and adenocarcinoma rates rising. International journal of cancer Journal international du cancer *117*, 294-299.

Dewhirst, M. W. (1998). Concepts of oxygen transport at the microcirculatory level. Seminars in radiation oncology *8*, 143-150.

Digumarti, R., Wang, Y., Raman, G., Doval, D. C., Advani, S. H., Julka, P. K., Parikh, P. M., Patil, S., Nag, S., Madhavan, J.*, et al.* (2011). A randomized, double-blind, placebo-controlled, phase II study of oral talactoferrin in combination with carboplatin and paclitaxel in previously untreated locally advanced or metastatic non-small cell lung cancer. Journal of thoracic oncology : official publication of the International Association for the Study of Lung Cancer *6*, 1098-1103.

DiPersio, J. F., Micallef, I. N., Stiff, P. J., Bolwell, B. J., Maziarz, R. T., Jacobsen, E., Nademanee, A., McCarty, J., Bridger, G., Calandra, G., and Investigators (2009). Phase III prospective randomized double-blind placebo-controlled trial of plerixafor plus granulocyte colony-stimulating factor compared with placebo plus granulocyte colony-stimulating factor for autologous stem-cell mobilization and transplantation for patients with non-Hodgkin's lymphoma. Journal of clinical oncology : official journal of the American Society of Clinical Oncology *27*, 4767-4773.

Dong, C. (2008). TH17 cells in development: an updated view of their molecular identity and genetic programming. Nature reviews Immunology *8*, 337-348.

Dunn, G. P., Old, L. J., and Schreiber, R. D. (2004). The immunobiology of cancer immunosurveillance and immunoediting. Immunity *21*, 137-148.

Erreni, M., Solinas, G., Brescia, P., Osti, D., Zunino, F., Colombo, P., Destro, A., Roncalli, M., Mantovani, A., Draghi, R.*, et al.* (2010). Human glioblastoma tumours and neural cancer stem cells express the chemokine CX3CL1 and its receptor CX3CR1. Eur J Cancer *46*, 3383-3392.

Fakhoury, H. M., Noureddine, S., Tamim, H., Chmaisse, H., and Makki, R. (2012). Association of MMP3-1171(5A>6A) polymorphism with lung cancer in Lebanon. Genetic testing and molecular biomarkers *16*, 988-990.

Fehervari, Z., and Sakaguchi, S. (2004). CD4+ Tregs and immune control. The Journal of clinical investigation *114*, 1209-1217.

Ferlay, J., Shin, H. R., Bray, F., Forman, D., Mathers, C., and Parkin, D. M. (2010). Estimates of worldwide burden of cancer in 2008: GLOBOCAN 2008. International journal of cancer Journal international du cancer *127*, 2893-2917.

Fernandez-Aguilar, S., Jondet, M., Simonart, T., and Noel, J. C. (2006). Microvessel and lymphatic density in tubular carcinoma of the breast: comparative study with invasive low-grade ductal carcinoma. Breast *15*, 782-785.

Ferretti, E., Bertolotto, M., Deaglio, S., Tripodo, C., Ribatti, D., Audrito, V., Blengio, F., Matis, S., Zupo, S., Rossi, D.*, et al.* (2011). A novel role of the CX3CR1/CX3CL1 system in the cross-talk between chronic lymphocytic leukemia cells and tumor microenvironment. Leukemia *25*, 1268-1277.

Finberg, K. E., Sequist, L. V., Joshi, V. A., Muzikansky, A., Miller, J. M., Han, M., Beheshti, J., Chirieac, L. R., Mark, E. J., and Iafrate, A. J. (2007). Mucinous differentiation correlates with absence of EGFR mutation and presence of KRAS mutation in lung adenocarcinomas with bronchioloalveolar features. The Journal of molecular diagnostics : JMD *9*, 320-326.

Fitzpatrick, F. A. (2001). Inflammation, carcinogenesis and cancer. International immunopharmacology *1*, 1651-1667.

Fleetwood, A. J., Dinh, H., Cook, A. D., Hertzog, P. J., and Hamilton, J. A. (2009). GM-CSF- and M-CSF-dependent macrophage phenotypes display differential dependence on type I interferon signaling. Journal of leukocyte biology *86*, 411-421.

Fong, L., and Small, E. J. (2008). Anti-cytotoxic T-lymphocyte antigen-4 antibody: the first in an emerging class of immunomodulatory antibodies for cancer treatment. Journal of clinical oncology : official journal of the American Society of Clinical Oncology *26*, 5275-5283.

Freire, T., and Osinaga, E. (2012). The sweet side of tumor immunotherapy. Immunotherapy *4*, 719-734.

Galli, S. J., Borregaard, N., and Wynn, T. A. (2011). Phenotypic and functional plasticity of cells of innate immunity: macrophages, mast cells and neutrophils. Nature immunology *12*, 1035-1044.

Gandhi, L., and Johnson, B. E. (2006). Paraneoplastic syndromes associated with small cell lung cancer. Journal of the National Comprehensive Cancer Network : JNCCN *4*, 631-638.

Gao, Y., Goldstein, A. M., Consonni, D., Pesatori, A. C., Wacholder, S., Tucker, M. A., Caporaso, N. E., Goldin, L., and Landi, M. T. (2009). Family history of cancer and nonmalignant lung diseases as risk factors for lung cancer. International journal of cancer Journal international du cancer *125*, 146-152.

Garin, A., Tarantino, N., Faure, S., Daoudi, M., Lecureuil, C., Bourdais, A., Debre, P., Deterre, P., and Combadiere, C. (2003). Two novel fully functional isoforms of CX3CR1 are potent HIV coreceptors. J Immunol *171*, 5305-5312.

Gazzaniga, S., Bravo, A. I., Guglielmotti, A., van Rooijen, N., Maschi, F., Vecchi, A., Mantovani, A., Mordoh, J., and Wainstok, R. (2007). Targeting tumor-associated macrophages and inhibition of MCP-1 reduce angiogenesis and tumor growth in a human melanoma xenograft. The Journal of investigative dermatology *127*, 2031-2041.

Geissmann, F., Jung, S., and Littman, D. R. (2003). Blood monocytes consist of two principal subsets with distinct migratory properties. Immunity *19*, 71-82.

Gelboin, H. V. (1980). Benzo[alpha]pyrene metabolism, activation and carcinogenesis: role and regulation of mixed-function oxidases and related enzymes. Physiological reviews *60*, 1107-1166.

Gill, J. H., Kirwan, I. G., Seargent, J. M., Martin, S. W., Tijani, S., Anikin, V. A., Mearns, A. J., Bibby, M. C., Anthoney, A., and Loadman, P. M. (2004). MMP-10 is overexpressed, proteolytically active, and a potential target for therapeutic intervention in human lung carcinomas. Neoplasia *6*, 777-785.

Goetzl, E. J., Banda, M. J., and Leppert, D. (1996). Matrix metalloproteinases in immunity. J Immunol *156*, 1-4.

Gordon, S., and Martinez, F. O. (2010). Alternative activation of macrophages: mechanism and functions. Immunity *32*, 593-604.

Graeber, T. G., Osmanian, C., Jacks, T., Housman, D. E., Koch, C. J., Lowe, S. W., and Giaccia, A. J. (1996). Hypoxia-mediated selection of cells with diminished apoptotic potential in solid tumours. Nature *379*, 88-91.

Greten, F. R., Arkan, M. C., Bollrath, J., Hsu, L. C., Goode, J., Miething, C., Goktuna, S. I., Neuenhahn, M., Fierer, J., Paxian, S.*, et al.* (2007). NF-kappaB is a negative

regulator of IL-1beta secretion as revealed by genetic and pharmacological inhibition of IKKbeta. Cell *130*, 918-931.

Gridelli, C., Rossi, A., Maione, P., Ferrara, M. L., Castaldo, V., and Sacco, P. C. (2009). Vaccines for the treatment of non-small cell lung cancer: a renewed anticancer strategy. The oncologist *14*, 909-920.

Grunewald, M., Avraham, I., Dor, Y., Bachar-Lustig, E., Itin, A., Jung, S., Chimenti, S., Landsman, L., Abramovitch, R., and Keshet, E. (2006). VEGF-induced adult neovascularization: recruitment, retention, and role of accessory cells. Cell *124*, 175-189.

Hamilton, J. A. (2008). Colony-stimulating factors in inflammation and autoimmunity. Nature reviews Immunology *8*, 533-544.

Hanahan, D., and Folkman, J. (1996). Patterns and emerging mechanisms of the angiogenic switch during tumorigenesis. Cell *86*, 353-364.

Hanahan, D., and Weinberg, R. A. (2000). The hallmarks of cancer. Cell *100*, 57-70.

Haura, E. B. (2001). Treatment of advanced non-small-cell lung cancer: a review of current randomized clinical trials and an examination of emerging therapies. Cancer control : journal of the Moffitt Cancer Center *8*, 326-336.

Herbst, R. S., Heymach, J. V., and Lippman, S. M. (2008). Lung cancer. The New England journal of medicine *359*, 1367-1380.

Hirsch, F. R., Herbst, R. S., Olsen, C., Chansky, K., Crowley, J., Kelly, K., Franklin, W. A., Bunn, P. A., Jr., Varella-Garcia, M., and Gandara, D. R. (2008). Increased EGFR gene copy number detected by fluorescent in situ hybridization predicts outcome in non-small-cell lung cancer patients treated with cetuximab and chemotherapy. Journal of clinical oncology : official journal of the American Society of Clinical Oncology *26*, 3351-3357.

Hodi, F. S., O'Day, S. J., McDermott, D. F., Weber, R. W., Sosman, J. A., Haanen, J. B., Gonzalez, R., Robert, C., Schadendorf, D., Hassel, J. C.*, et al.* (2010). Improved survival with ipilimumab in patients with metastatic melanoma. The New England journal of medicine *363*, 711-723.

Iida, S., Kohro, T., Kodama, T., Nagata, S., and Fukunaga, R. (2005). Identification of CCR2, flotillin, and gp49B genes as new G-CSF targets during neutrophilic differentiation. Journal of leukocyte biology *78*, 481-490.

Imai, T., Hieshima, K., Haskell, C., Baba, M., Nagira, M., Nishimura, M., Kakizaki, M., Takagi, S., Nomiyama, H., Schall, T. J., and Yoshie, O. (1997). Identification and

molecular characterization of fractalkine receptor CX3CR1, which mediates both leukocyte migration and adhesion. Cell *91*, 521-530.

Irani, A. A., Schechter, N. M., Craig, S. S., DeBlois, G., and Schwartz, L. B. (1986). Two types of human mast cells that have distinct neutral protease compositions. Proceedings of the National Academy of Sciences of the United States of America *83*, 4464-4468.

Izzo, J. G., Correa, A. M., Wu, T. T., Malhotra, U., Chao, C. K., Luthra, R., Ensor, J., Dekovich, A., Liao, Z., Hittelman, W. N.*, et al.* (2006). Pretherapy nuclear factor-kappaB status, chemoradiation resistance, and metastatic progression in esophageal carcinoma. Molecular cancer therapeutics *5*, 2844-2850.

Janssen-Heijnen, M. L., and Coebergh, J. W. (2001). Trends in incidence and prognosis of the histological subtypes of lung cancer in North America, Australia, New Zealand and Europe. Lung cancer *31*, 123-137.

Johnson, D. H., Fehrenbacher, L., Novotny, W. F., Herbst, R. S., Nemunaitis, J. J., Jablons, D. M., Langer, C. J., DeVore, R. F., 3rd, Gaudreault, J., Damico, L. A.*, et al.* (2004). Randomized phase II trial comparing bevacizumab plus carboplatin and paclitaxel with carboplatin and paclitaxel alone in previously untreated locally advanced or metastatic non-small-cell lung cancer. Journal of clinical oncology : official journal of the American Society of Clinical Oncology *22*, 2184-2191.

Jung, S., Aliberti, J., Graemmel, P., Sunshine, M. J., Kreutzberg, G. W., Sher, A., and Littman, D. R. (2000). Analysis of fractalkine receptor CX(3)CR1 function by targeted deletion and green fluorescent protein reporter gene insertion. Molecular and cellular biology *20*, 4106-4114.

Justilien, V., Regala, R. P., Tseng, I. C., Walsh, M. P., Batra, J., Radisky, E. S., Murray, N. R., and Fields, A. P. (2012). Matrix metalloproteinase-10 is required for lung cancer stem cell maintenance, tumor initiation and metastatic potential. PloS one *7*, e35040.

Kalemkerian, G. P., and Gadgeel, S. M. (2013). Modern staging of small cell lung cancer. Journal of the National Comprehensive Cancer Network : JNCCN *11*, 99-104.

Kampen, G. T., Stafford, S., Adachi, T., Jinquan, T., Quan, S., Grant, J. A., Skov, P. S., Poulsen, L. K., and Alam, R. (2000). Eotaxin induces degranulation and chemotaxis of eosinophils through the activation of ERK2 and p38 mitogen-activated protein kinases. Blood *95*, 1911-1917.

Karin, M., Lawrence, T., and Nizet, V. (2006). Innate immunity gone awry: linking microbial infections to chronic inflammation and cancer. Cell *124*, 823-835.

Karnoub, A. E., Dash, A. B., Vo, A. P., Sullivan, A., Brooks, M. W., Bell, G. W., Richardson, A. L., Polyak, K., Tubo, R., and Weinberg, R. A. (2007). Mesenchymal stem cells within tumour stroma promote breast cancer metastasis. Nature *449*, 557-563.

Kelly, P. M., Davison, R. S., Bliss, E., and McGee, J. O. (1988). Macrophages in human breast disease: a quantitative immunohistochemical study. British journal of cancer *57*, 174-177.

Kelly, R. J., Gulley, J. L., and Giaccone, G. (2010). Targeting the immune system in non-small-cell lung cancer: bridging the gap between promising concept and therapeutic reality. Clinical lung cancer *11*, 228-237.

Kenfield, S. A., Wei, E. K., Stampfer, M. J., Rosner, B. A., and Colditz, G. A. (2008). Comparison of aspects of smoking among the four histological types of lung cancer. Tobacco control *17*, 198-204.

Khatwa, U. A., Kleibrink, B. E., Shapiro, S. D., and Subramaniam, M. (2010). MMP-8 promotes polymorphonuclear cell migration through collagen barriers in obliterative bronchiolitis. Journal of leukocyte biology *87*, 69-77.

Kim, K. W., Vallon-Eberhard, A., Zigmond, E., Farache, J., Shezen, E., Shakhar, G., Ludwig, A., Lira, S. A., and Jung, S. (2011). In vivo structure/function and expression analysis of the CX3C chemokine fractalkine. Blood *118*, e156-167.

Kito, K., Morishita, K., and Nishida, K. (2001). MCP-1 receptor binding affinity is up-regulated by pre-stimulation with MCP-1 in an actin polymerization-dependent manner. Journal of leukocyte biology *69*, 666-674.

Kitowska, K., Zakrzewicz, D., Konigshoff, M., Chrobak, I., Grimminger, F., Seeger, W., Bulau, P., and Eickelberg, O. (2008). Functional role and species-specific contribution of arginases in pulmonary fibrosis. American journal of physiology Lung cellular and molecular physiology *294*, L34-45.

Kohrmann, A., Kammerer, U., Kapp, M., Dietl, J., and Anacker, J. (2009). Expression of matrix metalloproteinases (MMPs) in primary human breast cancer and breast cancer cell lines: New findings and review of the literature. BMC cancer *9*, 188.

Koivunen, J. P., Mermel, C., Zejnullahu, K., Murphy, C., Lifshits, E., Holmes, A. J., Choi, H. G., Kim, J., Chiang, D., Thomas, R.*, et al.* (2008). EML4-ALK fusion gene and efficacy of an ALK kinase inhibitor in lung cancer. Clinical cancer research : an official journal of the American Association for Cancer Research *14*, 4275-4283.

Koshiba, T., Hosotani, R., Miyamoto, Y., Ida, J., Tsuji, S., Nakajima, S., Kawaguchi, M., Kobayashi, H., Doi, R., Hori, T.*, et al.* (2000). Expression of stromal cell-derived factor 1 and CXCR4 ligand receptor system in pancreatic cancer: a possible role for tumor progression. Clinical cancer research : an official journal of the American Association for Cancer Research *6*, 3530-3535.

Kugathasan, K., Roediger, E. K., Small, C. L., McCormick, S., Yang, P., and Xing, Z. (2008). CD11c+ antigen presenting cells from the alveolar space, lung parenchyma and spleen differ in their phenotype and capabilities to activate naive and antigen-primed T cells. BMC immunology *9*, 48.

Kuhne, M. R., Mulvey, T., Belanger, B., Chen, S., Pan, C., Chong, C., Cao, F., Niekro, W., Kempe, T., Henning, K. A.*, et al.* (2013). BMS-936564/MDX-1338: a fully human anti-CXCR4 antibody induces apoptosis in vitro and shows antitumor activity in vivo in hematologic malignancies. Clinical cancer research : an official journal of the American Association for Cancer Research *19*, 357-366.

Kundu, J. K., and Surh, Y. J. (2008). Inflammation: gearing the journey to cancer. Mutation research *659*, 15-30.

Kwak, E. L., Bang, Y. J., Camidge, D. R., Shaw, A. T., Solomon, B., Maki, R. G., Ou, S. H., Dezube, B. J., Janne, P. A., Costa, D. B.*, et al.* (2010). Anaplastic lymphoma kinase inhibition in non-small-cell lung cancer. The New England journal of medicine *363*, 1693-1703.

Lackner, C., Jukic, Z., Tsybrovskyy, O., Jatzko, G., Wette, V., Hoefler, G., Klimpfinger, M., Denk, H., and Zatloukal, K. (2004). Prognostic relevance of tumour-associated macrophages and von Willebrand factor-positive microvessels in colorectal cancer. Virchows Archiv : an international journal of pathology *445*, 160-167.

Landsman, L., Bar-On, L., Zernecke, A., Kim, K. W., Krauthgamer, R., Shagdarsuren, E., Lira, S. A., Weissman, I. L., Weber, C., and Jung, S. (2009). CX3CR1 is required for monocyte homeostasis and atherogenesis by promoting cell survival. Blood *113*, 963-972.

Langheinrich, A. C., Bohle, R. M., Breithecker, A., Lommel, D., and Rau, W. S. (2004). [Micro-computed tomography of the vasculature in parenchymal organs and lung alveoli]. Rofo *176*, 1219-1225.

Langheinrich, A. C., Yeniguen, M., Ostendorf, A., Marhoffer, S., Dierkes, C., von Gerlach, S., Nedelmann, M., Kampschulte, M., Bachmann, G., Stolz, E., and Gerriets, T.

(2010). In vitro evaluation of the sinus sagittalis superior thrombosis model in the rat using 3D micro- and nanocomputed tomography. Neuroradiology *52*, 815-821.

Laskin, D. L., Weinberger, B., and Laskin, J. D. (2001). Functional heterogeneity in liver and lung macrophages. Journal of leukocyte biology *70*, 163-170.

Lawrence, T., and Natoli, G. (2011). Transcriptional regulation of macrophage polarization: enabling diversity with identity. Nature reviews Immunology *11*, 750-761.

Le Chevalier, T., Brisgand, D., Douillard, J. Y., Pujol, J. L., Alberola, V., Monnier, A., Riviere, A., Lianes, P., Chomy, P., Cigolari, S., and et al. (1994). Randomized study of vinorelbine and cisplatin versus vindesine and cisplatin versus vinorelbine alone in advanced non-small-cell lung cancer: results of a European multicenter trial including 612 patients. Journal of clinical oncology : official journal of the American Society of Clinical Oncology *12*, 360-367.

Lee, S. J., Namkoong, S., Kim, Y. M., Kim, C. K., Lee, H., Ha, K. S., Chung, H. T., and Kwon, Y. G. (2006). Fractalkine stimulates angiogenesis by activating the Raf-1/MEK/ERK- and PI3K/Akt/eNOS-dependent signal pathways. Am J Physiol Heart Circ Physiol *291*, H2836-2846.

Leek, R. D., Hunt, N. C., Landers, R. J., Lewis, C. E., Royds, J. A., and Harris, A. L. (2000). Macrophage infiltration is associated with VEGF and EGFR expression in breast cancer. The Journal of pathology *190*, 430-436.

Leifeld, L., Fielenbach, M., Dumoulin, F. L., Speidel, N., Sauerbruch, T., and Spengler, U. (2002). Inducible nitric oxide synthase (iNOS) and endothelial nitric oxide synthase (eNOS) expression in fulminant hepatic failure. Journal of hepatology *37*, 613-619.

Leuschner, F., Dutta, P., Gorbatov, R., Novobrantseva, T. I., Donahoe, J. S., Courties, G., Lee, K. M., Kim, J. I., Markmann, J. F., Marinelli, B.*, et al.* (2011). Therapeutic siRNA silencing in inflammatory monocytes in mice. Nature biotechnology *29*, 1005-1010.

Levental, K. R., Yu, H., Kass, L., Lakins, J. N., Egeblad, M., Erler, J. T., Fong, S. F., Csiszar, K., Giaccia, A., Weninger, W.*, et al.* (2009). Matrix crosslinking forces tumor progression by enhancing integrin signaling. Cell *139*, 891-906.

Lewis, C. E., and Pollard, J. W. (2006). Distinct role of macrophages in different tumor microenvironments. Cancer research *66*, 605-612.

Li, C. Y., Shan, S., Cao, Y., and Dewhirst, M. W. (2000). Role of incipient angiogenesis in cancer metastasis. Cancer metastasis reviews *19*, 7-11.

Li, Y., Qiu, X., Zhang, S., Zhang, Q., and Wang, E. (2009). Hypoxia induced CCR7 expression via HIF-1alpha and HIF-2alpha correlates with migration and invasion in lung cancer cells. Cancer biology & therapy *8*, 322-330.

Lin, E. Y., and Pollard, J. W. (2004). Role of infiltrated leucocytes in tumour growth and spread. British journal of cancer *90*, 2053-2058.

Lindmark, G., Gerdin, B., Sundberg, C., Pahlman, L., Bergstrom, R., and Glimelius, B. (1996). Prognostic significance of the microvascular count in colorectal cancer. Journal of clinical oncology : official journal of the American Society of Clinical Oncology *14*, 461-466.

Lo, C. M., Wang, H. B., Dembo, M., and Wang, Y. L. (2000). Cell movement is guided by the rigidity of the substrate. Biophysical journal *79*, 144-152.

Lynch, T. J., Bell, D. W., Sordella, R., Gurubhagavatula, S., Okimoto, R. A., Brannigan, B. W., Harris, P. L., Haserlat, S. M., Supko, J. G., Haluska, F. G.*, et al.* (2004). Activating mutations in the epidermal growth factor receptor underlying responsiveness of non-small-cell lung cancer to gefitinib. The New England journal of medicine *350*, 2129-2139.

MacLeod, M. C., and Tang, M. S. (1985). Interactions of benzo(a)pyrene diol-epoxides with linear and supercoiled DNA. Cancer research *45*, 51-56.

Malvezzi, M., Bertuccio, P., Levi, F., La Vecchia, C., and Negri, E. (2012). European cancer mortality predictions for the year 2012. Annals of oncology : official journal of the European Society for Medical Oncology / ESMO *23*, 1044-1052.

Mantovani, A., Sozzani, S., Locati, M., Allavena, P., and Sica, A. (2002). Macrophage polarization: tumor-associated macrophages as a paradigm for polarized M2 mononuclear phagocytes. Trends in immunology *23*, 549-555.

Mao, L., Lee, J. S., Kurie, J. M., Fan, Y. H., Lippman, S. M., Lee, J. J., Ro, J. Y., Broxson, A., Yu, R., Morice, R. C.*, et al.* (1997). Clonal genetic alterations in the lungs of current and former smokers. Journal of the National Cancer Institute *89*, 857-862.

McCarthy, W. J., Meza, R., Jeon, J., and Moolgavkar, S. H. (2012). Chapter 6: Lung cancer in never smokers: epidemiology and risk prediction models. Risk analysis : an official publication of the Society for Risk Analysis *32 Suppl 1*, S69-84.

McDonald, D. M., and Choyke, P. L. (2003). Imaging of angiogenesis: from microscope to clinic. Nature medicine *9*, 713-725.

Mellado, M., Rodriguez-Frade, J. M., Aragay, A., del Real, G., Martin, A. M., Vila-Coro, A. J., Serrano, A., Mayor, F., Jr., and Martinez, A. C. (1998). The chemokine

monocyte chemotactic protein 1 triggers Janus kinase 2 activation and tyrosine phosphorylation of the CCR2B receptor. J Immunol *161*, 805-813.

Micke, P., Faldum, A., Metz, T., Beeh, K. M., Bittinger, F., Hengstler, J. G., and Buhl, R. (2002). Staging small cell lung cancer: Veterans Administration Lung Study Group versus International Association for the Study of Lung Cancer--what limits limited disease? Lung cancer *37*, 271-276.

Moilanen, M., Pirila, E., Grenman, R., Sorsa, T., and Salo, T. (2002). Expression and regulation of collagenase-2 (MMP-8) in head and neck squamous cell carcinomas. The Journal of pathology *197*, 72-81.

Mok, T. S., Wu, Y. L., Yu, C. J., Zhou, C., Chen, Y. M., Zhang, L., Ignacio, J., Liao, M., Srimuninnimit, V., Boyer, M. J.*, et al.* (2009). Randomized, placebo-controlled, phase II study of sequential erlotinib and chemotherapy as first-line treatment for advanced non-small-cell lung cancer. Journal of clinical oncology : official journal of the American Society of Clinical Oncology *27*, 5080-5087.

Molina, R., Filella, X., Auge, J. M., Fuentes, R., Bover, I., Rifa, J., Moreno, V., Canals, E., Vinolas, N., Marquez, A.*, et al.* (2003). Tumor markers (CEA, CA 125, CYFRA 21-1, SCC and NSE) in patients with non-small cell lung cancer as an aid in histological diagnosis and prognosis. Comparison with the main clinical and pathological prognostic factors. Tumour biology : the journal of the International Society for Oncodevelopmental Biology and Medicine *24*, 209-218.

Monti, P., Leone, B. E., Marchesi, F., Balzano, G., Zerbi, A., Scaltrini, F., Pasquali, C., Calori, G., Pessi, F., Sperti, C.*, et al.* (2003). The CC chemokine MCP-1/CCL2 in pancreatic cancer progression: regulation of expression and potential mechanisms of antimalignant activity. Cancer research *63*, 7451-7461.

Moore, U. M., Kaplow, J. M., Pleass, R. D., Castro, S. W., Naik, K., Lynch, C. N., Daly, S., Roach, A. G., Jaye, M., and Williams, R. J. (1997). Monocyte chemoattractant protein-2 is a potent agonist of CCR2B. Journal of leukocyte biology *62*, 911-915.

Morikawa, S., Baluk, P., Kaidoh, T., Haskell, A., Jain, R. K., and McDonald, D. M. (2002). Abnormalities in pericytes on blood vessels and endothelial sprouts in tumors. The American journal of pathology *160*, 985-1000.

Morrison, C., Mancini, S., Cipollone, J., Kappelhoff, R., Roskelley, C., and Overall, C. (2011). Microarray and proteomic analysis of breast cancer cell and osteoblast co-cultures: role of osteoblast matrix metalloproteinase (MMP)-13 in bone metastasis. The Journal of biological chemistry *286*, 34271-34285.

Mosser, D. M., and Edwards, J. P. (2008). Exploring the full spectrum of macrophage activation. Nature reviews Immunology *8*, 958-969.

Motoi, N., Szoke, J., Riely, G. J., Seshan, V. E., Kris, M. G., Rusch, V. W., Gerald, W. L., and Travis, W. D. (2008). Lung adenocarcinoma: modification of the 2004 WHO mixed subtype to include the major histologic subtype suggests correlations between papillary and micropapillary adenocarcinoma subtypes, EGFR mutations and gene expression analysis. The American journal of surgical pathology *32*, 810-827.

Mroczko, B., Groblewska, M., Wereszczynska-Siemiatkowska, U., Okulczyk, B., Kedra, B., Laszewicz, W., Dabrowski, A., and Szmitkowski, M. (2007). Serum macrophage-colony stimulating factor levels in colorectal cancer patients correlate with lymph node metastasis and poor prognosis. Clinica chimica acta; international journal of clinical chemistry *380*, 208-212.

Muller, A., Homey, B., Soto, H., Ge, N., Catron, D., Buchanan, M. E., McClanahan, T., Murphy, E., Yuan, W., Wagner, S. N.*, et al.* (2001). Involvement of chemokine receptors in breast cancer metastasis. Nature *410*, 50-56.

Munk, M. E., and Emoto, M. (1995). Functions of T-cell subsets and cytokines in mycobacterial infections. The European respiratory journal Supplement *20*, 668s-675s.

Murdoch, C., Giannoudis, A., and Lewis, C. E. (2004). Mechanisms regulating the recruitment of macrophages into hypoxic areas of tumors and other ischemic tissues. Blood *104*, 2224-2234.

Murray, P. J., and Wynn, T. A. (2011). Protective and pathogenic functions of macrophage subsets. Nature reviews Immunology *11*, 723-737.

Nannuru, K. C., Futakuchi, M., Varney, M. L., Vincent, T. M., Marcusson, E. G., and Singh, R. K. (2010). Matrix metalloproteinase (MMP)-13 regulates mammary tumor-induced osteolysis by activating MMP9 and transforming growth factor-beta signaling at the tumor-bone interface. Cancer research *70*, 3494-3504.

Nars, M. S., and Kaneno, R. (2012). Immunomodulatory effects of low dose chemotherapy and perspectives of its combination with immunotherapy. International journal of cancer Journal international du cancer.

Noh, S., and Shim, H. (2012). Optimal combination of immunohistochemical markers for subclassification of non-small cell lung carcinomas: A tissue microarray study of poorly differentiated areas. Lung cancer *76*, 51-55.

Numasaki, M., Fukushi, J., Ono, M., Narula, S. K., Zavodny, P. J., Kudo, T., Robbins, P. D., Tahara, H., and Lotze, M. T. (2003). Interleukin-17 promotes angiogenesis and tumor growth. Blood *101*, 2620-2627.

Numasaki, M., Watanabe, M., Suzuki, T., Takahashi, H., Nakamura, A., McAllister, F., Hishinuma, T., Goto, J., Lotze, M. T., Kolls, J. K., and Sasaki, H. (2005). IL-17 enhances the net angiogenic activity and in vivo growth of human non-small cell lung cancer in SCID mice through promoting CXCR-2-dependent angiogenesis. J Immunol *175*, 6177-6189.

Oonakahara, K., Matsuyama, W., Higashimoto, I., Kawabata, M., Arimura, K., and Osame, M. (2004). Stromal-derived factor-1alpha/CXCL12-CXCR 4 axis is involved in the dissemination of NSCLC cells into pleural space. American journal of respiratory cell and molecular biology *30*, 671-677.

Orimo, A., Gupta, P. B., Sgroi, D. C., Arenzana-Seisdedos, F., Delaunay, T., Naeem, R., Carey, V. J., Richardson, A. L., and Weinberg, R. A. (2005). Stromal fibroblasts present in invasive human breast carcinomas promote tumor growth and angiogenesis through elevated SDF-1/CXCL12 secretion. Cell *121*, 335-348.

Paez, J. G., Janne, P. A., Lee, J. C., Tracy, S., Greulich, H., Gabriel, S., Herman, P., Kaye, F. J., Lindeman, N., Boggon, T. J.*, et al.* (2004). EGFR mutations in lung cancer: correlation with clinical response to gefitinib therapy. Science *304*, 1497-1500.

Palframan, R. T., Jung, S., Cheng, G., Weninger, W., Luo, Y., Dorf, M., Littman, D. R., Rollins, B. J., Zweerink, H., Rot, A., and von Andrian, U. H. (2001). Inflammatory chemokine transport and presentation in HEV: a remote control mechanism for monocyte recruitment to lymph nodes in inflamed tissues. The Journal of experimental medicine *194*, 1361-1373.

Palleroni, A. V., Varesio, L., Wright, R. B., and Brunda, M. J. (1991). Tumoricidal alveolar macrophage and tumor infiltrating macrophage cell lines. International journal of cancer Journal international du cancer *49*, 296-302.

Pao, W., Miller, V., Zakowski, M., Doherty, J., Politi, K., Sarkaria, I., Singh, B., Heelan, R., Rusch, V., Fulton, L.*, et al.* (2004). EGF receptor gene mutations are common in lung cancers from "never smokers" and are associated with sensitivity of tumors to gefitinib and erlotinib. Proceedings of the National Academy of Sciences of the United States of America *101*, 13306-13311.

Parikh, P. M., Vaid, A., Advani, S. H., Digumarti, R., Madhavan, J., Nag, S., Bapna, A., Sekhon, J. S., Patil, S., Ismail, P. M.*, et al.* (2011). Randomized, double-blind,

placebo-controlled phase II study of single-agent oral talactoferrin in patients with locally advanced or metastatic non-small-cell lung cancer that progressed after chemotherapy. Journal of clinical oncology : official journal of the American Society of Clinical Oncology *29*, 4129-4136.

Pelosof, L. C., and Gerber, D. E. (2010). Paraneoplastic syndromes: an approach to diagnosis and treatment. Mayo Clinic proceedings Mayo Clinic *85*, 838-854.

Petersen, R. P., Campa, M. J., Sperlazza, J., Conlon, D., Joshi, M. B., Harpole, D. H., Jr., and Patz, E. F., Jr. (2006). Tumor infiltrating Foxp3+ regulatory T-cells are associated with recurrence in pathologic stage I NSCLC patients. Cancer *107*, 2866-2872.

Phillips, D. H. (1983). Fifty years of benzo(a)pyrene. Nature *303*, 468-472.

Piccard, H., Muschel, R. J., and Opdenakker, G. (2012). On the dual roles and polarized phenotypes of neutrophils in tumor development and progression. Critical reviews in oncology/hematology *82*, 296-309.

Picchio, M. C., Scala, E., Pomponi, D., Caprini, E., Frontani, M., Angelucci, I., Mangoni, A., Lazzeri, C., Perez, M., Remotti, D.*, et al.* (2008). CXCL13 is highly produced by Sezary cells and enhances their migratory ability via a synergistic mechanism involving CCL19 and CCL21 chemokines. Cancer research *68*, 7137-7146.

Pivetta, E., Scapolan, M., Pecolo, M., Wassermann, B., Abu-Rumeileh, I., Balestreri, L., Borsatti, E., Tripodo, C., Colombatti, A., and Spessotto, P. (2011). MMP-13 stimulates osteoclast differentiation and activation in tumour breast bone metastases. Breast cancer research : BCR *13*, R105.

Polentarutti, N., Allavena, P., Bianchi, G., Giardina, G., Basile, A., Sozzani, S., Mantovani, A., and Introna, M. (1997). IL-2-regulated expression of the monocyte chemotactic protein-1 receptor (CCR2) in human NK cells: characterization of a predominant 3.4-kilobase transcript containing CCR2B and CCR2A sequences. J Immunol *158*, 2689-2694.

Pollard, J. W. (2004). Tumour-educated macrophages promote tumour progression and metastasis. Nature reviews Cancer *4*, 71-78.

Pucci, F., Venneri, M. A., Biziato, D., Nonis, A., Moi, D., Sica, A., Di Serio, C., Naldini, L., and De Palma, M. (2009). A distinguishing gene signature shared by tumor-infiltrating Tie2-expressing monocytes, blood "resident" monocytes, and embryonic macrophages suggests common functions and developmental relationships. Blood *114*, 901-914.

Qian, B. Z., Li, J., Zhang, H., Kitamura, T., Zhang, J., Campion, L. R., Kaiser, E. A., Snyder, L. A., and Pollard, J. W. (2011). CCL2 recruits inflammatory monocytes to facilitate breast-tumour metastasis. Nature *475*, 222-225.

Qian, B. Z., and Pollard, J. W. (2010). Macrophage diversity enhances tumor progression and metastasis. Cell *141*, 39-51.

Quint, L. E., Tummala, S., Brisson, L. J., Francis, I. R., Krupnick, A. S., Kazerooni, E. A., Iannettoni, M. D., Whyte, R. I., and Orringer, M. B. (1996). Distribution of distant metastases from newly diagnosed non-small cell lung cancer. The Annals of thoracic surgery *62*, 246-250.

Raftopoulos, H. (2007). Diagnosis and management of hyponatremia in cancer patients. Supportive care in cancer : official journal of the Multinational Association of Supportive Care in Cancer *15*, 1341-1347.

Raschke, W. C., Baird, S., Ralph, P., and Nakoinz, I. (1978). Functional macrophage cell lines transformed by Abelson leukemia virus. Cell *15*, 261-267.

Reed, J. R., Stone, M. D., Beadnell, T. C., Ryu, Y., Griffin, T. J., and Schwertfeger, K. L. (2012). Fibroblast growth factor receptor 1 activation in mammary tumor cells promotes macrophage recruitment in a CX3CL1-dependent manner. PloS one *7*, e45877.

Rehman, S., and Jayson, G. C. (2005). Molecular imaging of antiangiogenic agents. The oncologist *10*, 92-103.

Riely, G. J., Kris, M. G., Rosenbaum, D., Marks, J., Li, A., Chitale, D. A., Nafa, K., Riedel, E. R., Hsu, M., Pao, W.*, et al.* (2008). Frequency and distinctive spectrum of KRAS mutations in never smokers with lung adenocarcinoma. Clinical cancer research : an official journal of the American Association for Cancer Research *14*, 5731-5734.

Rodriguez-Frade, J. M., Vila-Coro, A. J., de Ana, A. M., Albar, J. P., Martinez, A. C., and Mellado, M. (1999). The chemokine monocyte chemoattractant protein-1 induces functional responses through dimerization of its receptor CCR2. Proceedings of the National Academy of Sciences of the United States of America *96*, 3628-3633.

Romagnani, S., Parronchi, P., D'Elios, M. M., Romagnani, P., Annunziato, F., Piccinni, M. P., Manetti, R., Sampognaro, S., Mavilia, C., De Carli, M.*, et al.* (1997). An update on human Th1 and Th2 cells. International archives of allergy and immunology *113*, 153-156.

Roussos, E. T., Condeelis, J. S., and Patsialou, A. (2011). Chemotaxis in cancer. Nature reviews Cancer *11*, 573-587.

Russell, P. A., Wainer, Z., Wright, G. M., Daniels, M., Conron, M., and Williams, R. A. (2011). Does lung adenocarcinoma subtype predict patient survival?: A clinicopathologic study based on the new International Association for the Study of Lung Cancer/American Thoracic Society/European Respiratory Society international multidisciplinary lung adenocarcinoma classification. Journal of thoracic oncology : official publication of the International Association for the Study of Lung Cancer *6*, 1496-1504.

Sancar, A. (1995). DNA repair in humans. Annual review of genetics *29*, 69-105.

Sanders, S. K., Crean, S. M., Boxer, P. A., Kellner, D., LaRosa, G. J., and Hunt, S. W., 3rd (2000). Functional differences between monocyte chemotactic protein-1 receptor A and monocyte chemotactic protein-1 receptor B expressed in a Jurkat T cell. J Immunol *165*, 4877-4883.

Sandler, A., Gray, R., Perry, M. C., Brahmer, J., Schiller, J. H., Dowlati, A., Lilenbaum, R., and Johnson, D. H. (2006). Paclitaxel-carboplatin alone or with bevacizumab for non-small-cell lung cancer. The New England journal of medicine *355*, 2542-2550.

Sandler, A. B., Nemunaitis, J., Denham, C., von Pawel, J., Cormier, Y., Gatzemeier, U., Mattson, K., Manegold, C., Palmer, M. C., Gregor, A.*, et al.* (2000). Phase III trial of gemcitabine plus cisplatin versus cisplatin alone in patients with locally advanced or metastatic non-small-cell lung cancer. Journal of clinical oncology : official journal of the American Society of Clinical Oncology *18*, 122-130.

Sangha, R., and Butts, C. (2007). L-BLP25: a peptide vaccine strategy in non small cell lung cancer. Clinical cancer research : an official journal of the American Association for Cancer Research *13*, s4652-4654.

Sarrafzadegan, N., Rabiei, K., Shirani, S., Kabir, A., Mohammadifard, N., and Roohafza, H. (2007). Drop-out predictors in cardiac rehabilitation programmes and the impact of sex differences among coronary heart disease patients in an Iranian sample: a cohort study. Clinical rehabilitation *21*, 362-372.

Sato, M., Shames, D. S., Gazdar, A. F., and Minna, J. D. (2007). A translational view of the molecular pathogenesis of lung cancer. Journal of thoracic oncology : official publication of the International Association for the Study of Lung Cancer *2*, 327-343.

Savai, R., Schermuly, R. T., Pullamsetti, S. S., Schneider, M., Greschus, S., Ghofrani, H. A., Traupe, H., Grimminger, F., and Banat, G. A. (2007). A combination hybrid-based

vaccination/adoptive cellular therapy to prevent tumor growth by involvement of T cells. Cancer research *67*, 5443-5453.

Schwartz, A. G., and Ruckdeschel, J. C. (2006). Familial lung cancer: genetic susceptibility and relationship to chronic obstructive pulmonary disease. American journal of respiratory and critical care medicine *173*, 16-22.

Sciume, G., Soriani, A., Piccoli, M., Frati, L., Santoni, A., and Bernardini, G. (2010). CX3CR1/CX3CL1 axis negatively controls glioma cell invasion and is modulated by transforming growth factor-beta1. Neuro-oncology *12*, 701-710.

Serbina, N. V., Jia, T., Hohl, T. M., and Pamer, E. G. (2008). Monocyte-mediated defense against microbial pathogens. Annual review of immunology *26*, 421-452.

Sharma, S. V., Bell, D. W., Settleman, J., and Haber, D. A. (2007). Epidermal growth factor receptor mutations in lung cancer. Nature reviews Cancer *7*, 169-181.

Shi, C., and Pamer, E. G. (2011). Monocyte recruitment during infection and inflammation. Nature reviews Immunology *11*, 762-774.

Shibayama, T., Ueoka, H., Nishii, K., Kiura, K., Tabata, M., Miyatake, K., Kitajima, T., and Harada, M. (2001). Complementary roles of pro-gastrin-releasing peptide (ProGRP) and neuron specific enolase (NSE) in diagnosis and prognosis of small-cell lung cancer (SCLC). Lung cancer *32*, 61-69.

Sica, A., Larghi, P., Mancino, A., Rubino, L., Porta, C., Totaro, M. G., Rimoldi, M., Biswas, S. K., Allavena, P., and Mantovani, A. (2008). Macrophage polarization in tumour progression. Seminars in cancer biology *18*, 349-355.

Sica, A., Saccani, A., Bottazzi, B., Bernasconi, S., Allavena, P., Gaetano, B., Fei, F., LaRosa, G., Scotton, C., Balkwill, F., and Mantovani, A. (2000). Defective expression of the monocyte chemotactic protein-1 receptor CCR2 in macrophages associated with human ovarian carcinoma. J Immunol *164*, 733-738.

Siddiqui, S. A., Frigola, X., Bonne-Annee, S., Mercader, M., Kuntz, S. M., Krambeck, A. E., Sengupta, S., Dong, H., Cheville, J. C., Lohse, C. M.*, et al.* (2007). Tumor-infiltrating Foxp3-CD4+CD25+ T cells predict poor survival in renal cell carcinoma. Clinical cancer research : an official journal of the American Association for Cancer Research *13*, 2075-2081.

Siegel, R., Naishadham, D., and Jemal, A. (2013). Cancer statistics, 2013. CA: a cancer journal for clinicians *63*, 11-30.

Siegel, R., Ward, E., Brawley, O., and Jemal, A. (2011). Cancer statistics, 2011: the impact of eliminating socioeconomic and racial disparities on premature cancer deaths. CA: a cancer journal for clinicians *61*, 212-236.

Sierra-Filardi, E., Vega, M. A., Sanchez-Mateos, P., Corbi, A. L., and Puig-Kroger, A. (2010). Heme Oxygenase-1 expression in M-CSF-polarized M2 macrophages contributes to LPS-induced IL-10 release. Immunobiology *215*, 788-795.

Soda, M., Choi, Y. L., Enomoto, M., Takada, S., Yamashita, Y., Ishikawa, S., Fujiwara, S., Watanabe, H., Kurashina, K., Hatanaka, H.*, et al.* (2007). Identification of the transforming EML4-ALK fusion gene in non-small-cell lung cancer. Nature *448*, 561-566.

Sounni, N. E., and Noel, A. (2013). Targeting the tumor microenvironment for cancer therapy. Clinical chemistry *59*, 85-93.

Sozzani, S., Ghezzi, S., Iannolo, G., Luini, W., Borsatti, A., Polentarutti, N., Sica, A., Locati, M., Mackay, C., Wells, T. N.*, et al.* (1998). Interleukin 10 increases CCR5 expression and HIV infection in human monocytes. The Journal of experimental medicine *187*, 439-444.

Spira, A., Beane, J., Shah, V., Liu, G., Schembri, F., Yang, X., Palma, J., and Brody, J. S. (2004). Effects of cigarette smoke on the human airway epithelial cell transcriptome. Proceedings of the National Academy of Sciences of the United States of America *101*, 10143-10148.

Stadlmann, S., Pollheimer, J., Moser, P. L., Raggi, A., Amberger, A., Margreiter, R., Offner, F. A., Mikuz, G., Dirnhofer, S., and Moch, H. (2003). Cytokine-regulated expression of collagenase-2 (MMP-8) is involved in the progression of ovarian cancer. Eur J Cancer *39*, 2499-2505.

Stewart, S. A., Dykxhoorn, D. M., Palliser, D., Mizuno, H., Yu, E. Y., An, D. S., Sabatini, D. M., Chen, I. S., Hahn, W. C., Sharp, P. A.*, et al.* (2003). Lentivirus-delivered stable gene silencing by RNAi in primary cells. RNA *9*, 493-501.

Stoyanov, E., Uddin, M., Mankuta, D., Dubinett, S. M., and Levi-Schaffer, F. (2012). Mast cells and histamine enhance the proliferation of non-small cell lung cancer cells. Lung cancer *75*, 38-44.

Strauss, L., Bergmann, C., Szczepanski, M., Gooding, W., Johnson, J. T., and Whiteside, T. L. (2007). A unique subset of CD4+CD25highFoxp3+ T cells secreting interleukin-10 and transforming growth factor-beta1 mediates suppression in the tumor

microenvironment. Clinical cancer research : an official journal of the American Association for Cancer Research *13*, 4345-4354.

Strnad, H., Lacina, L., Kolar, M., Cada, Z., Vlcek, C., Dvorankova, B., Betka, J., Plzak, J., Chovanec, M., Sachova, J.*, et al.* (2010). Head and neck squamous cancer stromal fibroblasts produce growth factors influencing phenotype of normal human keratinocytes. Histochemistry and cell biology *133*, 201-211.

Stupp, R., Monnerat, C., Turrisi, A. T., 3rd, Perry, M. C., and Leyvraz, S. (2004). Small cell lung cancer: state of the art and future perspectives. Lung cancer *45*, 105-117.

Sugimoto, H., Mundel, T. M., Kieran, M. W., and Kalluri, R. (2006). Identification of fibroblast heterogeneity in the tumor microenvironment. Cancer biology & therapy *5*, 1640-1646.

Sun, L., Louie, M. C., Vannella, K. M., Wilke, C. A., LeVine, A. M., Moore, B. B., and Shanley, T. P. (2011). New concepts of IL-10-induced lung fibrosis: fibrocyte recruitment and M2 activation in a CCL2/CCR2 axis. American journal of physiology Lung cellular and molecular physiology *300*, L341-353.

Sun, S., Schiller, J. H., and Gazdar, A. F. (2007). Lung cancer in never smokers--a different disease. Nature reviews Cancer *7*, 778-790.

Tacha, D., Yu, C., Bremer, R., Qi, W., and Haas, T. (2012). A 6-antibody panel for the classification of lung adenocarcinoma versus squamous cell carcinoma. Applied immunohistochemistry & molecular morphology : AIMM / official publication of the Society for Applied Immunohistochemistry *20*, 201-207.

Tanaka, K., Kurebayashi, J., Sohda, M., Nomura, T., Prabhakar, U., Yan, L., and Sonoo, H. (2009). The expression of monocyte chemotactic protein-1 in papillary thyroid carcinoma is correlated with lymph node metastasis and tumor recurrence. Thyroid : official journal of the American Thyroid Association *19*, 21-25.

Tang, Q., and Bluestone, J. A. (2008). The Foxp3+ regulatory T cell: a jack of all trades, master of regulation. Nature immunology *9*, 239-244.

Tardaguila, M., Mira, E., Garcia-Cabezas, M. A., Feijoo, A. M., Quintela-Fandino, M., Azcoitia, I., Lira, S. A., and Manes, S. (2013). CX3CL1 promotes breast cancer via transactivation of the EGF pathway. Cancer research *73*, 4461-4473.

Tarhini, A. A., and Iqbal, F. (2010). CTLA-4 blockade: therapeutic potential in cancer treatments. OncoTargets and therapy *3*, 15-25.

Taylor, R., Najafi, F., and Dobson, A. (2007). Meta-analysis of studies of passive smoking and lung cancer: effects of study type and continent. International journal of epidemiology *36*, 1048-1059.

Terme, M., Pernot, S., Marcheteau, E., Sandoval, F., Benhamouda, N., Colussi, O., Dubreuil, O., Carpentier, A. F., Tartour, E., and Taieb, J. (2013). VEGFA-VEGFR Pathway Blockade Inhibits Tumor-Induced Regulatory T-cell Proliferation in Colorectal Cancer. Cancer research *73*, 539-549.

Thun, M. J., Hannan, L. M., Adams-Campbell, L. L., Boffetta, P., Buring, J. E., Feskanich, D., Flanders, W. D., Jee, S. H., Katanoda, K., Kolonel, L. N.*, et al.* (2008). Lung cancer occurrence in never-smokers: an analysis of 13 cohorts and 22 cancer registry studies. PLoS medicine *5*, e185.

Travis, W. D., Brambilla, E., Noguchi, M., Nicholson, A. G., Geisinger, K. R., Yatabe, Y., Beer, D. G., Powell, C. A., Riely, G. J., Van Schil, P. E.*, et al.* (2011). International association for the study of lung cancer/american thoracic society/european respiratory society international multidisciplinary classification of lung adenocarcinoma. Journal of thoracic oncology : official publication of the International Association for the Study of Lung Cancer *6*, 244-285.

Truong, T., Hung, R. J., Amos, C. I., Wu, X., Bickeboller, H., Rosenberger, A., Sauter, W., Illig, T., Wichmann, H. E., Risch, A.*, et al.* (2010). Replication of lung cancer susceptibility loci at chromosomes 15q25, 5p15, and 6p21: a pooled analysis from the International Lung Cancer Consortium. Journal of the National Cancer Institute *102*, 959-971.

Trzonkowski, P., Szmit, E., Mysliwska, J., Dobyszuk, A., and Mysliwski, A. (2004). CD4+CD25+ T regulatory cells inhibit cytotoxic activity of T CD8+ and NK lymphocytes in the direct cell-to-cell interaction. Clin Immunol *112*, 258-267.

Tsang, J. Y., Ni, Y. B., Chan, S. K., Shao, M. M., Kwok, Y. K., Chan, K. W., Tan, P. H., and Tse, G. M. (2013). CX3CL1 expression is associated with poor outcome in breast cancer patients. Breast cancer research and treatment *140*, 495-504.

Tsao, M. S., Sakurada, A., Cutz, J. C., Zhu, C. Q., Kamel-Reid, S., Squire, J., Lorimer, I., Zhang, T., Liu, N., Daneshmand, M.*, et al.* (2005). Erlotinib in lung cancer - molecular and clinical predictors of outcome. The New England journal of medicine *353*, 133-144.

Uguccioni, M., D'Apuzzo, M., Loetscher, M., Dewald, B., and Baggiolini, M. (1995). Actions of the chemotactic cytokines MCP-1, MCP-2, MCP-3, RANTES, MIP-1 alpha and MIP-1 beta on human monocytes. European journal of immunology *25*, 64-68.

Um, S. J., Choi, Y. J., Shin, H. J., Son, C. H., Park, Y. S., Roh, M. S., Kim, Y. S., Kim, Y. D., Lee, S. K., Jung, M. H.*, et al.* (2010). Phase I study of autologous dendritic cell tumor vaccine in patients with non-small cell lung cancer. Lung cancer *70*, 188-194.

van Rooijen, N., Bakker, J., and Sanders, A. (1997). Transient suppression of macrophage functions by liposome-encapsulated drugs. Trends in biotechnology *15*, 178-185.

Van Rooijen, N., and Sanders, A. (1994). Liposome mediated depletion of macrophages: mechanism of action, preparation of liposomes and applications. Journal of immunological methods *174*, 83-93.

van Rooijen, N., and van Kesteren-Hendrikx, E. (2002). Clodronate liposomes: perspectives in research and therapeutics. Journal of liposome research *12*, 81-94.

Vaupel, P., Kallinowski, F., and Okunieff, P. (1989). Blood flow, oxygen and nutrient supply, and metabolic microenvironment of human tumors: a review. Cancer research *49*, 6449-6465.

Vayrynen, J. P., Vornanen, J., Tervahartiala, T., Sorsa, T., Bloigu, R., Salo, T., Tuomisto, A., and Makinen, M. J. (2012). Serum MMP-8 levels increase in colorectal cancer and correlate with disease course and inflammatory properties of primary tumors. International journal of cancer Journal international du cancer *131*, E463-474.

Veglia, F., Vineis, P., Overvad, K., Boeing, H., Bergmann, M., Trichopoulou, A., Trichopoulos, D., Palli, D., Krogh, V., Tumino, R.*, et al.* (2007). Occupational exposures, environmental tobacco smoke, and lung cancer. Epidemiology *18*, 769-775.

Verreck, F. A., de Boer, T., Langenberg, D. M., Hoeve, M. A., Kramer, M., Vaisberg, E., Kastelein, R., Kolk, A., de Waal-Malefyt, R., and Ottenhoff, T. H. (2004). Human IL-23-producing type 1 macrophages promote but IL-10-producing type 2 macrophages subvert immunity to (myco)bacteria. Proceedings of the National Academy of Sciences of the United States of America *101*, 4560-4565.

Wakabayashi, O., Yamazaki, K., Oizumi, S., Hommura, F., Kinoshita, I., Ogura, S., Dosaka-Akita, H., and Nishimura, M. (2003). CD4+ T cells in cancer stroma, not CD8+ T cells in cancer cell nests, are associated with favorable prognosis in human non-small cell lung cancers. Cancer science *94*, 1003-1009.

Wang, X. R., Yu, I. T., Chiu, Y. L., Qiu, H., Fu, Z., Goggins, W., Au, J. S., Tse, L. A., and Wong, T. W. (2009). Previous pulmonary disease and family cancer history increase the risk of lung cancer among Hong Kong women. Cancer causes & control : CCC *20*, 757-763.

Weaver, C. T., Harrington, L. E., Mangan, P. R., Gavrieli, M., and Murphy, K. M. (2006). Th17: an effector CD4 T cell lineage with regulatory T cell ties. Immunity *24*, 677-688.

Wei, Q., Cheng, L., Amos, C. I., Wang, L. E., Guo, Z., Hong, W. K., and Spitz, M. R. (2000). Repair of tobacco carcinogen-induced DNA adducts and lung cancer risk: a molecular epidemiologic study. Journal of the National Cancer Institute *92*, 1764-1772.

Wei, Q., and Spitz, M. R. (1997). The role of DNA repair capacity in susceptibility to lung cancer: a review. Cancer metastasis reviews *16*, 295-307.

Welsh, T. J., Green, R. H., Richardson, D., Waller, D. A., O'Byrne, K. J., and Bradding, P. (2005). Macrophage and mast-cell invasion of tumor cell islets confers a marked survival advantage in non-small-cell lung cancer. Journal of clinical oncology : official journal of the American Society of Clinical Oncology *23*, 8959-8967.

Westra, W. H. (2000). Early glandular neoplasia of the lung. Respiratory research *1*, 163-169.

Willenborg, S., Lucas, T., van Loo, G., Knipper, J. A., Krieg, T., Haase, I., Brachvogel, B., Hammerschmidt, M., Nagy, A., Ferrara, N.*, et al.* (2012). CCR2 recruits an inflammatory macrophage subpopulation critical for angiogenesis in tissue repair. Blood *120*, 613-625.

Wistuba, II, Berry, J., Behrens, C., Maitra, A., Shivapurkar, N., Milchgrub, S., Mackay, B., Minna, J. D., and Gazdar, A. F. (2000). Molecular changes in the bronchial epithelium of patients with small cell lung cancer. Clinical cancer research : an official journal of the American Association for Cancer Research *6*, 2604-2610.

Wolf, M. J., Hoos, A., Bauer, J., Boettcher, S., Knust, M., Weber, A., Simonavicius, N., Schneider, C., Lang, M., Sturzl, M.*, et al.* (2012). Endothelial CCR2 signaling induced by colon carcinoma cells enables extravasation via the JAK2-Stat5 and p38MAPK pathway. Cancer cell *22*, 91-105.

Wong, L. M., Myers, S. J., Tsou, C. L., Gosling, J., Arai, H., and Charo, I. F. (1997). Organization and differential expression of the human monocyte chemoattractant protein 1 receptor gene. Evidence for the role of the carboxyl-terminal tail in receptor trafficking. The Journal of biological chemistry *272*, 1038-1045.

Xian, X., Hakansson, J., Stahlberg, A., Lindblom, P., Betsholtz, C., Gerhardt, H., and Semb, H. (2006). Pericytes limit tumor cell metastasis. The Journal of clinical investigation *116*, 642-651.

Xing, F., Saidou, J., and Watabe, K. (2010). Cancer associated fibroblasts (CAFs) in tumor microenvironment. Frontiers in bioscience : a journal and virtual library *15*, 166-179.

Xue, W., Meylan, E., Oliver, T. G., Feldser, D. M., Winslow, M. M., Bronson, R., and Jacks, T. (2011). Response and resistance to NF-kappaB inhibitors in mouse models of lung adenocarcinoma. Cancer discovery *1*, 236-247.

Yancopoulos, G. D., Davis, S., Gale, N. W., Rudge, J. S., Wiegand, S. J., and Holash, J. (2000). Vascular-specific growth factors and blood vessel formation. Nature *407*, 242-248.

Yang, X., Lu, P., Ishida, Y., Kuziel, W. A., Fujii, C., and Mukaida, N. (2006). Attenuated liver tumor formation in the absence of CCR2 with a concomitant reduction in the accumulation of hepatic stellate cells, macrophages and neovascularization. International journal of cancer Journal international du cancer *118*, 335-345.

Zaynagetdinov, R., Sherrill, T. P., Polosukhin, V. V., Han, W., Ausborn, J. A., McLoed, A. G., McMahon, F. B., Gleaves, L. A., Degryse, A. L., Stathopoulos, G. T.*, et al.* (2011). A critical role for macrophages in promotion of urethane-induced lung carcinogenesis. J Immunol *187*, 5703-5711.

Zhang, J., and Patel, J. M. (2010). Role of the CX3CL1-CX3CR1 axis in chronic inflammatory lung diseases. International journal of clinical and experimental medicine *3*, 233-244.

Zhang, J., Patel, L., and Pienta, K. J. (2010). CC chemokine ligand 2 (CCL2) promotes prostate cancer tumorigenesis and metastasis. Cytokine & growth factor reviews *21*, 41-48.

Zhang, P., Summer, W. R., Bagby, G. J., and Nelson, S. (2000). Innate immunity and pulmonary host defense. Immunological reviews *173*, 39-51.

Zheng, S., Chang, Y., Hodges, K. B., Sun, Y., Ma, X., Xue, Y., Williamson, S. R., Lopez-Beltran, A., Montironi, R., and Cheng, L. (2010). Expression of KISS1 and MMP-9 in non-small cell lung cancer and their relations to metastasis and survival. Anticancer research *30*, 713-718.

Zhu, X. D., Zhang, J. B., Zhuang, P. Y., Zhu, H. G., Zhang, W., Xiong, Y. Q., Wu, W. Z., Wang, L., Tang, Z. Y., and Sun, H. C. (2008). High expression of macrophage

colony-stimulating factor in peritumoral liver tissue is associated with poor survival after curative resection of hepatocellular carcinoma. Journal of clinical oncology : official journal of the American Society of Clinical Oncology *26*, 2707-2716.

Ziegler-Heitbrock, L. (2007). The CD14+ CD16+ blood monocytes: their role in infection and inflammation. Journal of leukocyte biology *81*, 584-592.

Zudaire, I., Lozano, M. D., Vazquez, M. F., Pajares, M. J., Agorreta, J., Pio, R., Zulueta, J. J., Yankelevitz, D. F., Henschke, C. I., and Montuenga, L. M. (2008). Molecular characterization of small peripheral lung tumors based on the analysis of fine needle aspirates. Histology and histopathology *23*, 33-40.

11 Appendix

Coordinate	Target	Alternate Nomenclature
A1-2	Positive Control	Control (+)
A23-24	Positive Control	Control (+)
B1-2	BLC	CXCL13/BCA-1
B3-4	C5a	Complement Component 5a
B5-6	G-CSF	
B7-8	GM-CSF	
B9-10	I-309	CCl1/TCA-3
B11-12	Eotaxin	CCL11
B13-14	siCAM-1	CD54
B15-16	IFNγ	
B17-18	IL-1α	IL-1F1
B19-20	Il-1β	IL-1F2
B21-22	IL-1ra	IL-1F3
B23-24	IL-2	
C1-2	IL-3	
C3-4	IL-4	
C5-6	IL-5	
C7-8	IL-6	
C9-10	IL-7	
C11-12	IL-10	
C13-14	IL-13	
C15-16	IL-12 p70	
C17-18	IL-16	
C19-20	IL-17	
C21-22	IL-23	
C23-24	IL-27	
D1-2	IP-10	CXCL10/CRG-2

D3-4	I-TAC	CXCL11
D5-6	KC	
D7-8	M-CSF	
D9-10	JE	CCL2/MCP-1
D11-12	MCP-5	CCL12
D13-14	MIG	CXCL9
D15-16	MIP-1α	CCL3
D17-18	MIP-1β	CCL4
D19-20	MIP-2	
D21-22	RANTES	CCL5
D23-24	SDF-1	CXCL12
E1-2	TARC	CCL17
E3-4	TIMP-1	
E5-6	TNFα	TNFSF2
E7-8	TREM-1	
F1-2	Positive Control	Control (+)
F23-24	PBS (Negative Control)	Control (-)

Table 17 **Cytokine Array coordinate**

12 Statement of Authenticity

Erklärung zur Dissertation

„Hiermit erkläre ich, dass ich die vorliegende Arbeit selbständig und ohne unzulässige Hilfe oder Benutzung anderer als der angegebenen Hilfsmittel angefertigt habe. Alle Textstellen, die wörtlich oder sinngemäß aus veröffentlichten oder nichtveröffentlichten Schriften entnommen sind, und alle Angaben, die auf mündlichen Auskünften beruhen, sind als solche kenntlich gemacht. Bei den von mir durchgeführten und in der Dissertation erwähnten Untersuchungen habe ich die Grundsätze guter wissenschaftlicher Praxis, wie sie in der „Satzung der Justus-Liebig-Universität Gießen zur Sicherung guter wissenschaftlicher Praxis“ niedergelegt sind, eingehalten sowie ethische, datenschutzrechtliche und tierschutzrechtliche Grundsätze befolgt. Ich versichere, dass Dritte von mir weder unmittelbar noch mittelbar geldwerte Leistungen für Arbeiten erhalten haben, die im Zusammenhang mit dem Inhalt der vorgelegten Dissertation stehen, oder habe diese nachstehend spezifiziert. Die vorgelegte Arbeit wurde weder im Inland noch im Ausland in gleicher oder ähnlicher Form einer anderen Prüfungsbehörde zum Zweck einer Promotion oder eines anderen Prüfungsverfahrens vorgelegt. Alles aus anderen Quellen und von anderen Personen übernommene Material, das in der Arbeit verwendet wurde oder auf das direkt Bezug genommen wird, wurde als solches kenntlich gemacht. Insbesondere wurden alle Personen genannt, die direkt und indirekt an der Entstehung der vorliegenden Arbeit beteiligt waren. Mit der Überprüfung meiner Arbeit durch eine Plagiatserkennungssoftware bzw. ein internetbasiertes Softwareprogramm erkläre ich mich einverstanden.“

13 Acknowledgement

It is a pleasure to express my sincere gratitude to everybody contributing to this thesis. Without the support, patience and guidance of the following people, this study would not have been completed.

First of all, I would like to especially thank Prof. Dr. Werner Seeger for providing me the opportunity to perform my studies in his department and further for giving valuable advices regarding my project over the last three years.

I feel honored to express my gratitude to my supervisors Prof. Dr. rer. nat. Ralph Schermuly and Prof. Dr. rer. nat. Michael Martin for their scientific guidance and support during my thesis.

I am deeply grateful for the supervising, guidance and support of Dr. biol. hum. Rajkumar Savai. I appreciate your commitment and enthusiasm for science and my project. Thank you for intensive and fruitful discussions.

I received generous support and encouragement from PD Dr. med Susanne Herold, PhD, Dr. med Marian Kampschulte, Gunhild Martels and Dr. rer. nat. Astrid Wietelmann. I have greatly benefited from illuminating discussions and help with Flow cytometry, computed tomography and magnetic resonance imaging.

I would like to show my greatest appreciation to all faculty and administrative members of Molecular Biology and Medicine of the Lung (MBML), especially Dr. Rory E. Morty, Dr. Soni Pullamsetti, Dr. Grazyna Kwapiszewska-Marsh and Dr. Malgorzata Wygrecka for excellent training.

In particular I would like to thank my lab mates and all colleagues from Seeger Department, especially Dr. Aleksandra Tretyn, Marianne Hoeck, Yanina Knepper, Vanessa Golchert, Nefertiti El-Nikhely, Alina Asafova and Poonam Sarode.

Finally, I owe my deepest gratitude to my friends, my boyfriend Hamza Al-Tamari and most notably my family, especially my sister Jana for unconditional support, love and endless patience with me and my work.

14 Curriculum vitae

Der Lebenslauf wurde aus der elektronischen Version der Arbeit entfernt.